Electric Distribution Reliability Analysis Considering Time-varying Load, Weather Conditions and Reconfiguration with Distributed Generation

Dan Zhu

Dissertation Submitted to the Faculty of the
Virginia Polytechnic Institute and State University
in partial fulfillment of the requirements for the degree of

Doctor of Philosophy
In
Electrical Engineering

Dr. Robert P. Broadwater (Chairman)

Dr. Kwa-Sur Tam

Dr. Yilu Liu

Dr. Walling Cyre

Dr. James D. Arthur

March 27, 2007
Blacksburg, Virginia

Keywords: Power Distribution System, Reliability Analysis, Reliability Improvement, Storm Outage Prediction, Reconfiguration for Restoration, DG, Time-varying Load.

Electric Distribution Reliability Analysis Considering Time-varying Load, Weather Conditions, and Reconfiguration with Distributed Generation

Dan Zhu

ABSTRACT

This dissertation is a systematic study of electric power distribution system reliability evaluation and improvement. Reliability evaluation of electric power systems has traditionally been an integral part of planning and operation. Changes in the electric utility coupled with aging electric apparatus create a need for more realistic techniques for power system reliability modeling.

This work presents a reliability evaluation technique that combines set theory and Graph Trace Analysis (GTA). Unlike the traditional Markov approach, this technique provides a fast solution for large system reliability evaluation by managing computer memory efficiently with iterators, assuming a single failure at a time. A reconfiguration for restoration algorithm is also created to enhance the accuracy of the reliability evaluation, considering multiple concurrent failures. As opposed to most restoration simulation methods used in reliability analysis, which convert restoration problems into mathematical models and only can solve radial systems, this new algorithm seeks the

reconfiguration solution from topology characteristics of the network itself. As a result the new reconfiguration algorithm can handle systems with loops.

In analyzing system reliability, this research takes into account time-varying load patterns, and seeks approaches that are financially justified. An exhaustive search scheme is used to calculate optimal locations for Distributed Generators (DG) from the reliability point of view. A Discrete Ascent Optimal Programming (DAOP) load shifting approach is proposed to provide low cost, reliability improvement solutions.

As weather conditions have an important effect on distribution component failure rates, the influence of different types of storms has been incorporated into this study. Storm outage models are created based on ten years' worth of weather and power outage data. An observer is designed to predict the number of outages for an approaching or on going storm. A circuit corridor model is applied to investigate the relationship between power outages and lightning activity.

ACKNOWLEDGEMENTS

I would like to acknowledge the invaluable guidance and concern of my advisor, Dr. Robert Broadwater. Throughout this writing and research process, he always accepted my ideas with an open mind and gave me the maximum opportunity to contribute to the program. I am grateful for his mentorship, friendship, guidance and patience not only during my Ph.D program, but over the past five years.

I would like to thank Electric Distribution Design (EDD) Inc. for providing facilities to finish this research work, and the Distribution Engineering Workstation (DEW) for benchmark analysis of the power flow calculations.

Thanks are also due to Dr. Kwa-Sur Tam, Dr. Yilu Liu, Dr. Walling Cyre and Dr. James D. Arthur for serving on my committee, especially, Dr. Cyre. He helped me to review the dissertation report and offered me valuable comments.

All of this would not be possible without the support from my parents, Longchang Zhu and Xiuzhen Zhong, who always have believed in me and been proud of me.

My husband, Max, deserves special thanks. His unselfish support and encouragement has allowed me to keep my perspective throughout this adventure.

This Dissertation is dedicated to

My lovely family

Especially to my son Cato

TABLE OF CONTENTS

LIST OF FIGURES

LIST OF TABLES

CHAPTER 1 INTRODUCTION

1.1 Introduction to Power System Reliability

'One of the really difficult problems faced by those responsible for planning of electric supply systems is that of deciding how far they are justified in increasing the investment on their properties to improve service reliability. ' [1938, Dean] Reliability is not a new topic in the electric power industry. Nevertheless, it has intrigued a number of engineers and scientists in the past decade due to costly blackouts.

The function of an electric power system is to satisfy the system load requirement with a reasonable assurance of continuity and quality. The ability of the system to provide an adequate supply of electrical energy is usually designated by the term of reliability. The concept of power-system reliability is extremely broad and covers all aspects of the ability of the system to satisfy the customer requirements. There is a reasonable subdivision of the concern designated as "system reliability", which is shown in Figure 1.1.

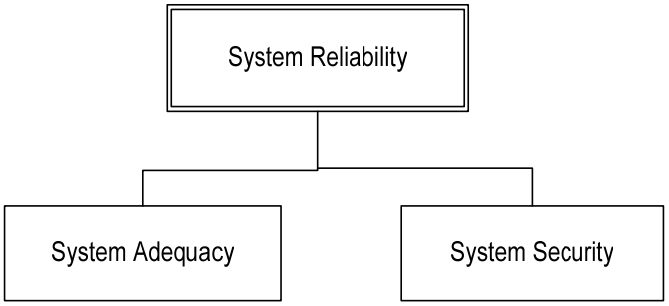

Figure 1.1 System Reliability Subdivisions

Figure 1.1 represents two basic aspects of a power system: system adequacy and security. Adequacy relates to the existence of sufficient facilities within the system to satisfy the consumer load demand. These include the facilities necessary to generate sufficient energy and the associated transmission and distribution facilities required to transport the energy to the actual consumer load points. Security relates to the ability of the system to respond to disturbances arising within that system. Security is therefore associated with the response of the system to whatever perturbations it is subject to [1]. Most of the probabilistic techniques presently available for power-system reliability evaluations are in the domain of adequacy assessment. The major techniques presented in this work are also in this domain.

Intuitively, adequacy is tied to forecasting (load and capacity). However, power system reliability evaluations are usually conducted separately in the functional zones of generation, transmission and distribution. Assessments are also made in the combined generation and transmission systems, called composite or bulk system evaluation. In generation system reliability evaluation, the total system generation capacity is examined to determine its adequacy to meet the total system load requirement. Generation adequacy analysis is not intended to provide the reliability indices for individual load

points. On the other hand, the distribution system is usually analyzed as a separate entity. In this case, the focus is on the impact of distribution element failures on individual customer load points. The effect of the bulk system on the distribution system is usually ignored in the analysis. Since this study concentrates on the power distribution system, we assume there is always sufficient power supplied by the substations, (the failures of components within the substation, such as transformers and switches, are taken into account). Therefore the main focus of this study is on the availability of the distribution facilities required to transport the power to customer load points.

1.2 Challenges in Power Systems

According to the U.S. Department of Energy's Energy Information Administration (EIA), consumer demand for electricity is projected to grow at an average rate of 1.5 percent per year through 2030. Overall, electricity consumption is expected to increase 45 percent by 2030 [2]. Traditionally, new delivery capacity would be added to handle load increases. However, due to the current difficulty in obtaining permits and the uncertainty about achieving an adequate rate of return on investment, total circuit miles added annually are declining while total demand for delivery resources continues to grow. The smaller transmission reserve makes the power system more vulnerable during emergency situations. Moreover, even without the rapid growth in electricity demand and the limit of transmission and distribution capacity, with more than 100 years of history, the power system itself is becoming more vulnerable due to the aging equipment. The cascading blackout in North America during August 2003 was a good illustration of vulnerabilities in the power system. This event increased the interest in reliability analysis.

In parallel with the current reliability challenges, distributed generation (DG) is receiving considerable attention. DG is typically defined as small generators, usually less than 30-MW, that are connected to transmission or distribution systems. The emerging new techniques such as small combustion turbines, fuel cells, photovoltaics, and superconducting magnetic energy storage (SMES) make DGs more and more affordable and popular. While large scale power plants remain critical to the national energy supply, studies have predicted that DGs may account for up to 20% of all new generation going online by the year 2010[3].

This work observes the trend of using DG for operation and management support, and considers DGs in power system reliability analysis. Time-varying load conditions and some environmental conditions are also taken into account in the reliability assessments considered here.

1.3 Research Objective and Contribution

1.3.1 Objective of This Research

This research seeks to achieve a more thorough understanding of the factors that affect power system reliability. A new approach to systems analysis, Graph Trace Analysis (GTA), is applied in the reliability and reconfiguration for restoration calculations.

1.3.2 Contribution of This Research

This dissertation outlines research efforts concerning electrical power distribution system reliability analysis. There are five contributions that are sought which are:

- Apply GTA algorithm notation in the solution of reliability analysis and reconfiguration for restoration.
- Develop a reconfiguration for restoration algorithm to enhance the accuracy of reliability assessment.
- Analyze system reliability as a function of time varying system load.
- Analyze system reliability as a function of distributed generation.
- Apply Discrete Ascent Optimal Programming on load shifting to improve system reliability
- Model reliability parameters as a function of different types of storms.
- Seek a relationship between lightning flash density and outages.

In this study, the algorithm used to evaluate power system reliability is implemented with topological iterators and graph trace sets. A Graph Trace Analysis (GTA) notation is introduced to present the computer algorithm in fine details without involving any specific computer languages.

Distribution network reconfiguration is the process of altering the topology of the system by changing the open/closed status of the sectionalizing devices such that no

feeder overloads or abnormal voltages are created. This research focuses on reconfiguration for service restoration as an intermediate process in reliability analysis. Reconfiguration for restoration improves system reliability by reducing customer down times following power outages. In this research, a reconfiguration for restoration algorithm is developed that takes into account multiple concurrent failures and also load priorities. The reconfiguration algorithm is implemented with Graph Trace Analysis.

A system's loading can affect its reliability level in two ways. First, it can accelerate or decelerate the process of component aging, which changes the probability of component failure. Second, within an interconnected distribution system, if alternative power sources are available from adjacent feeders, the power interchange capability influences the system's reliability. That is, the power interchange capability is a function of the system loading. It will be shown that as the system load fluctuates over time, system reliability will change as a stepwise function of load.

Distributed generators (DGs) sometimes provide the lowest cost solution for handling low voltage or overload problems. In conjunction with handling such problems, a DG can be placed for optimum efficiency or optimum reliability. The impact of DG placement on reliability and efficiency with time-varying loads is addressed in [4]. The difference in DG placement between optimum efficiency and optimum reliability varies with loading conditions. Recommendations concerning DG placement for optimum reliability and efficiency are provided. Economic considerations are also discussed.

Balancing the load among adjacent circuits is also a low cost measure to improve overall system reliability. This work applies Discrete Ascent Optimal Programming

(DAOP) to re-distribute loads among the interconnected circuits so that optimal system reliability can be obtained.

This research seeks to extend the application of reliability analysis during storm conditions. Utility companies spend large amounts of money on storm outage restoration. Improvements in reliability for storms can translate into significant savings for electric utilities. As part of this effort, an investigation of how storms impact the power distribution system is performed.

Power facilities are vulnerable to adverse weather conditions, and failures are very much a function of weather conditions. Knowing reliability levels during storms, including how long and how often interruptions are expected to happen, is valuable for outage management. In this work, storm categories in terms of temperatures, wind speeds, and lightning activity are defined. For each storm category the outage and recovery distributions are developed and analyzed. An observer is designed to predict equipment failures. The observer uses historical outage distributions and real time outage records [5]. In this way, storm outages can be better managed and overall system reliability can be improved.

Lightning is a primary cause of outages during summer storms. Research has been initiated to seek the relation between summer lightning activity and power outages within certain ranges of circuit corridors. Results are presented on a possible relationship between flash density and outages.

1.4 Literature Review

An electric power system includes three hierarchies: generation, transmission and distribution (known as hierarchical level 3, HL3). An overall reliability evaluation is normally not conducted because of the enormity of the problem. Instead, reliability evaluations of generating facilities, of composite generation and transmission systems, and of distribution system are conducted independently. Some efforts have been devoted to performing comprehensive reliability evaluation considering impacts of all parts of the power system. [6] [7]

Analysis of customer failure statistics [8] has indicated that the distribution system makes the greatest individual contribution to overall customer supply unavailability. Statistics such as these and others collected by the Canadian Electrical Association (CEA) for all its member electric power utilities [9] indicate that the bulk power system contributes only a relatively small component to the overall HL3 customer indices, which are performance indices obtained from historical event reporting. Therefore, this research focuses on distribution system reliability evaluation and improvement.

1.4.1 Evaluation techniques

The Markov process is one of the common techniques employed in reliability analysis [10]. The application of Markov Chains in the power system reliability field was illustrated in Reference [11]. However, the Markov approach is limited in application because of computer storage requirements and the rounding errors which occur in the solution of large systems. This report presents a reliability analysis method that combines

set theory and Graph Trace Analysis (GTA), which provides a rapid reliability evaluation, assuming single failures at a time. Unlike the Markov process, this method utilizes iterators to manage computer memory, which enables it to handle computations for large systems.

An accurate reliability evaluation of radial distribution systems must take restoration into account. Most conventional techniques [12], [13] developed for reliability analyses are generally based on minimal cut set approach (MCSA) or failure mode and effect analysis (FMEA) [14]. For a distribution system, which consists of a wide variety of components and a great number of load points connected in complex configuration and operating in different modes, it is quite a tedious procedure to determine minimal cut sets for each load point and each contingency. Besides, modeling the overlapping outage times associated with the minimal cut-sets leading to a load point failure is a drawback of this technique. The list of basic failure events using FMEA can also be very lengthy. A generalized method [15] converting complex distribution systems to their equivalent networks for reliability evaluation has been proposed to simplify the analytical process. It is, however, very difficult to determine the network equivalent of a sub-feeder when network constraints and restoration sequence are considered. The impact of two-stage service restoration on distribution reliability has been investigated [16]. A simple restoration procedure has been considered [17]. A radial distribution system is represented dynamically using a tree data structure in this technique. The techniques can be used to consider complicated restoration procedures. However, the tree data structure prevents this approach from solving the restoration problems in a system with loops. In this work, a reconfiguration algorithm is developed to handle systems with loops.

1.4.2 Reliability Improvement

New techniques have been developed to improve distribution system reliability, such as automatic learning techniques [18], automatic switches [19], Microprocessor Relays [20], and so on. However, the financial aspect of these new techniques is seldom considered. This work investigates new approaches to improving system reliability, which are financially justified, including optimal DG location and DAOP load shifting.

As weather conditions have an important effect on network failure rates, it is necessary to take into account the influence of the weather in the performance of the components located in open-air environments. Previous research has been performed on storm related power outages. Early in the 1980's, [21] proposed using a database of customer no-light calls to generate outage patterns. However, the outage patterns were not successful for use in identifying faulted sections. [22] uses a two-stage Monte Carlo simulation to evaluate the impact of high wind storms. This work quantifies storm interruptions in a power distribution system. In order to improve outage restoration, [23] suggests a rule-based prediction for determining outage locations from the available call patterns and telemetered data. None of the 'prediction' models in [21]-[23] provide an outage forecast ahead of time.

[24] proposes a predictor which applies a data grouping method and neural networks to estimate the amount of damage due to typhoons. Similar to [24], the work here uses a two stage process. Instead of typhoons, typical storms in the northeastern section of the United States are analyzed and an observer [25] is used instead of neural networks in the second stage.

[26] presents a general procedure for storm outage management. It utilizes the information from weather forecasts and historical data to predict the storm damage in advance, and uses the prediction to manage the crews. However, [26] did not provide any specific storm outage models, and furthermore did not provide the details of how storm related information may be used to produce storm outage models. In this research, reliability parameters are modeled for different types of storms, and a model of circuit corridors is created to investigate a possible relationship between flash density and outages.

1.5 Outline of Dissertation

The remainder of this dissertation is organized as follows. Chapter 2 provides a review of the factors that influence power system reliability. Chapter 3 reviews reliability evaluation techniques and introduces a reliability algorithm for analyzing single failures in terms of set theory and graph trace analysis, where GTA algorithm notations are applied. In Chapter 3, a reconfiguration algorithm is introduced to assist reliability evaluation for multiple failure situations. Chapter 4 provides a detailed investigation of reliability improvements from various aspects discussed in Chapter 2. In the course of this investigation, system reliability is analyzed as a function of time varying system load and distributed generation location. Reliability parameters are also developed as a function of weather and lightning conditions. Chapter 5 presents the conclusions deduced from this research and includes ideas for future study.

CHAPTER 2 FACTORS INFLUENCING POWER SYSTEM RELIABILITY

The factors influencing power system reliability can be broken down into four categories. They are component reliability, environmental conditions, loading, and system configuration.

2.1 Component Statistics

A power system consists of various components, such as lines, cables, transformers, breakers, switches, reactors, and capacitors. Any single component outage may cause a partial or even entire system outage. The availability of component functionally is characterized by failure rates and repair or replacement times.

2.1.1 Failure rate

Component failures can be divided into aging failures and chance failures. Aging failure is a conditional failure that depends on the component's history. Fig 2.1 shows a bath-tub curve of a component's failure rate change during its life time. An aging failure can happen suddenly after a component enters its Wear-out period. Fig 2.1 indicates that a component failure rate is not a constant. Failure rate distributions are different from component type to component type. Some expensive components, like transformers, come with a set of reliability data provided by the manufacturer, including the

component's life cycle statistical distribution. Nowadays, the infant mortality period of some expensive components is usually consumed by manufacturers so that when these components are put into service they are already in a reliable state.

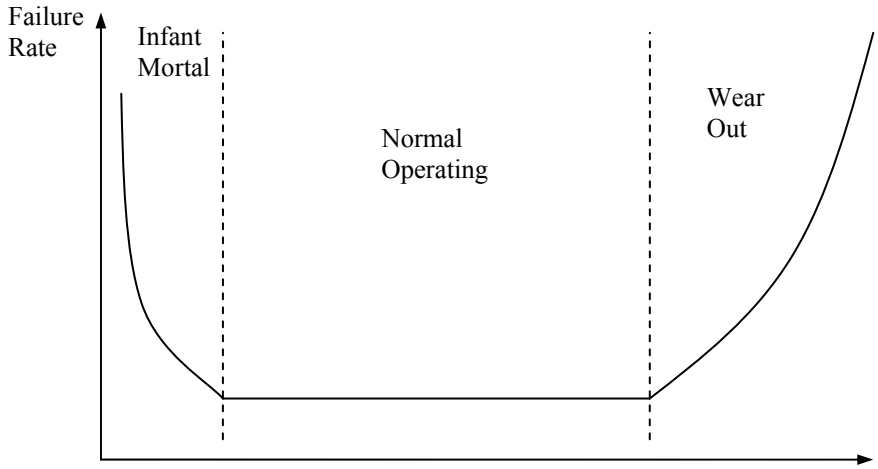

Figure 2.1 Bath-tub curve of a component's life

Chance failure is a random fatal failure [27]. We notice from Fig 2.1 that the failure rate in the normal operation period is a constant failure rate, and it does not depend on a component's age. Therefore, chance failure can be modeled as an exponential distribution. (Exponential distribution is the only distribution that has a constant failure rate. [28])

This statistic usually can be obtained under normal operating conditions from the manufacture. However, loading and environmental conditions often contribute to equipment failures. Failure rates for operating under abnormal conditions are difficult for manufactures to provide. The influence of these abnormal conditions will be discussed later in this dissertation.

2.1.2 Repair Time

There are no good models for repair time (or down time), since the repair time for failed equipment depends upon many things, such location, crew dispatch policy, different failed parts in a type of component and so on. One of the common practices is to use the exponential model, which assumes reparations are statistically independent events and the repair time can be represent by the global average. Historical data shows that the repair time is also affected by weather conditions. Stormy conditions usually prolong the process of customer down time.

2.2 System Configurations

System configurations include various issues, including topology, transportation capacity, protection/coordination schemes, and DG placement. These factors all influence the reliability level of a system to some extent. Basically, assuming the protection and coordination scheme permits, more connectivity between feeders means more potential alternate feeds to the interconnected feeders, and whether the potential alternate feeds can actually provide alternate power during contingency situations is determined by the capacity of the feeders themselves. However, adding DGs in a system shapes this relationship. Later in this dissertation, an investigation is conducted to seek the optimal location to install a DG based on different criteria.

2.3 Time-varying Load

The load demands in distribution systems vary from time to time, and each class of customers follows a different pattern. Figure 2.2 shows the daily load change for a residential building in a weekday of January. The difference between the maximum load point and minimum load point is 4800 -2400 = 2400 KW, which is 50% of the peak load. It is obvious that the applicability of a reliability analysis algorithm to a practical system is limited if only a constant load model is considered.

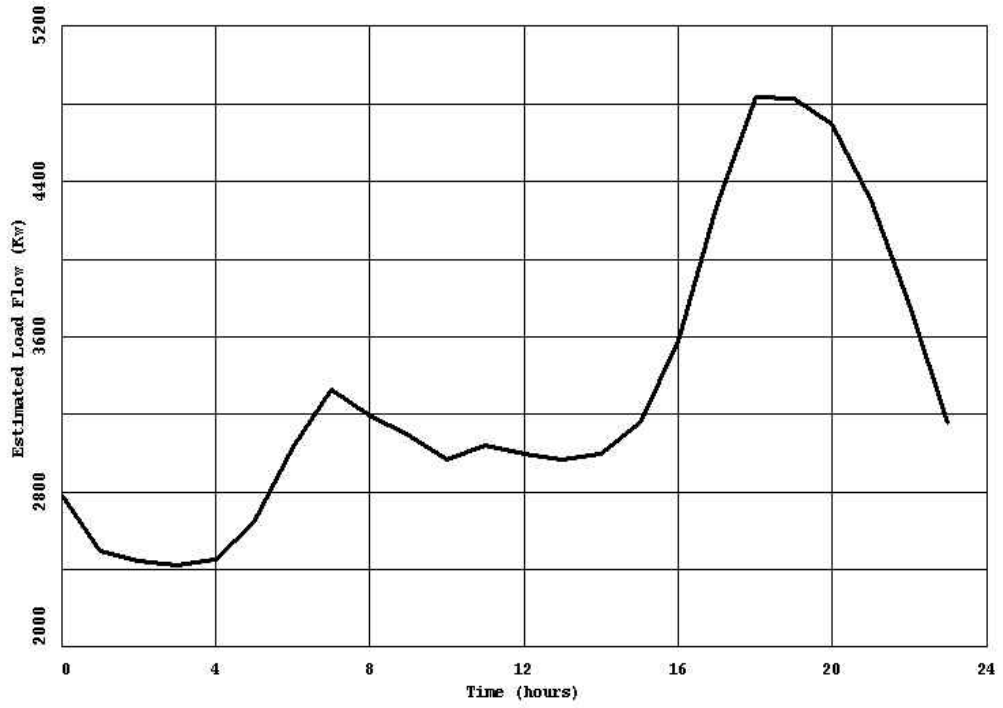

Figure 2.2 Daily Load Pattern of a Residential Load in a Weekday of January

The loading condition changes the system reliability in two different ways. First, excess load speeds up equipment aging; on the other hand, mild load may prolong the life-span of an electric component. Second, loading conditions change the power

interchange capability among the adjacent circuits. Power system networks are interconnected, often by open tie switches. For many load points, there are alternative sources of power if switching operations are permitted. When an alternative source is available, whether the alternative source is able to supply power to a particular load point is determined by power interchange capability among the adjacent circuits. So for a given configuration of the power system, loading conditions also affect the system reliability. In Chapter 3 it will considered how power system reliability can be modeled as a function of load conditions.

2.4 Environmental Conditions

Power system components are exposed to various weather conditions and hazards. Animals, motor vehicle accidents, rain, ice, and tree contact can all lead to faults and failures. Environment dependent failures may be of short duration. However, during such events, the probability of failure of components increases dramatically. Many utility companies have given this increased attention, especially with weather dependent failures.

It is difficult to develop an accurate model for the catastrophic environment since its probability of occurrence and the impact range can only be based on a rough estimate. Usually weather condition modeling is better designed than the other environmental conditions since historical weather data is always available. For example, if we divide the weather conditions into two basic states: normal and adverse, and the failure rates and repair times of components for these two states are available, the system reliability can be evaluated separately for the two weather states and the resulting reliability indices can be weighted by the probability of the weather states.

CHAPTER 3 RELIABILITY EVALUATION

3.1 Reliability Evaluation Techniques

Reliability analysis has a wide range of engineering applications. These applications involve either qualitative or quantitative techniques. Qualitative techniques imply that reliability assessment must depend solely upon engineering experience and judgment. Quantitative methodologies use statistical approaches to reinforce engineering judgments. Quantitative techniques describe the historical performance of existing systems and utilize the historical performance to predict the effects of changing conditions on system performance. Reliability is an inherent characteristic of a system, and therefore it should be expressed in quantitative terms in order to compare alternative configurations or perform economic analysis. In this research, quantitative techniques are used to estimate reliability with changing configurations, generation, and load patterns.

The majority of distribution systems are designed to operate with a radial topology. Radial distribution systems have a set of series components between a substation and a load point, including breakers, lines, cables, transformers, switches, fuses and other equipment. A failure of any component in the series path results in the outage of a load point. Sectionalizing devices provide a means of isolating a faulted section. In some systems there is an alternative supply source for sections that become disconnected from their original source after the failure is isolated. Figure 3.1 shows a simple radial distribution configuration with an alternative source.

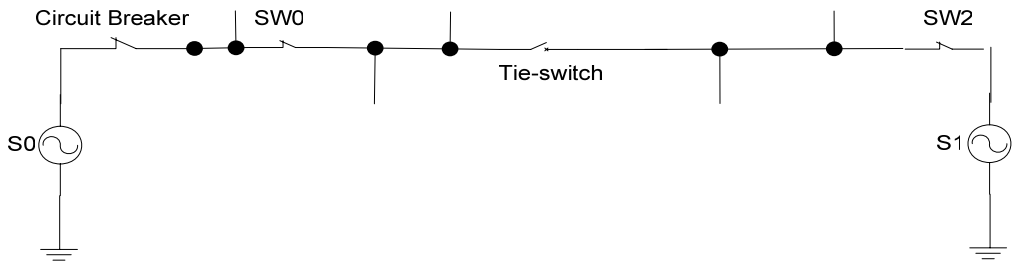

Figure 3.1 A Simple radial distribution system

3.2 Analytical Method

The analytical approach to estimate radial system reliability has been used for years [27]. In this case, the components between load points and the substations are in series. The non-series characteristic of the distribution system is tackled by the reliability sets discussed in the next section.

For example, in a series network with two components, as shown in Figure 3.2, the failure rate of the network is

$$FR=Fr_1+Fr_2 \tag{3.1}$$

where Fr_j = the failure rate for component ***j***

The system unavailability, U, is

$$U=1-(1-U_1)(1-U_2) \tag{3.2}$$

where U_j = the unavailability for component ***j***

System unavailability can be also expressed as

$$U = 1 - \frac{FR}{FR + \frac{1}{REP}} \tag{3.3}$$

where REP = the equivalent repair time of a system.

And component unavailability can expressed as

$$U_i = 1 - \frac{Fr_i}{Fr_i + \frac{1}{\mathrm{Re}\, p_i}} \tag{3.4}$$

Where Rep_j = the average repair time for component ***j***

From 3.2 to 3.4 we can get

$$(1 - \frac{FR}{FR + \frac{1}{REP}}) = (1 - \frac{Fr_1}{Fr_1 + \frac{1}{\mathrm{Re}\, p_1}})(1 - \frac{Fr_2}{Fr_2 + \frac{1}{\mathrm{Re}\, p_2}}) \tag{3.5}$$

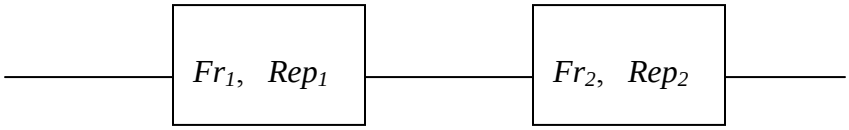

Figure 3.2 Series Network

Substituting 3.1 into 3.5, the expected repair time for the series system can be calculated by

$$REP = \frac{Fr_1 \times \mathrm{Re}\, p_1 + Fr_2 \times \mathrm{Re}\, p_2 + Fr_1 \times \mathrm{Re}\, p_1 \times Fr_2 \times \mathrm{Re}\, p_2}{Fr_1 + Fr_2} \tag{3.6}$$

Generally, the condition of $Fr_1 \times \mathrm{Re}\, p_1 \times Fr_2 \times \mathrm{Re}\, p_2 << Fr_1 \times \mathrm{Re}\, p_1$ or $Fr_2 \times \mathrm{Re}\, p_2$ holds true in distribution systems, so 3.4 can be approximated by

$$REP = \frac{Fr_1 \times \mathrm{Re}\, p_1 + Fr_2 \times \mathrm{Re}\, p_2}{Fr_1 + Fr_2} \tag{3.7}$$

3.1 and 3.5 can be extended to the case of any number of components in series:

$$FR = \sum_{j=1}^{n} Fr_j \tag{3.8}$$

$$REP = \frac{\sum_{j=1}^{n} Fr_j \times \mathrm{Re}\, p_j}{\sum_{j=1}^{n} Fr_j} \tag{3.9}$$

Once the indices at all load points are obtained, system reliability performance indices can be calculated. However, in a system with thousands of nodes, computing the indices at all load points would be exhausting. A computer algorithm employing set theory and graph trace analysis may be used to calculate the indices for all load points automatically. This algorithm will be presented in the following sections.

3.3 Reliability Analysis Sets

Before introducing the computer algorithm, let us first address the concept of a segment. In essence, there are two types of equipment in a distribution system. One consists of lines, transformers, and other components that are involved in transmitting power from the distribution substation to customers. The second type of equipment represents protective devices and consists of fuses, reclosers, circuit breakers, etc. Protective devices are designed to detect unusual conditions on the power delivery system and isolate portions of system that are responsible for those conditions from the

rest of the network. The location of protective components on the distribution system and their response to failures can have an important impact on reliability indices.

Protective devices together with switches will be referred to as sectionalizing devices. Sectionalizing devices are used to group components. Thus, a sectionalizing device is any component that is designed to break the electrical circuit topology. The distribution system will be considered to be divided into segments, where a segment a group of components whose entry component is a sectionalizing device (that is, a switch or a protective device). Each segment has one and only one sectionalizing device. For example, in the circuit indicated in Figure 3.1, there are four segments: segment Circuit Breaker, segment SW0, segment SW2 and segment Tie-switch. Note that segment Tie-switch has only one component, which is the open tie switch itself. In the following pages, the power system is not modeled in terms of components, but segments.

In Figure 3.3, the only protection on the feeder is the station breaker B. Segment B consists of nine components. They are B, 1, 2, 3…… and 8. The failure of any of the components in segment B can cause an interruption at load point 1. It is the same for the other load points (3, 5, 7 and 8). No temporary restoration is possible. For this configuration, the reliability of all the load points (1, 3, 5, 7, and 8) is identical.

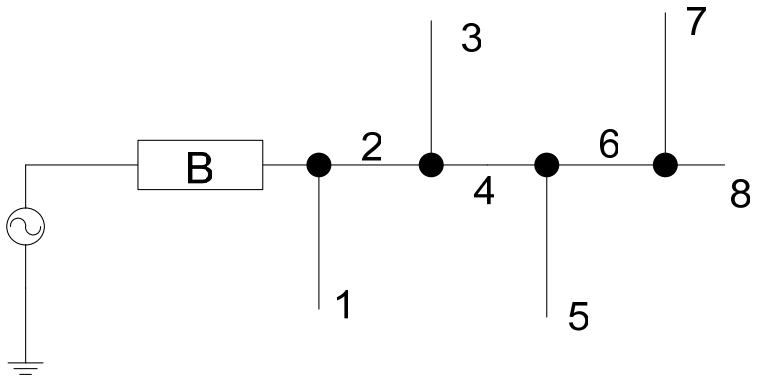

Figure 3.3 Sample segment

A segment's name is the same as that of its sectionalizing device. In Figure 3.3, there is only one segment, which is segment B. Breaker B and components 1, 2, 3, 4 and 5 all belong to segment B.

Modeling the power system in terms of segments speeds up the reliability calculations. The algorithm can be programmed to run faster since only the sectionalizing devices are processed.

In order to analyze the reliability of distribution systems, the Electric Power Research Institute (EPRI) defined sets [29] needed for calculating the reliability of a given load point. Figure 3.4 illustrates the relation among these sets.

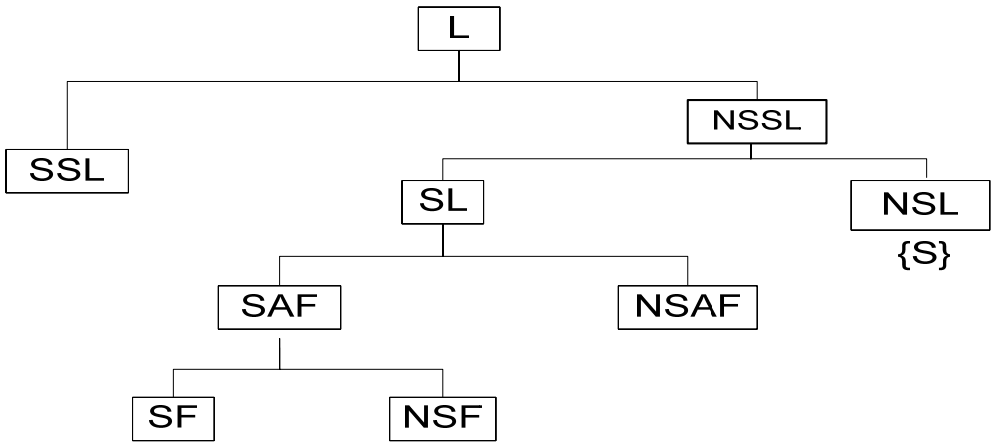

Figure 3.4 Reliability Analysis Sets

In reliability analysis, the failure of all components that can cause a lost of service to a particular load point must be considered. (This load point will be presented in terms

of a segment, which is the segment of interest *S*.) All system components are either located on the continuous path between the source and the segment of interest, or not located on the path. The failure of any continuous path components can cause an interruption at the load point. And the failure of components not in the path can also cause an interruption at the load point, unless the component is separated from the path by a protective device that responds automatically to the component failure. The effects of non-series components and temporary restoration are now considered in the sets shown in Figure 3.4, as will now be explained.

The L set shown in Figure 3.4 contains all segments within a circuit whose failure can cause loss of power to the segment of interest *S*. This L set includes all segments that are not separated from the continuous path between the source (substation, generator, etc.) and the segment of interest *S* by an automatic protective device. Now we partition the L set into the sets SSL and NSSL:

- The SSL set consists of the segments that may be isolated from the continuous path between ***S*** and the original source
- The NSSL set consists of the segments that can**not** be switched away from the continuous path between *S* and the original source.

The SSL set contains any segments separated from the continuous path by manually operated switches. If any component of this set fails, the segment of interest *S* can be temporarily restored from the original source before the failed component is repaired or replaced.

Examining those segments that cannot be separated from the continuous path, we can further partition the set NSSL into SL and NSL:

- The SL set consists of the segments that can be switched away from the segment of interest ***S***, so that if the failure occurs in the SL set, ***S*** may be fed by an alternate source
- The NSL set consists of the segments that can**not** be switched away from the segment of interest ***S***. That is the segment of interest itself, so this set only contains the component {S}.

If any thing fails in the NSL set, all the components within that segment have to experience the full repair or replacement time of the failed component. Temporary restoration is not possible. Considering the SL set, we can divide it into SAF and NSAF:

- For the SAF set, if the failed component lies in these segments, it is possible to restore power to ***S*** by an alternate source
- For the NSAF set, if the failed segment belongs to this set, the segment of interest ***S*** cannot be temporarily restored from an alternate feed.

The set SAF contains the segments that can be isolated from both the segment of interest ***S*** and the alternative source, which make the temporary restoration topologically possible. Sometimes, system constraints may limit the restoration options; the alternate source might not have the capacity to support the particular load point of interest. So the set SAF is partitioned into SF and NSF:

- The SF set consists of all segments that can be isolated from ***S*** and an alternative source, allowing power to be restored to ***S*** from the alternative source (for segments in this set, system constraint violations do not occur during the restoration)
- The NSF set consists of all segments which may be isolated from ***S*** and an alternative source, but for which it is **not** possible to restore power to ***S*** because of violating system constraints.

The set L, including all the segments for calculating the reliability indices, is decomposed into a number of sets as given by

$$L = SSL \cup NSSL; \tag{3.10}$$

$$NSSL = SL \cup \{S\}; \tag{3.11}$$

$$SL = SAF \cup NSAF; \tag{3.12}$$

$$SAF = SF \cup NSF \tag{3.13}$$

3.8, 3.9, 3.10 and 3.11 yield

$$L = SSL \cup SF \cup \{S\} \cup NSAF \cup NSF \tag{3.14}$$

To sum up, if the failed component from the L set is placed in the SSL set, it is possible to restore power to the load point of interest *S* from the original source. If the failure occurs in the SF set, the power can be restored to *S* from an alternative source without violating system constraints. But if the failed component lies in either of the {s}, NSAF or NSF sets, then the failed component must be completely repaired before power can be restored to *S*.

We use several additional reliability analysis (RA) sets to calculate the sets in 3.12, as given by

SIC = set of all the segments in the circuit

SW = set of all the sectionalizing devices in the circuit

AF = set of available alternate sources

IS = set of sectionalizing devices that will isolate the segment of interest *S* from the original sources

NIS = set of switches that do not isolate the original source from the segment of interest

EC = set of ending components for the circuit

PD = set of protective devices that isolate the load point of interest from its original source.

3.4 Graph Trace Analysis with Iterators

The Distributed Engineering Workstation, DEW, provides a computer aided engineering environment that may be used for the design and analysis of electric distribution systems [30]. The reliability analysis application presented here is developed within the DEW.

Reliability analysis is complicated by a number of factors. One of these is the size of distribution systems. Large metropolitan areas may contain tens of thousands of devices with many separated circuits supplied by different substations. Calculation of reliability for a system is an extensive logistical problem. Fundamental to reliability improvement is manipulation of large amounts of interrelated data. This data includes distribution system configuration, system fault protection, customer density, failure rates and repair times. The methods with which this data is stored, displayed and modeled determine the effectiveness of the computerized method. In DEW, information about the distribution system under study is permanently stored in data base tables. Initialization of the environment results in the most commonly used circuit model data being loaded into the workstation active memory [31]. This data is immediately available to and shared by application modules, such as the reliability analysis application. In this way, the number of accesses to the relational database is minimized. The most commonly used application modules run entirely in high speed memory and do not have to access the hard disk. This approach provides rapid graphical display operations and engineering analysis computation.

3.4.1 Iterators

An iterator is an object which allows an algorithm to traverse through all the elements of a collection, regardless of its specific implementation. Depending on the language and intended use, iterators may also provide additional operations or exhibit different behaviors. Since DEW is developed in the C and C++ languages, pointers are used as the iterators, and the data schema is described in terms of them. Since C doesn't have classes, objects will include instances of struct types.

With large amounts of data in active memory, data structure manipulation is a primary concern. A feature of the C/C++ language which has a significant impact on this problem is the pointer. A pointer is a variable that holds the address of an object or function. Pointers permit the construction of linked lists of objects in computer memory [31]. In DEW, pointers are used to access all data objects. Applications share circuit information via pointers, and also use pointers to manipulate data objects hidden inside the applications. A pointer may be thought of as a topological iterator in DEW, because it may be used to process the topology of the circuit.

In distribution systems, a single circuit model may contain thousands of components, and an entire system model consisting of hundreds of circuits may contain millions of components. With such large systems, modeling methods have a direct impact on the ability to perform engineering analysis. Using of pointers in linked lists allow system interconnects and equipment parameters to be directly available for analysis without complex search algorithms. Intrinsic in the graphical creation of the circuits is the creation of linked lists. The DEW memory model links together sources and components

of each circuit. In this way, it is possible to trace from circuit to circuit, through an individual circuit, or through a particular branch of a circuit.

Application programmers work with DEW defined objects. These objects are manipulated and accessed via iterators and indices into arrays of iterators. The pointers provided that pertain to component traces for reliability analysis are:

- Forward Iterator—forward direction for doubly linked list of circuit components
- Backward Iterator— backward direction for doubly linked list of circuit components
- Feeder Path Iterator —the feeder path iterator of a given component is the next component toward the reference substation that feeds the given component
- Brother Iterator — a given component's brother iterator points to the first component connected in its forward path which is not fed by the given component. (It is used to detect dead ends or physical jumps in connectivity.)
- Adjacent Iterator — a given component's adjacent iterator points to a component that is physically connected to the given component but has a different feeder path than the given component. (It is used to detect alternate feeds.)

Take the simple circuit in Figure 3.3 as an example:

- Component 1's Forward Iterator points to Component 2;
- Component 1's Backward Iterator points to Breaker B;
- Component 1's Feeder Path Iterator points to Breaker B;
- Component 1's Brother Iterator points to Component 2.

- Adjacent Iterators of all the components point to null, since there is no alternate feed for any of the components in this circuit.

Because of these contained links and iterators, each component's data object is known as a "trace" struct. A struct is C's and C++'s notion of a composite type, a data type that composes a fixed set of labeled fields or members. Struct is short for structure or, more precisely, user-defined data structure. Table 3.1 lists the elements in the component struct that are related to the reliability analysis module.

Table 3.1 Partial Component Struct Elements

Element Name	**Data Type**
Circuit number	Short integer
Substation number	Short integer
Equipment index number	Short integer
Component type number	Short integer
Component name	String
Forward Iterator (f)	Pointer to component
Backward Iterator (b)	Pointer to component
Feeder Path Iterator (fp)	Pointer to component
Brother Iterator (br)	Pointer to component
Adjacent Iterator (pAdjCmp)	Pointer to component
//…Elements added for reliability analysis module	

Segment Iterator	Pointer to component
Forward Segment Iterator	Pointer to component
Backward Segment Iterator	Pointer to component
Feeder Path Segment Iterator	Pointer to component
Primary Protective Device (ppd)	Pointer to component

Due to the large size of the trace structure, only the elements which are employed by the reliability analysis module are listed in Table 3.1. Several segment trace iterators are included in the structure. The Segment Iterator is used to find the primary sectionalizing device for a component. Sectionalizing devices in a circuit are linked in a doubly linked list via the Forward Segment Iterator and the Backward Segment Iterator. Sectionalizing devices are also linked with the Feeder Path Segment Iterator, which is similar to components are linked with the Feeder Path Iterator, except that only sectionalizing devices are in the linked list.

3.4.2 Graph Traces

Graph traces, also referred to as circuit traces, and are applied in determining the reliability analysis (RA) sets shown in Figure 3.4. Graph traces employ the topology iterators and linked lists discussed previously. Graph traces represent the order in which an algorithm processes the components of the system. As indicated earlier, a circuit

analysis program must efficiently manage large quantities of system and equipment data. The iterators and linked lists compact the data storage and reduce algorithm execution time.

Here we provide an overview of using graph traces. Figure 3.5 is an example circuit used to illustrate the application of circuit traces. Source S0 is the original source of the circuit of interest, and S1 is the alternate source. S1 is separated from the circuit of interest by the open

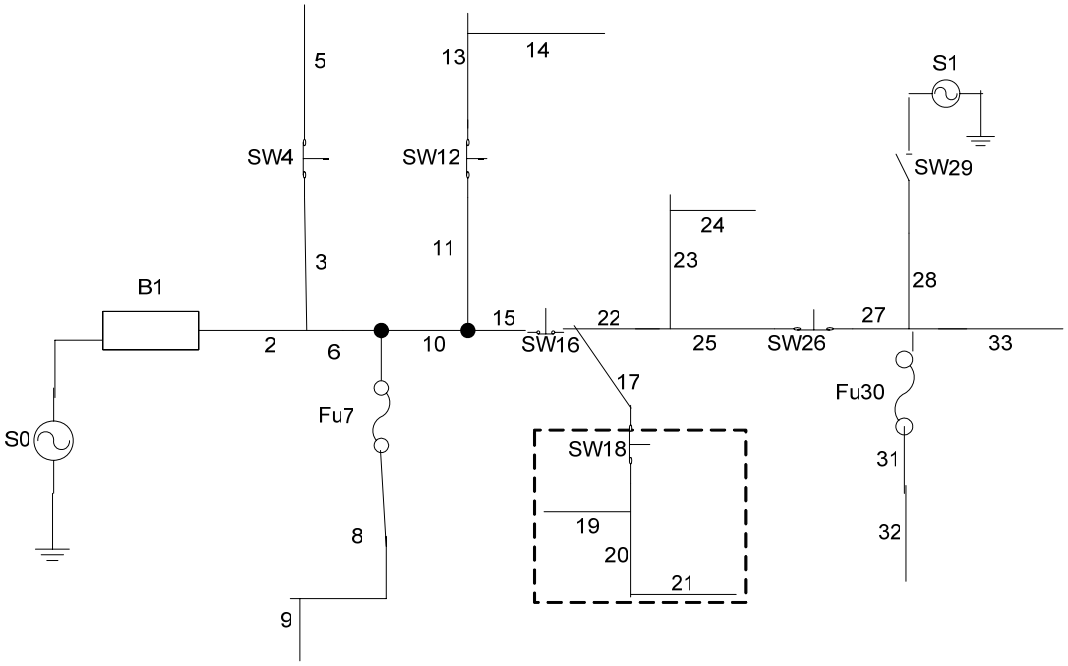

Figure 3.5 Sample Circuit

switch SW29. In Figure 3.5, only the sectionalizing devices are indicated with B (breaker), Fu (fuse) and SW (switch); and the rest of the components are represented by numerical symbol, which can stands for arbitrary component type, expect sectionalizing device.

Each graph trace represents a particular linked list tracing through the components of the circuit. We will apply five types of graph traces to construct the reliability sets. These traces yield five basic sets as follow:

FT_m = forward component trace beginning with component *m* (if *m* is not specified, FT begins from the substation). FT using the Forward Iterator in the example circuit is given by

$$FT = B1 \rightarrow 2 \rightarrow 3 \rightarrow 4 \rightarrow 5 \rightarrow 6\ldots\ldots \rightarrow 33 \quad (3.15)$$

BT_m= backward component trace beginning with *m* using the Backward Iterator, as illustrated by

$$BT_{15} = 15 \rightarrow SW14 \rightarrow 13 \rightarrow 12 \rightarrow SW11 \rightarrow 10 \ldots\ldots \rightarrow B1 \quad (3.16)$$

FPT_m = component *m*'s feeder path component trace using Feeder Path Iterator, as illustrated by

$$FPT_{15} = 15 \rightarrow 10 \rightarrow 6 \rightarrow 2 \rightarrow B1 \quad (3.17)$$

ECT = ending component trace using the Forward Iterator, here for the example circuit is given by

$$ECT = 5 \rightarrow 9 \rightarrow 14 \rightarrow 21 \rightarrow 24 \rightarrow SW29 \rightarrow 32 \rightarrow 33 \quad (3.18)$$

The circuit traces discussed above are basic circuit traces. For reliability analysis, it is more efficient to work with iterators to segments and to perform traces based on these iterators. The segment circuit traces used in this research are as follows:

FST_m = forward segment trace from segment ***m***, (if m is not specified, the forward trace will begin with the substation). In the example circuit, FST using the Forward Segment Iterator is given by

$$FST = B1 \rightarrow SW4 \rightarrow Fu7 \rightarrow SW12 \ldots\ldots \rightarrow Fu30 \quad (3.19)$$

$FPST_m$ = feeder path segment trace (It is performed relative to a given segment ***m***). For instance, if we trace from the segment of interest, segment SW18, $FPST_{SW18}$ with Feeder Path Segment Iterator is given by

$$FPST_{SW18} = SW18 \rightarrow SW16 \rightarrow B1. \quad (3.20)$$

AFT = alternative feed trace. In the example circuit, there is only one alternative source, so AFT is given by

$$AFT = SW29 \tag{3.21}$$

If there is more than one alternative feed for the circuit, then the AFT would consist of the linked list of all alternative feeds.

3.5 Computer Algorithm

This chapter presents the algorithm used to develop the reliability analysis (RA) sets. The algorithm is implemented with topological iterators and graph trace sets. A Graph Trace Analysis (GTA) notation is introduced. The GTA notation builds on the Object Constraint Language [32]. A software design for implementing the algorithm is also discussed. Along with the presentation of the algorithm, the example circuit illustrated in Figure 3.5 is used to explain the development of the RA sets.

The Object Constraint Language is used to specify constraints on objects in the Unified Modeling Language (UML). It has the power (but not syntax) of the Lower order Predicate Calculus (LPC) plus simple set theory. For instance, any query that can be expressed with the Structured Query Language [33] can also be expressed in OCL. GTA builds on OCL by adding assignment, topological iterators, and sets that result for the repeated application of the topological iterators. Since GTA uses the operator = for assignment, GTA also uses a different operator for equality than OCL, which is = =.

Graph Trace Analysis notation will now be introduced. Let v be a variable of Type T, and e (v) is an expression of v. R is an ordered set to contain the operation result.

R = C->select(v : T | e(v)), generates a collection by taking only elements referred to by the iterator *v* in *C* for which *e*(*v*) is true, and places these elements in the set R. Thus, v is an iterator that processes the elements of C in the order used by the iterator.

R = C->collect(v : T | e(v)), generates a collection made up of *e*(*v*) as *v* goes through the collection *C*, and places these elements in the set R.

C->iterate(v : T1 ; a : T2 = = e0 | e(v,a)) The variable *v* is the iterator, as in the definition of select above. *v* takes each value in the collection *C* in turn. The variable *a* is the accumulator. The *a* is initialized to the value *e0*. The *e(v,a)* is an expression that is repeatedly assigned to *a*. For example: *C->iterate(v, a=0 | a+=v).*

In what follows, we assume for the example circuit that the segment of interest is given by

$$\{\boldsymbol{S}\} = \{\text{SW18}\} \tag{3.22}$$

We first conduct a forward component trace, beginning with the substation, so that we can determine the SW set.

SW = FT -> select (p | p . bCmpTyp = = SD) (3.23)

where p is a component iterator, p . bCmpTyp is the component type introduced in Table 3.1, and SD stands for sectionalizing device. The expression (3.23) is read as the Forward Trace (FT) yields the SW set. For the example circuit,

SW = {B1, SW4, Fu7, SW12, SW16, SW18, SW26, SW29, Fu30 }

(3.24)

In the forward trace, we can also find the ending components that make up the EC set by using the following condition: if a component's forward iterator is the same as its brother iterator, then this component is an ending component. Thus,

$$EC = FT \text{ -> select (p | p. br = = p . f)} \tag{3.25}$$

Since IS consists of all the sectionalizing devices in the feeder path of ***S***, we can use a $FPST_s$ to obtain the IS set, as well as the PD (set of protective devices), as given by

$$IS = FPST_s \tag{3.26}$$

$$PD = FPST_s \text{ -> select (p | p. bCmpTyp = = pd)} \tag{3.27}$$

Where pd stands for protective device. For the segment of interest ***S*** in the example circuit,

$$IS= \{SW18, SW16, B1\} \quad (3.28)$$

$$PD = \{B1\} \quad (3.29)$$

The logic used to develop the L set is as follows:

Perform a FST. When the FST encounters a segment whose primary protective device belongs to the PD set, this segment is in the L set.

Otherwise, when the FST encounters a segment whose primary protective device does not belong to the PD set, the segment is not in the L set. Thus,

$$L = FST \text{ -> } select (p \mid p.\ ppd \in PD) \quad (3.30)$$

Where p-> ppd is the primary protective device listed in Table 3.1. Following this logic, we obtain the L set for the segment of interest ***S***

$$L= \{B1, SW4, SW12, SW16, SW18, SW26\} \quad (3.31)$$

The segments in the SSL set may be isolated from ***S*** and the original source, so that the power can be restored from the original source. SSL is given by the following set operations

$$SSL=L \cap NIS \quad (3.32)$$

where NIS= SW – IS.

Applying Equation (3.32) in the example circuit, and using expressions (3.24), (3.28) and (3.31), we obtain

$$SSL= \{SW4, SW12, SW26\} \tag{3.33}$$

The NSL set has only one component – the segment of interest ***S***. All the failed components in the segment of interest must be completely repaired before power can be restored to ***S***.

The segments in the SL set can be switched away from the segment of interest *S*, so that if the failure occurs in the SL set, *S* may be fed from an alternative source. The SL set is given by the following set operation

$$SL= L \cap IS – \{S\} \tag{3.34}$$

In the example circuit, applying expressions (3.22), (3.28) and (3.31), we obtain

$$SL= \{B1, SW16\} \tag{3.35}$$

If the failed component lies in the SAF set, it is possible to restore power to ***S*** when system constraints are not violated. The system constraints that are of interest here are the power handling capabilities of the equipment. Of particular interest is the remaining

power handling capability of each piece of equipment. In order to find the SAF set, we conduct feeder path segment traces both from an alternate source and the segment of interest ***S***, $FPST_{AF}$ and $FPST_S$, respectively. When these traces encounter a common path, then the SAF set is not empty. The SAF set includes the segments in the common path. Thus,

$$SAF = FPST_{AFT} \text{ -> select } (p \mid p \in FPST_S)$$

In the example circuit,

$$SAF= \{B1\} \tag{3.37}$$

The NSAF set includes all the segments for which it is not possible to restore power to *S* from an alternative source. All the failed components in these segments must be completely repaired before restoring power to ***S***.

The NSAF set is given by set operation:

$$NASF = SL – SAF \tag{3.38}$$

In the example circuit, using expression (3.35) and (3.37), we get

$$NSAF= \{SW16\} \tag{3.39}$$

The segments in the SF set may be isolated from ***S*** and an alternative source, so that power can be restored to ***S*** from the alternative source without violating system constraints.

The NSF set includes all the segments which may be isolated from ***S*** and an alternative source, but for which it is not possible to restore power to ***S*** because of system constraint violations. All the failed components in these segments must be completely repaired before power can be restored to ***S***.

To achieve the SF set, the power required by ***S*** must be compared to the smallest remaining capacity of the components along the feeder path from each of the alternative feeds in the set AF. If there is more than one alternative feed in the system, the minimum capacities encountered in the feeder path component traces FPT_{AF} for all the available sources in the AF set must be compared. For instance, there are n alternative feeds in the system. Let

C_{AFk} = minimum remaining component power capacity in the FPT_{AF} for the *k*th alternative feed, k =1, 2, 3 …n

(3.40)

$$C_{AFm} = \max_{k} \{C_{AFk}\}$$

(3.41)

Thus C_{AFm} represents the greatest minimum remaining capacity available among the alternative sources. For example, as demonstrated in Figure 7.1, there are two

alternative sources, AF_1 and AF_2. The segment of interest is marked as ***S***. As indicated in the figure, the power required by ***S*** is 5 KW. The numbers on the alternative feed components stand for the remaining capacity (units of KW) of the components.

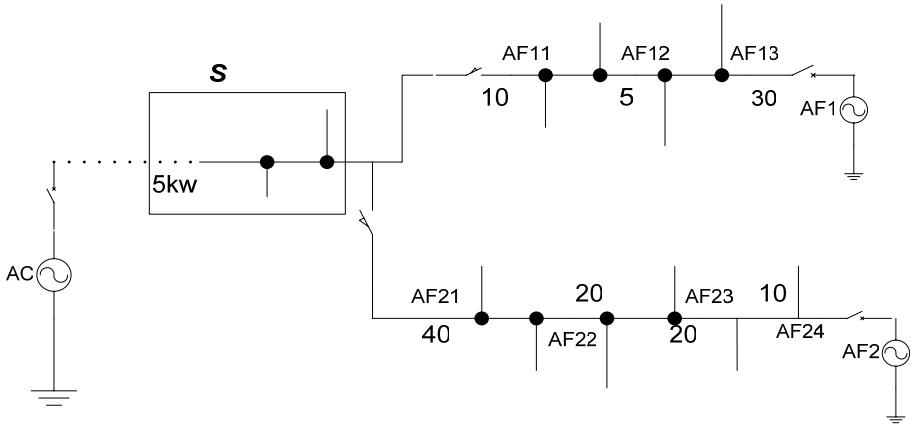

Figure 3.6 Illustrating Selection of Alternative Feed

According to Equation (3.40) and (3.41), we can obtain

$$C_{AF1} = \min \{10, 5, 30\} = 5 \quad (3.42)$$

$$C_{AF2} \min \{40, 20, 20, 10\} = 10 \quad (3.43)$$

$$C_{AFm} = \max \{ C_{AF11} , C_{AF21}\}$$

$$= \max \{5, 10\}$$

$$= 10 \quad (3.44)$$

So

$$AFm = AF_2 \quad (3.45)$$

Even though the minimum remaining capacity on the feeder path from AF_1 is equal to the required power in ***S***, pulling the power from AF_1 to ***S*** will fully utilize component AF_{12}. Thus AF_2 is chosen since it has more remaining capacity on the feeder path. In the general case, the segment of interest is not directly connected to the alternative feeds as shown in Figure 9. So FPT traces in the circuit of interest are also required to determine remaining power handling capabilities. In essence, component traces from the segment of interest to all alternative sources are required to check power handling capacities. To express the operations in terms of GTA, let pf[p] be a power flow algorithm array of results that may be indexed by iterator p. The attribute pf[p].Remain returns the remaining capacity in Amps for the circuit component referenced by the iterator p. Let AF_k be the kth component in the AF set. Thus,

$$\begin{aligned} &AF \text{ -> collect (} AF_k \text{ | } FPT_{AFk} \text{ ->iterate (p, } C_{AFk} = \text{LargeNumber |} \\ &\qquad\qquad \text{if p.Remain} < C_{AFk} \\ &\qquad\qquad \text{then } C_{AFk} = \text{p.Remain))} \end{aligned} \tag{3.46}$$

Then we can obtain C_{AFm} from (3.41), if C_{AFm} > the current load in ***S***, all the components in set SAF belong to set SF, otherwise, they belong to set NSF. In the example circuit, if C_{AFm} > the current load in ***S***,

$$SF = \{B1\} \tag{3.47}$$

$$NSF = \Phi \tag{3.48}$$

3.6 Reliability Index Calculations

This calculation relies on two general classes of information to estimate the reliability: component reliability parameters and system structure. Using system structure and component performance data, we can evaluate the reliability of specific load points or the whole distribution system. The structure information is achieved by the circuit traces presented previously. In the following paragraphs the performance data is discussed.

3.6. 1 Functional characterization

The availability of component functionally is characterized by the following indices:

- Annual Failure Rate = the annual average frequency of failure
- Annual Down Time = the annual outage duration experienced at a load point.

Predictive reliability techniques suffer from data collection difficulties. Simplifying assumptions (default values) are required for practical analysis of distribution systems. When this data is not available, default values are fetched from a table in the relational database which has generic average failure rates and repair times for each type of device.

The equivalent failure rate (FR) and equivalent down time (referred to as repair time, REP) can be obtained from equations (3.8) and (3.9), respectively.

3.6.2 Calculation of Reliability Indices Using RA sets

After finding the reliability analysis sets for the segment of interest ***S***, we can calculate the reliability indices. If there is only a single failure incident at a time, the failure rate and repair time can be calculated repeatedly for every segment contained in the set L, using equations (3.6) and (3.7). The down time for the segment $\boldsymbol{S}, DT_{S,w}$ is given by

$$DT_{S,w} = \sum_{\substack{i \in NSL, \\ NSAF, \\ NSF}} FR_{i,w} \times REP_i + \sum_{\substack{i \in SSL, \\ SF}} FR_{i,w} \times SOT_i$$

(3.49)

$$DT_S = \sum_w DT_{S,w}$$

(3.50)

SOTi = switch operation time to re-supply segment ***S*** due to the failure of segment ***i;***

FRi, w= Fri, w $\times P_w \times 365 \, {}^{days}\!/_{year}$

where Fri, w= expected failures per hour for segment ***i*** *under weather condition* ***w;***

REP_i= average repair time for a segment ***i***.

Pw = probability of weather ***w.***

Note that the reliability analysis algorithm presented here assumes that switch operations can always be performed faster than repairs.

The customer average interruption duration index (CAIDI) is sum of all customer interruption durations divided by total number of customer interruptions. CAIDI can also be viewed as the average restoration time. For a segment, it is the same as DT_s

$$CAIDI = DT_s \tag{3.51}$$

Once the predictive down time for each segment is calculated, and given the number of customers attached to each segment, the total customer down time, *DTC*, for a given circuit ***j*** can be calculated by

$$DTC_j = \sum_{i \in circuit} DT_i \times C_i \tag{3.52}$$

where C_i = the number of customers attached to segment ***i.***

Since the failure rate and down time are known at each segment on the feeder, the system index SAIDI (system average interruption duration index) for circuit ***j*** is then given by

$$SAIDI_j = \frac{DTC_j}{\sum_{i \in circuit} C_i} \tag{3.53}$$

In a distribution system consisting of multiple circuits, $SAIDI_{SYS}$, is defined as the average of SAIDI over all the circuits in the system.

$$SAIDI_{SYS} = \frac{\sum_{j=1}^{n} SAIDI_j}{n} \tag{3.54}$$

where n = number of circuits in the system.

3.6.3 Relative Reliability Index

A new measure of reliability, referred to as 'Relative_CAIDI' is introduced here. $Relative\_CAIDI_i$ helps to identify the areas that need reliability improvement. $Relative\_CAIDi_j$ is given by

$$Relative\ \_CAIDI_{\ i} = \frac{CAIDI_{\ ckt}}{CAIDI_{\ i}} \tag{3.55}$$

where

$CAIDI_{ckt}$ = average CAIDI for the circuit of interest

$CAIDI_i$ = CAIDI for segment ***i***.

Thus

If $Relative\_CAIDI_i = 1$, then the customers in segment ***i*** have the average reliability for the circuit of interest;

If $Relative\_CAIDI_i < 1$, then the reliability of the customers in segment ***i*** is less than average;

If $Relative\_CAIDI_i > 1$, then customers in segment ***i*** have reliability better than average.

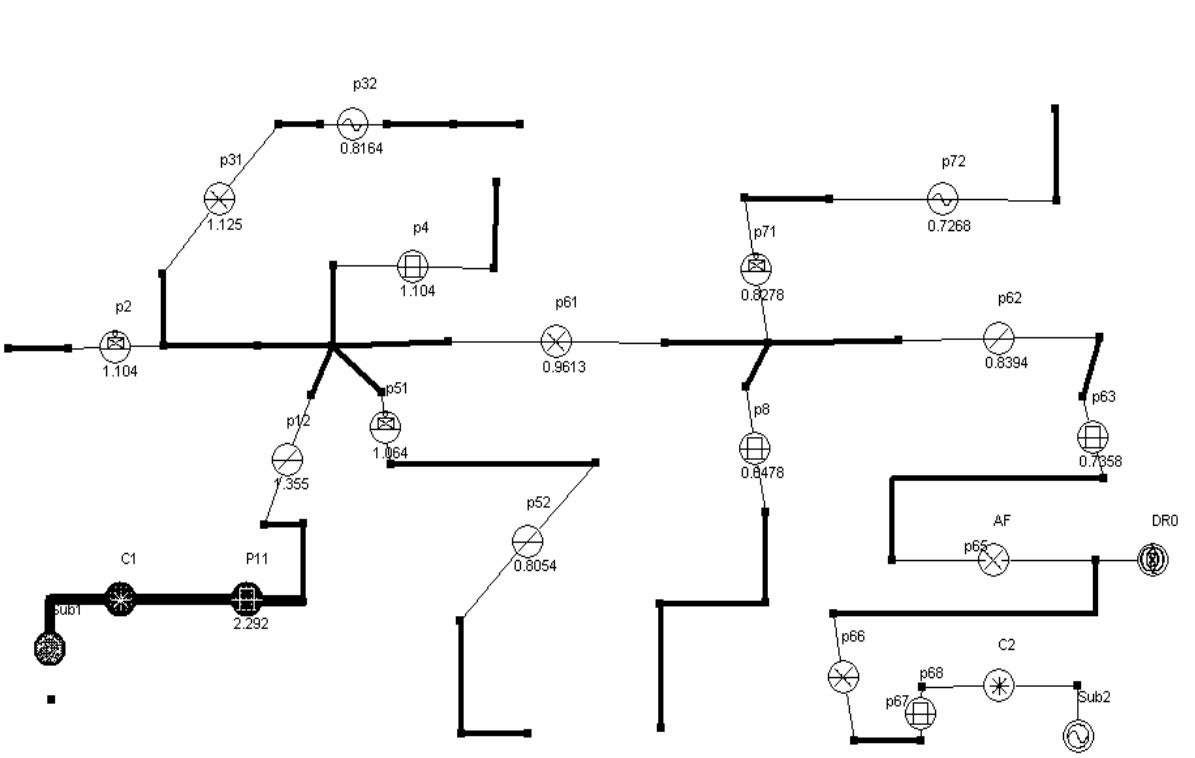

Figure 3.7 Example Circuit for Relative_CAIDI

Consider the two-circuit system shown in Figure 3.8 as an example. The Relative_CAIDI of each segment in circuit C1 is provided in Table 3.2. We can see segments such as P11, P12, P2, P31, and P4, have reliabilities greater than the average level of Circuit C1, while segments such as P52, P71, P72, P63, have reliabilities poorer than the average value.

Table 3.2 Relative_CAIDI of Segments in Circuit C1

Segment Name	Relative_CAIDI
p11	2.292
p12	1.355
p2	1.104

p31	1.125
p32	0.8164
p4	1.104
p51	1.064
p52	0.8054
p61	0.9613
p62	0.8394
p63	0.7358
p71	0.8278
p72	0.7268
p8	0.8478

In Figure 3.8, the *Relative_CAIDI* is also attached to each sectionalizing device for that segment. This makes it easier to observe that the components close to the power source (or substation in this case) have better reliability than the components approaching the end of the circuit.

3.6.4 Dependency Diagram

There are several algorithms incorporated in the reliability assessment and the dependency among these algorithms is exhibited in Figure. 3.9. From Figure. 3.9 note that any algorithm in the dependency chain depends upon all the algorithms below it in the chain. Thus, Reliability depends upon Load Estimation, as does Power Flow. Each algorithm has its specific responsibilities, as defined below:

Reliability Algorithm Responsibilities = to fail component k (only single failures are considered) and to calculate segment, circuit, and system reliability indices for system configurations where constraints are checked by Power Flow and Protection-Coordination [34, 35]. Reliability also sets the time point t for analysis.

Restoration Algorithm Responsibilities = given a failed component k, perform switching operations to isolate the failed component to a minimum outaged region and then determine switching operations to restore the maximum power possible without violating constraints as calculated by Power Flow and Protection-Coordination [35].

Protection-Coordination Responsibilities = given a failed component k and a switching configuration, insure that system protection works [36].

Fault Analysis Responsibility = given a failed component k and a switching configuration, calculate fault currents for all types of possible faults due to the failed component.

Power Flow Responsibilities = given a switching configuration, a failed component k, and loading at time t, check to see if all loads can be supplied while satisfying all constraints on voltage, current, and power flow values.

Load Estimation Responsibility = determine loading at time t.

Thus, Reliability fails a component and then requests Restoration to find a switching configuration that maximizes power restoration while maintaining system constraints. For some proposed restoration configuration, Restoration delegates the checking of system constraints to Power Flow and Protection/Coordination. Note that in the study presented here, the checking of the Protection/Coordination constraints was not performed. However, it is included in the formulation of the problem for completeness.

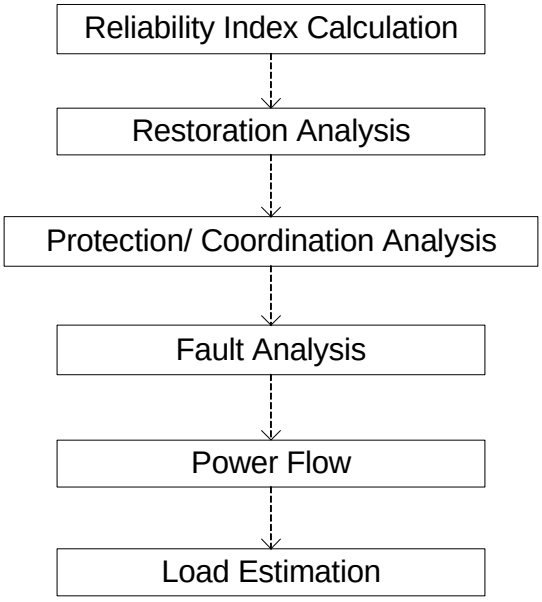

Figure 3.8 Dependency Diagram

3.7 Reconfiguration for Restoration Algorithm

Figure 3.9 indicates the dependency between reliability index calculations and restoration analysis. Even though there is no restoration analysis actually performed, a restoration plan is assumed during the process of developing the reliability sets, considering possible alternate feeds such that system constraints are not violated.(In this research, line section overloads and 6% below nominal voltage are regarded as constraint violations.) This approach to the reliability analysis provides a rapid assessment for system reliability that may be used to compare various configuration plans. However, this approach has its limitation. The approach is based on the assumption that there is only a single failure at a time, as indicated in section 3.6. When system reliability needs to be evaluated more closely, multiple failures should be taken into account, and an actual reconfiguration for restoration analysis should be carried out as part of this assessment.

In this work, a research effort has been devoted to developing a reconfiguration for restoration program. The results of this effort are described in this section.

3.7.1 Introduction

Distribution reconfiguration studies may be divided into following:

- Capacitor placement
- Network reconfigurations
- Voltage and reactive control
- State estimation
- Distributed generation placement
- Service restoration

In this research, service restoration is the major concern. Service restoration aims at minimizing service downtime to out-of-power loads during post fault conditions by using sectionalizing devices. The service restoration problem is a combinatorial, nonlinear, and constrained optimization problem, and as a result is hard to solve. As the number of the switches increases, the number combinations of possible switch operations increase exponentially. In the past, considerable efforts have been put into the subject of service restoration in electric power distribution system. Approaches to solving the problem include heuristic algorithms [37][38], expert systems [39], fuzzy inference [40] and genetic algorithms (GA) [41]. It should be noted that all these methods except GA may converge to a locally optimal solution.

The GA approach is based on concepts of natural selection from biology. A set of solution candidates called populations are prepared to perform a multi-point search. GA makes use of genetic operators such as cross-overs and mutations within the population to create a better solution. The genetic operators are controlled by probability to keep the diversity of solution candidates.

As opposed to the above approaches that solve the combinational problem, the author has created a reconfiguration algorithm in terms of graph trace analysis, which seeks the reconfiguration solution from topology characteristics of the network itself. This new algorithm is more efficient than GA and other combinatorial algorithms in terms of computational efforts, and holds the potential for real-time reconfiguration for restoration solutions. Another major advantage of this new algorithm is it can tackle a system with loops, which is neglected in most reconfiguration algorithms.

3.7.2 Reconfiguration/Restoration Using Graph Trace Analysis

The main objective in this restoration algorithm is to restore as many loads as possible by transferring de-energized loads via network reconfigurations to sources without violating operational constraints such as specified in the beginning of Section 3.7. The proposed algorithm is carried out at follows:

Step 1. Create the set of failed components, FC, as follows

$$FC = FT \text{ -> select (p| p.fStatus = = FAIL)} \tag{3.56}$$

Where fStatus is an attribute of the iterator p that represents the operational status of a component.

Step 2. Isolate the failed components.

Let Pf be a failed component (to be isolated) and STO be a set of isolating devices to operate.

STO_1= FPT_{Pf} -> select (p| p. bCmpTyp = = SD and p. ms = = UNLOCKED ,

quit when STO_1 ! = Φ). (3.57)

where ms represents the movable status of a component and p. bCmpTyp = = SD is the same condition as in (3.23).

Assume pO is the component contained in STO_1, then

STO_2= FT_{pO}-> select (p| p. bCmpTyp = = SD and p. ms= = UNLOCKED,

if p. sd = =true and p. ms= = UNLOCKED

then p = p. br,

quit when p. f = = pO. br then) (3.58)

STO3= STO2-> select (P| null != (FTP -> select (P'|P'.adjCkt != null,

if P'.f == P.br

then quit))) (3.59)

$STO = STO_1 \bigcup STO_3$ (3.60)

STO -> collect (p | p. fSectDev = OPEN) (3.61)

Step 3. Search for candidate alternate feeds.

Let CAF be the set of candidate alternate feeds, which is referred to by the open tie switches on the feeders.

CAF = FT -> select (p | p. bCmpTyp = = SD and p. fSectDev = = OPEN

and p. ms= = UNLOCKED) (3.62)

where fSectDev stands for the status of a sectionalizing component.

Step 4. Search for a sectionalizing device that has voltage on only one side from the candidate list.

Let PSD be the set of sectionalizing devices the have voltage on only one side, then

PSD = CAT -> select (p |

p. fp. fLostPrw = = TRUE and p. pAdjCmp. fLostPrw = = FALSE

or p. fp. fLostPrw = = FALSE and p. pAdjCmp. fLostPrw = = TRUE

quit when PSD != Φ) (3.63)

where p. pAdjCmp the Adjacent Iterator that introduced in Table 3.1.

p. fLostPrw stands for loss of power status.

Step 5. perform a feeder path trace from the selected sectionalizing device and form a list of segments to drop. In case the available power supplies are not sufficient to restore the whole out-of-service areas, then this list will be used to drop segments in an attempt to retore part of the outaged area. The trace stops when it encounters a transformer or when it finds a component that does not lose power.

Let SegTD be a set of segments to drop, and pSD be the component contained in the set PSD.

if PSD = = Φ then exit the program;

if PSD ! = Φ

then SegTD = FPT_{pSD} -> select (p | p. bCmpTyp = = SD,

if p. bCmpTyp = = TN or p. fLostPrw = = TRUE

then quit) (3.64)

where TN is transformer.

The transformers are sought because if there is a reverse current through a transformer, then the voltage on the primary side will generally be significantly reduced from its nominal value, due to the large impedance reflected to the primary side.

Step 6. Close the selected sectionalizing device, and run the power flow simulation. If the power flow can not converge, drop one segment at a time from the list of segments to drop until the power flow converges.

PSD -> collect (p | p . fSectDev = CLOSED) (3.65)

SegTD -> iterate (p, p . fSectDev = CLOSED |

if power flow dose not converge

then p . fSectDev = OPEN

if power flow converges

then LSeg = p and quit) (3.66)

where LSeg is the last segment that can be restored from the alternate feed. The upstream of LSeg will remain out of service because the alternate feed does not have sufficient supply margin to restore the entire area.

Step 7. Feeder path trace from the last segment restored, where VL is the set of components that have violations.

$$VL = FPT_{LSeg} \text{ -> select (p | pf [p] . ReCap < 0 or pf [p] . CusVolt < Min or pf [p] . CusVolt > Max)} \quad (3.67)$$

where pf [p] . ReCap is the remaining capacity of a component and is equal to the component rating minus the current going through the component;

pf [p] . CusVolt is the customer voltage of a component; Min and Max are the lower and upper limits on customer voltage, respectively. If VL is not empty**,** let pVL be the first component in set VL.

$$ESeg = FT_{pVL} \text{ -> select (p | p . br = = p . f, if p. f = = pVL . br then quit)} \quad (3.68)$$

Step 8. Repeatedly perform load shedding on the segment with the lowest priority and smallest load, one at a time, until no violations occur. Let pLS be an iterator corresponding to the segment that has lowest priority and smallest load among the set of ending segment found in step 7.

8.1 ESeg -> iterate (minP = H, minL = L, pLS = NULL |

if p.dLdPri < minP

then minP = p.dLdPri ,

if p.dLdPri = = minP

then if pf[p].dLoad < minL

then minL = pf[p].dLoad and pLS = p) (3.69)

where H is highest load priority in a system, and L is an extremely large number, which is certainly larger than the smallest load of all ending segments.

8.2 ESeg-> iterate (p, p. fSectDev = CLOSED |

if p = = pLS

then p . fSectDev = OPEN and

if (pf [pVL] . ReCap > 0 and

Max > pf [pVL] . CusVolt > Min)

then quit

else p . fSectDev = CLOSED and p = p. Segfp) (3.70)

Repeat step 8.1 and 8.2 until meet the condition to quit. And repeat step 7 and step 8 until set VL is empty.

Step 9. Go to step 4.

3.7.3 Application

This GTA reconfiguration algorithm simulates practical restoration procedures considering the distribution network constraints, which will enhance the accuracy of reliability analysis. This reliability analysis is conducted in three steps. First, contingency enumeration technique, such as combination selection screening, Monte Carlo state sampling method [42] and so on, is used to determine system states. Second, for each contingency case, the GTA reconfiguration program is applied to each to determine the number of customers that lose power due to faults and equipment failures. Then the reliability index like SAIDI, CAIDI can be summed up for the simulation period. Opposed to the GTA reliability set method presented in section 3.3-3.6, this approach takes a much longer time due to the larger number of contingency cases and larger number of power flows needed to run to check for system violations. However it provides a reliability assessment that is closer to reality, which is critical to utilities who must maintain their system to meet reliability standards.

CHAPTER 4 RELIABILITY IMPROVEMENT

Power delivery systems are subjected to abnormal operations caused by events such as accidents, component failures, and weather conditions. These events are random and are beyond the control of man. Such random events can be taken into account in designing a system that can sustain certain levels of disturbances.

How much should be invested in improving reliability? It will never be possible to make the system 100% reliable. A decision has to be made to accept a certain level of risk. In this decision-making process, quantitative reliability evaluation is the basis. On the other hand, this process is more than reliability evaluation, and it involves technical, economic, and environmental assessments.

In this research, we assess both the effectiveness and economic impacts of the reliability improvement methods that we address.

4.1 From component statistics point of view

First of all, from the component statistics point of view, component failures can be reduced by replacing aged components, especially those entering their wear out stage. This measure requires accurate statistical data. And there is the chance that equipment, such as transformers, can function for many years beyond their expected lifetime. Therefore, a replacement policy to improve reliability may be effective, but costly, to implement.

Looking at statistical data associated with equipment failure rates is sometimes not good enough. As mentioned in Chapter 2, equipment failures can be linked to other

external factors that may affect failures more than aging. Table 4.1 shows the failure rate in summer storms obtained by a utility company from analyzing ten years worth of outage data. From the table it may be seen that lightning contributes to 67.5% of the failures, which is much larger than the failures due to aging.

Table 4.1 Summer Storm Component Failure Rates (a)

Component Type	Transformer			Switch		
Cause	Tree Contact	Equipment Failure	Lightning	Tree Contact	Equipment Failure	Lightning
Number of Failure	4	5	144	11	6	5
Total Number of components	24779			1577		
Storm Failure Rate	0.000040	0.000050	0.00144	0.00095	0.00052	0.00043

Table 4.1 Summer Storm Component Failure Rates (b)

Component Type	Line & Cable			Fuse		
Cause	Tree Contact	Equipment Failure	Lightning	Tree Contact	Over Load	Lightning
Number of Failure	285	10	344	2	1	180
Total Number of components	795.30 (miles)			5591		
Storm Failure Rate	0.0896/per mile	0.0031/per mile	0.1081/per mile	0.00036	0.00018	0.032

Environmental conditions may be taken into account to perform effective reliability analysis. As indicated in equation (3.38), component failure rates need to be calculated

for different weather conditions. In this research, we also develop reliability parameters, like outage density, cumulative outages, based on different weather conditions to help outage management and reduce customer downtime. These reliability parameters are presented in Section 4.3, which addresses the analysis of storm data.

4.2 From system configuration point of view

From the system configuration point of view, setting up redundant paths is a common method of improving reliability. However, it is also commonly recognized that in most cases utilities cannot financially justify idle redundancy. So, the goal is to find some means to configure the system (flexible enough) so that alternative power supplies are available for use during contingencies without having dedicated backup power supply facilities. In this chapter, the reliability analysis approach discussed in Chapter 3 is applied to evaluate the reliability of different configurations.

In the analysis considered here, the GTA reliability evaluation method assuming single failures is used to compare alternative designs and configurations.

4.2.1 Reliability Improvements with DGs

A. Introduction

DGs sometimes provide the most economical solution to load growth. Low voltages or overloads that are created by load growth may only exist on a circuit for a small number of hours per year. There are many locations within the troubled circuit, or even in neighboring circuits, where a DG may be located to provide control needed to

eliminate the low voltage or overload. We assume that it has already been justified that a DG provides the lowest cost solution to a circuit problem and is to be installed to provide the needed control. The question that we seek to answer is "What is the best location in the system to add a DG?" Many DGs are currently placed in or near the substation, probably due to convenience of installation. However, placing DGs further out on the circuit can lead to improvements in losses, reliability, or both.

One of the criteria to find the optimal DG location is minimizing power loss. Several papers have been published that address the use of artificial intelligence algorithms to optimize DG placement [43-48] based on minimizing power loss. [43] solves the problem by an exhaustive algorithm, [44] employs the tabu search method, [45] uses a fuzzy genetic algorithm, and analytical approaches are presented in [46]. Other papers consider the cost of power interruptions [47] and minimizing peaks [48], but power loss minimization is still the base strategy employed.

All the simulations performed in [43-48] address a static load condition. Placing DGs to minimize loss based upon a single load point, such as the peak load, may not provide the same optimal solution as when the entire time-varying load pattern is considered. In this work time-varying loads are taken into account.

System load and additional generation (provided by DG) affect the system reliability. For a given case study, this work provides a comparison of the optimum reliability location with the minimum loss location. Similar to [43], an exhaustive search is applied. The manner in which these locations vary as a function of time-varying loading is considered. Differences in efficiencies and reliabilities of the two optimum

solutions are compared. A cost analysis is performed relative to the differences in efficiencies.

We assume here that a DG can be brought on line after the segment to which it is connected is switched to an alternate feed.

B. Reliability as a Function of Load

From equations 3.38 to 3.43, we can see that once a system is given, the number of customers and the number of circuits are constant, and so SAIDI is determined by the down time ($DT_{S,w}$). From equations 3.38 to 3.43, we can calculate SAIDI for a system under a given load condition. If the load condition changes, the elements of some of the reliability sets may change, which would then yield a different $DT_{S,w}$. Thus, we may get a different value of estimated SAIDI for a different load condition. Considering load condition ***l***, equations 3.38 - 3.43 become

$$DT_{S,w,l} = \sum_{\substack{i \in NSL, \\ NSAF, \\ NSF}} FR_{i,w} \times REP_i + \sum_{\substack{i \in SSL, \\ SF}} FR_{i,w} \times SOT_i \tag{4.1}$$

$$DT_{S,l} = \sum_{w} DT_{S,w,l} \tag{4.2}$$

$$DTC_{j,l} = \sum_{S \in circuit} DT_{S,l} \times C_S \tag{4.3}$$

$$SAIDI_{j,l} = \frac{DTC_{j,l}}{\sum_{S \in circuit} C_S} \tag{4.4}$$

$$SAIDI_{SYS,1} = \frac{\sum_{j=1}^{n} SAIDI_{j,l}}{n} \tag{4.5}$$

The relationship between reliability and load can be demonstrated with the example system shown in Figure. 4.1.

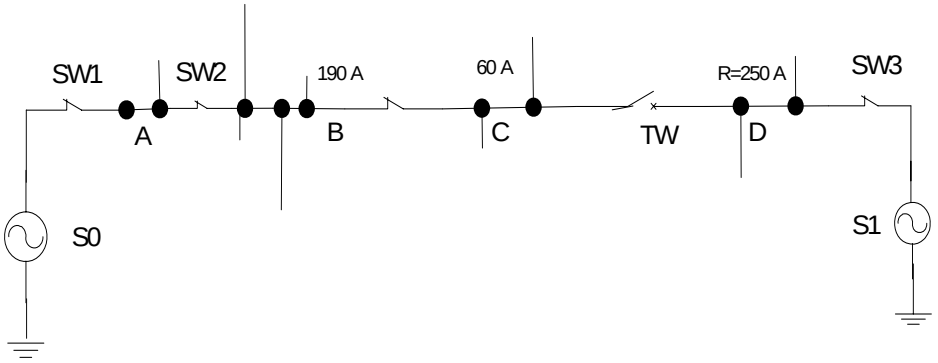

Figure 4.1 Example System

Circuits S0 and S1 are connected by the tie switch TW. Let us consider loading in terms of the current flow in the selected line sections, where all line sections are operating at the same voltage level. Line D is the line that has the least spare capacity in the feeder of S1. When line D has a load of 280 A, its remaining capacity is 250 A. The currents in lines B and C in circuit S0 are 190 and 60 A, respectively. Under this load condition, if A has a fault, it can be isolated by opening SW1 and SW2, and then the load in lines B and C can both be restored by closing TW. This is because S1 has plenty of spare capacity. When the load of D increases to 360 A, the remaining capacity of Line D

becomes 170 A. Assuming the load of S0 remains constant, if the same contingency occurs to S0, only the load of Line C can be picked up by its adjacent circuit without violating the current constraint. Under this new loading condition, all the segments in B's SF set move to its NSF set, and the expected down time of segment B increases, so SAIDI increases accordingly. Assume the load of S1 continues to increase. When the load reaches 500 A, the remaining capacity of Line D drops to 30 A, and then S1 cannot restore the load of either Line B or C. All the segments in C's SF set move to its NSF set, the expected down time of segment C increases, and SAIDI increases. Evaluating SAIDI under these three loading conditions

$$SAIDI_1 < SAIDI_2 < SAIDI_3 \tag{4.6}$$

where

$SAIDI_1 \Rightarrow (load_D < 340\ A)$

$SAIDI_2 \Rightarrow (340\ A < load_D < 470\ A)$

$SAIDI_3 \Rightarrow (load_D > 470\ A)$

Thus, SAIDI is a function of load. If we plot SAIDI against the load of S1, SAIDI increases (reliability decreases) in a stepwise fashion as the load increases. Practically, both of the loads in circuits S0 and S1 change with time, so the reliability of the system actually relates to the loading of both circuits.

C. Reliability as a Function of DG Location

As indicated in the above, $SAIDI_{SYS,l}$ depends upon $DTC_{j,l}$, which essentially is determined from the reliability sets. When a DG is added to a system, the elements in the SF and NSF sets may change. Seeking an optimal DG location for a given load condition L, the objective function becomes a function of DG location.

$$\min\{ SAIDI_{SYS,l}(DG\_Loc_{i,z})\} \tag{4.7}$$

where $DG\_Loc_{i,z}$ is the location of the DG for a given DG size ***z***, subject to the following constraints:

Protection works in the new configuration [34]. Note that the system configuration may change due to switching operations performed during the restoration.

Switching operations do not cause any under voltages, overloads or unbalanced conditions that exceed system limits.

Since we search the optimal location based on segments, $DG\_Loc_{i,z}$ represents the ***i***th segment in the system. To maximize the system reliability, we use an exhaustive search to seek the DG location that leads to the minimum for a given load condition and a given DG size.

D. Analysis Procedure

The procedure to determine the optimal location to place a DG in a system is given as follows.

Use load research statistics to determine the system hourly loading over some time period and plot the load versus hour of day curve.

Divide the load curve into different windows such that the loading in each window is relatively constant. These windows will be referred to as load windows, where in the analysis the loading condition in each load window is represented with a constant.

Corresponding to each load window, adjust the maximum allowable DG output to prevent back feed to the substation.

Corresponding to each load window, perform an exhaustive search over all segments to obtain the optimal DG placement location. This exhaustive search is performed once for the minimum loss criteria and again for the minimum SAIDI criteria.

For the specific case study considered, the optimum DG location for minimum loss is compared with the optimum location for minimum SAIDI. Also, we simulate that a DG may be brought back into service after a fault is isolated (if the DG is not in the failed segment).

E. Case Study

From previous work [49] we note that placing distributed generators further out on a circuit, instead of locating them at the substation, can help enhance a system's reliability. Also, from the same work we note that the reliability of a system may vary as a function of the time-varying load. In general, the system reliability may decrease as the loading increases. In the case study presented in this section we further investigate how DG placement affects system reliability and also power loss reduction. The placement of only a single DG is considered.

The system shown in Figure 4.2 consists of three interconnected circuits named C1, C2, and C3. These three circuits are supplied by substations named Sub1, Sub2 and Sub3, respectively. Along with the substation and circuit names, names of segments are also depicted in Figure 4.2. Segment names of particular interest that will be discussed are highlighted with ovals.

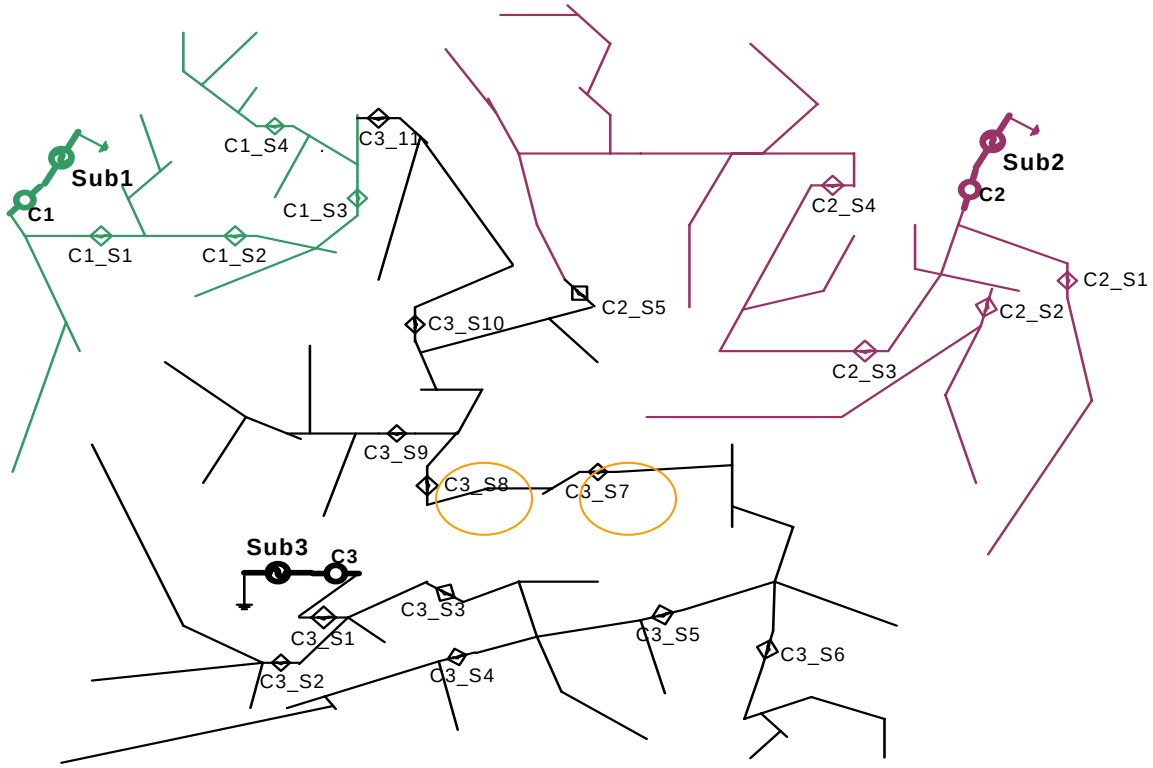

Figure 4.2 Three-Circuit System Used for Analysis

This system supplies two types of residential customers and one type of manufacturing customer. Different types of customers have different load patterns. Relevant features of the loads supplied by the individual circuits are listed in Table 4.2.

Table 4.2 Loading Features of the Three Circuits Shown in Figure. 4.2

Circuit Name	Peak Load Period	Peak Load (kW)
C1	6:00pm~7:00pm	8308
C2	7:00pm~8:00pm	9386
C3	10:00am~11:00am	11707

Figure 4.3 shows the daily load curves for a January week day for the individual circuits and the entire system. For the purposes of presentation here, time points 3am, 6am, 12pm and 6pm are selected for presenting results from both the reliability and power loss calculations. These time points are representative of four loading conditions, which are minimum load, medium load, normal work hour load, and maximum load, respectively. The DG output is adjusted as a function of placement and the time-varying loading condition so that the generation output is kept within 10-20% of the system load. This operation of the DG is to insure that reverse power flows into the substation do not occur, and also such operation does not interfere with circuit protection. Over these placements and loading conditions, the DG is operated at 1800 kW and 4750 kW, as indicated in Table 4.3.

Table 4.3 Output of DG at Various Time Points

Time point	3am	6am	12pm	6pm
DG Output (kW)	1800	1800	4750	4750

For the reliability calculations, switch operation times are assumed to be 1 hour. The device failure rates and repair times used in this analysis are listed in Table 4.4. The failure rates for the line sections (line, cable) in each circuit are indicated in Table 4.5.

Table 4.4 Device Failure Rates and Repair Times

Component Type	Failure Rate (Failures/Yr)	Average Repair Time (Hr)
Substation	0.1	5
Network Protector	0.001	5
Cable, Station Pole	0.001	5
Sectionalizing Device (switch, fuse, recloser, breaker)	0.001	5
Transformer	0.01	5
Voltage Regulator	0.01	5
Capacitor Bank	0.01	5
Arrester	0.001	5

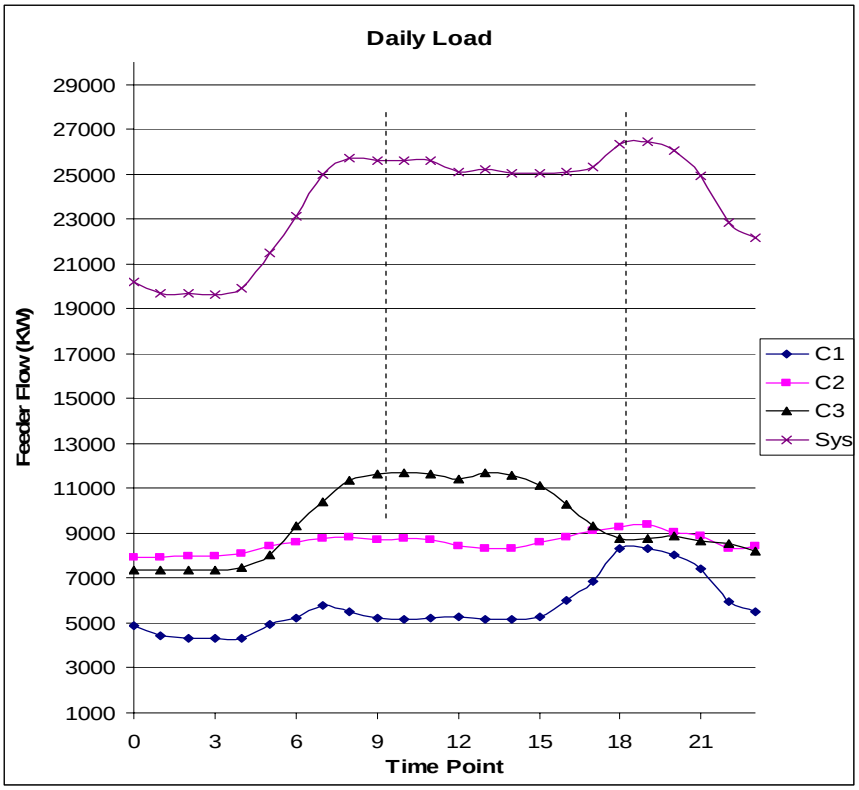

Figure 4.3 Time-varying Circuit and System Loading

Table 4.5 Line Section Failure Rates and Repair Times

Circuit Name	Line Section Failure Rate (Failures/Yr/1000Ft)	Line Section Repair Time (Hr)
C1	0.1	5
C2	0.01	5
C3	0.06	5

F. Analysis Results

In evaluating DG placement for optimum losses and reliability, an exhaustive search is performed. The DG is tried on each segment of all three circuits shown in Figure. 4.2. For every location evaluated, the total power loss and system reliability indices are computed. Power losses as a percentage of the total system power and percentage improvements in SAIDI are also calculated.

Working in terms of segments, the exhaustive search runs fairly fast on the example test system. A PC (Pentium 4 CPU 2.40GHz, 512MB of RAM) can finish the exhaustive search for a single time point in 90 seconds. Approximately 60 seconds is required for the reliability optimization and 30 seconds for the minimum loss. The reliability optimization takes longer because in checking for low voltages and overloads it has to run more power flow computations than the minimum loss calculation.

There are several reasons why an exhaustive search is used instead of a more complex optimization algorithm. First, the exhaustive search is easy to program. Second, the exhaustive search does run fairly fast for the problem considered. Third, in our work we wanted to insure that the global optimum location is found, and due to the nonlinearity of the problem, many optimization algorithms may become trapped at a local optimum,.

Table 4.6 shows optimum locations found for the four different load conditions - 3am, 6am, 12pm, and 6pm. It should be noted that the DG would not normally be operated at the light load conditions, such as 3am. However, there is still a reliability improvement available due to the DG at the light load condition. In Table V, the first column under each loading condition (or time point) shows the segment location for the best reliability

improvement. Thus, at 3am the DG should be located on segment C3_S8 for a reliability improvement of 20.96% with corresponding system losses of 4.23%.

The second column under each loading condition shows the location for the minimum power loss. Thus, at 3am the DG should be located on segment C1_S4 for a minimum loss condition of 4.14% and a reliability improvement of 10.18%.

The third column under each loading condition shows the differences in either system losses or reliability improvements between the optimum locations for reliability and loss. Thus, at 3am there is only a 0.09% difference in the losses and a 10.78% difference in the reliability improvements between the two placements.

Table 4.6 DG Effect on System Loss and Reliability in Locations for Optimal Loss and Optimal Reliability Shown at Various Time Points

Time point	3am			6am			12pm			6pm		
DG Location	C3_S8	C1_S4	diff	C3_S10	C1_S4	diff	C3_S8	C3_S7	diff	C1_S4	C1_S4	diff
System Loss (%)	4.23	4.14	0.09	5.26	4.19	1.07	4.35	3. 90	0.45	3.81	3.81	0
SAIDI Improvement (%)	20.96	10.18	10.78	21.61	19.60	2.01	32.16	25.63	6.53	19.60	19.60	0

From the Loss Reduction Point of View

Moving the DG away from the substation along the main feeder path, the system power losses improve up to a point. Table 4.6 shows a trend that the system loss percentage becomes less when the system has a higher loading. This is due to the DG supplying more power at the higher load conditions, as shown in Table II. Thus, more power supplied from the DG leads to reducing the system losses at the higher load levels.

For minimum loss, the DG should be placed in segment C3_S7 at 12 pm and in segment C1_S4 at 3am, 6am and 6pm. Since the system load does not change much during normal working hours (7am-5pm), the optimal DG location for 12pm also holds good for the period from 7am to 5pm, and this turns out to be the optimal location when the losses over the entire 24 hour load curve are considered.

From the Reliability Point of View

Simulation results obtained here support the conclusions of previous research [49]. In the previous work it was noted that placing a DG further out on the circuit as opposed to siting it near the substation can result in improvements in reliability.

As explained previously, if a circuit has tie switches with its adjacent circuits, the availability of an alternate source for the circuit depends on the spare capacity of the adjacent circuits. System reliability changes as a function of system load. This relationship is illustrated in Figure. 4.4. In Figure. 4.4, the Y-axis shown on the left hand side shows the total system loading, and the Y-axis on the right hand side shows the system SAIDI. Both the system loading and reliability are plotted as a function of time in the figure. The system reliability changes with the system loading in a step wise fashion. Note that the increase of SAIDI indicates a decrease of the system reliability. As seen in the Figure.4.4, as the system loading increases, the system reliability decreases.

In the previous work it was noted that applying a DG helps to enhance system reliability more during light load periods than during heavy load periods when all circuits in the system have the same loading pattern [49]. However, from Table 4.6 we notice that in this case study, the greatest reliability enhancement by the DG appears at 12pm,

when system load is heavy, but not yet at the maximum. At 12pm, siting the DG in segment C3_S8, SAIDI is improved by 32.16%. The reason for this improvement will now be explained.

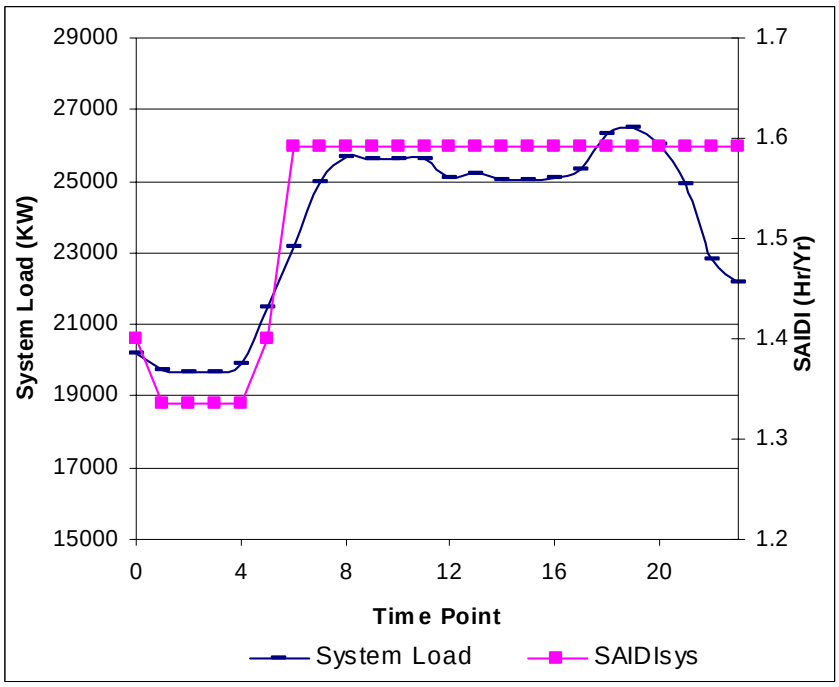

Figure 4.4 Change in SAIDI with Changing System Load

The three-circuit system considered here is populated with multiple customer types, which results in different loading patterns in the different circuits. At 12pm, the load is heavy from the system standpoint. However, if we look at the load curves of each circuit at 12pm, we will notice that circuit C3 is heavily loaded, but circuits C1 and C2 still have modest remaining capacities. Therefore, with the application of a DG in C3, the ability of C3 to re-supply power to C1 or C2 when contingencies happen in C1 or C2 increases. Furthermore, since C1 and C2 are only modestly loaded, they have an ability to re-supply power to portions of C3 in case of a contingency. Consequently, SAIDI is dramatically

improved by the DG placement under such a heavy system loading condition. Hence, if a system consists of multiple types of customers, which result in different loading patterns in each circuit, adding a DG may have the largest improvement in reliability during high demand periods.

Table 4.6 also indicates that depending on the load condition, the optimum DG locations for minimizing losses and for maximizing reliability could be in proximity or far apart. As shown in Table 4.6, during the light load period, such as 3am and 6am, the DG locations for minimizing losses and for maximizing reliability are quite different (for example, C3_S10 for reliability and C1_S4 for losses at 6 a.m.) . However, during the heavy load period (12pm and 6 pm), the optimum DG locations are very close to each other (for example, C3_S8 and C3_S7 at 12 p.m.). In the light load period, each circuit has plenty of spare capacity. With the flexibility provided by the spare capacity, the location where the DG is most needed for reliability improvement is not necessarily related to the DG location that helps to reduce the power losses. During the heavy load period, the heavily loaded circuit has little or no spare capacity. Under such a condition, adding the DG creates some spare capacity in the distribution circuit and improves reliability by shifting more elements into the SSL and SF set. At the same time, the addition of the DG reduces the need for power transmission and consequently the losses are also reduced.

How much spare capacity is created is now related to how much losses are reduced. During the heavy load period, the best DG locations for improving reliability and the best DG locations for reducing losses tend to be close to one another. This effect is even more

pronounced when the DG is operated at a higher output level as in this case (4750 kW at 12 p.m. versus 1800 kW at 6 a.m. as shown in Table 4.3).

With the support of a DG, an alternate source from a neighboring circuit may restore power to part of the load in the failed circuit without violating constraints. This reduces the duration of interruptions, which lowers the SAIDI. In this case, during power outages, the DG can benefit not only the neighboring circuits, but also the circuit to which it is attached. So under this operation mode, the optimum DG location for reliability improvement does not have to be in the circuit with the minimum failure rate. This is reflected by the result in Table 4.6. At the maximum load point(6pm), adding the DG in segment C1_S4 leads to the greatest reliability improvement, even though circuit C1 has the worst failure rate among the three circuits.

Similar to the minimum loss analysis, applying the result for the 7am-5pm period leads to the best performance over the 24-hour cycle. So segment C3_S8 is selected as the best location for reliability enhancement.

To summarize the simulation results, the optimum placements for the entire load pattern are as follows:

To minimize power loss, the DG should be placed in segment C3_S7.

To obtain the greatest reliability improvement, the DG should be sited in segment C3_S8.

Note that these locations are not the same as the optimums based upon the peak load condition, which is segment C1_S4 for optimum reliability and optimum loss.

Now consider placing the DG at the optimum locations attained under the peak load condition, instead of the optimum attained using the working hour load. Table 4.7 shows

the difference in losses between these two placements at 12pm, which holds true of the period 7am-5pm. Suppose power is worth 10 cents per kilowatt-hour during this period. The cost difference due to losses between these two results is calculated by

$$C_{dif} = P_{dif} \times \text{Unit\_Price} \times T_d \quad (4.8)$$

where C_{dif} = difference in total cost

P_{dif} = difference in power loss

Unit_Price = the power unit price

T_d = time duration of concern.

So if we want to minimize the loss, placing the DG based upon the peak load condition versus placing the DG based upon the load condition that exists for most of the day will cost $21 more per day, assuming the DG only operates during working hours.

Table 4.7 Power Losses for DG in Segment C1_S4 and Segment C3_S7 at 12pm

DG Location	Description	Losses (kW)	Percentage (%)
C1_S4	Optimum DG location for min loss (peak load condition)	996	3.98
C3_S7	Optimum DG location for min loss (work hours load condition)	975	3.90
Difference		21	0.08

Suppose the goal is to maximize the reliability improvement. Table 4.8 shows the difference in reliability improvement between placing the DG at C1_S4 and C3_S8 during working hours. If we use the result for the peak load rather than the result for working hours, we will lose 16.74 % reliability improvement in ten hours.

Table 4.8 Reliability Improvement for DG in Segment C1_S4 and Segment C3_S8 at 12pm

DG Location	Description	Reliability Improvement (%)
C1_S4	Optimum DG location for max reliability improvement (peak load condition)	15.32
C3_S8	Optimum DG location for max reliability improvement (work hours load condition)	32.16
Difference		16.74

It appears that from both the loss reduction and the reliability points of view, analyzing over the time-varying load pattern can lead to significantly different answers than just analyzing the peak load point.

G. Economic Considerations

We have considered two options for placing the DG. Which solution should be chosen depends on the viewpoint of the person making the decision. The economic effects of these two options and the results attained under a single load point versus the entire load pattern are considered in this section.

In the example presented in the case study, during the working hours 7am-5pm, assume the DG is placed in segment C3_S8, instead of segment C3_S7, to gain the optimal reliability enhancement. Using equation 4.8, we can calculate the difference in cost due to the differences in efficiencies between siting the DG in segment C3_S7 instead of segment C3_S8. The calculation is just performed for the working hours of 7am-5pm, the time period during which the DG is most likely to operate. The total power being supplied during 7am-5pm is approximately 25100 kW. Table 4.9 shows the power losses and $SAIDI_{SYS}$ improvement for the DG in segment C3_S8 and segment C3_S7 at 12pm. Applying equation (4.8) and using the same unit price that was applied to Table

4.8, we get that the variation in power loss between these two locations costs $12.20 for one hour. Since the result at 12pm approximately holds true for the period from 7am to 5pm, we can estimate that during this ten-hour period, a 6.53% reliability improvement (reflected by SAIDI) costs $122.

Table 4.9 Power Losses and $SAIDI_{SYS}$ Improvement for DG in Segment C3_S8 and Segment C3_S7 at 12pm

DG Location	Description	Losses (kW)	$SAIDI_{SYS}$ Improvement (%)
C3_S8	Optimum DG location for reliability improvement	1097	32.16
C3_S7	Optimum DG location for minimizing losses	975	25.63
Difference		122	6.53

The cost of $122 per ten-hour period during the working day provides one data point to be used in judging the cost of the 6.53% reliability improvement. But the fact is that once the power system fails, it fails. For some customers, like hospitals, or industries with continuous processing, such as food processing, the cost of power outages can be extremely expensive. Studies indicate that nationwide, power fluctuations cause annual losses of from $12 to $26 billion [50]. So considering the economic impact, the reliability of the power system should perhaps receive a higher priority than improving the efficiency related to power loss.

H. Summary

The observations from this work can be summarized as follows:

Improving reliability and efficiency in a single circuit

- Often DGs are placed at substations for convenience. However, placing a DG further out on a circuit as opposed to locating the DG at the substation can enhance circuit reliability and reduce power losses.
- In industry, often decisions are based on power flow analysis run for the peak load. Placing a DG where only the peak load condition is evaluated may not provide the best location for minimum loss or reliability improvement.

Improving reliability in a system of circuits

- If DGs are to be shut down when circuits experience outages, for the best improvement in system reliability DGs should be placed in circuits that have the lowest failure rates.
- If DGs can be quickly restarted following switching operations with alternate feeds, circuit component failure rate is not a determining factor in considering optimal DG placement for reliability improvement.

System reliability is influenced by loading patterns

- If all the circuits in a system exhibit the same loading pattern, then applying a DG may help to enhance system reliability more during light load periods than during heavy load periods.
- If the circuits in a system exhibit different loading patterns, adding a DG may yield the largest improvement in system reliability during periods of high load.

Comparing minimum loss with maximum reliability

- The optimal DG placements for minimum loss and maximum reliability are different during light load conditions and close to one another during heavy load periods.
- The cost of improvements in reliability can in part be evaluated by the trade off with the cost of the losses in efficiency.

There are additional practical constraints that must be considered, such as what locations are available to the utility for installing the DG. Also, modifying the protection system either due to the additional fault currents supplied by the DG or due to switching operations anticipated are other practical aspects that need to be considered.

4.2.2 Reliability Improvement by Load Shifting

The objective in this section is to select the system configuration that leads to the greatest improvement in power system reliability such that no system voltage or equipment current constraints are violated. In a system with interconnected circuits, the loads can be shifted among the circuits by opening and closing switches. Such load shifting can change the system reliability. We use the Discrete Ascent Optimal Programming (DAOP) [51] approach to solve this problem.

A. Algorithm

Here the configuration for maximum reliability will be defined as the one which results in all segments having the smallest possible value of DTC. Observed from

equation 3.42 that for a given system, where the number of the customer is constant, and the smallest DTC leads to the lowest value of SAIDI for the system. In determining the configuration for maximum reliability, the DAOP algorithm starts by opening all switches in the system. Next a list of candidate switches to be considered for closing is created. These candidate switches are at the end of the current flow, and thus only one side of each candidate switch has a voltage. Figure 4.5 shows the flow chart of this algorithm.

At each step, all candidate switches are closed in turn and the reliability index, H, is evaluated. The candidate switch that contributes to the minimum DTC is selected as the switch to close. After closing the switch that results in the minimum DTC, the list of candidate switches is updated and the evaluation of which switch to close is repeated. As progress toward the solution is made, more and more load is supplied and the DTC of the system continues to increase. The algorithm is terminated when all loads in the system are supplied.

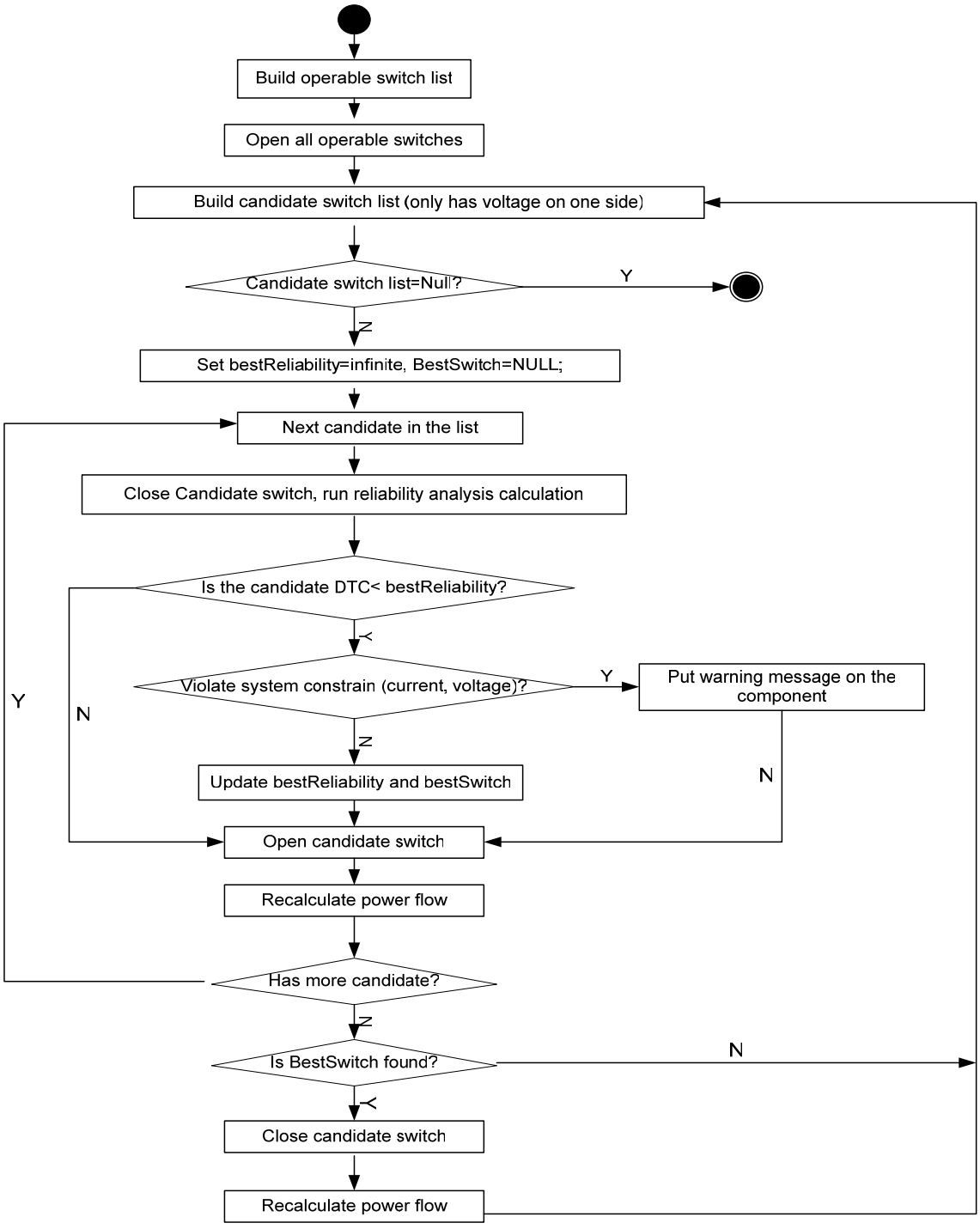

Figure 4.5 Flow Chart of DAOP Applied to the Reconfiguration Algorithm for Load Shifting

This algorithm is not an exhaustive state enumeration scheme. This algorithm follows the topology of the power system in the way that only a portion of the system is considered at each step. The reliability of loads closest to the sources are considered first. As loads become supplied during the course of analysis, reliability of other loads are considered until the system is fully loaded. So the reliability index SAIDI increases step by step according to the nature of the discrete ascent algorithm.

B. Advantage of DAOP

The DAOP algorithm converges to a solution which is the configuration with the segments having the minimum values of DTC (where system voltage and equipment current constraints are not violated) within a number of computation steps equal to the number of segments in the system.

C. Analysis result

During the optimal reliability analysis, the circuit that has best reliability always tries to reach out, taking over more load from adjacent circuits. However, the system and equipment constraints may limit the reconfiguration. For instance, in the 2-circuit model shown in Figure. 4.6, these two circuits are respectively supplied by two substations of the same type. In the original system, circuits C2 and C3 are interconnected by the open switch CTSW.

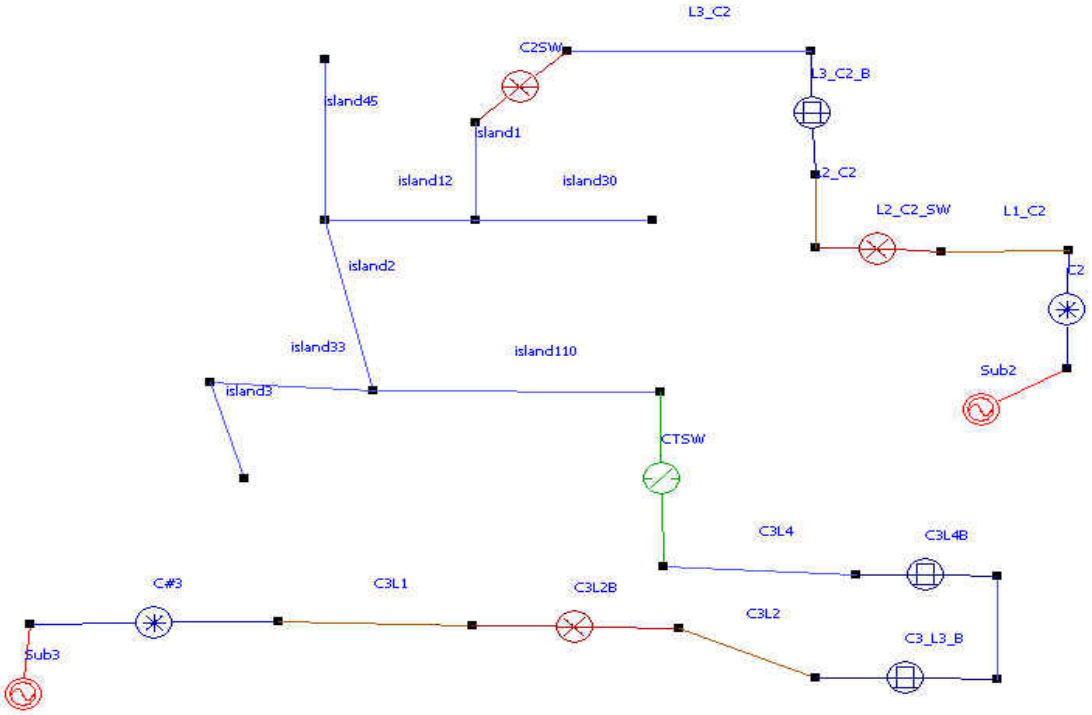

Figure 4.6 Original System

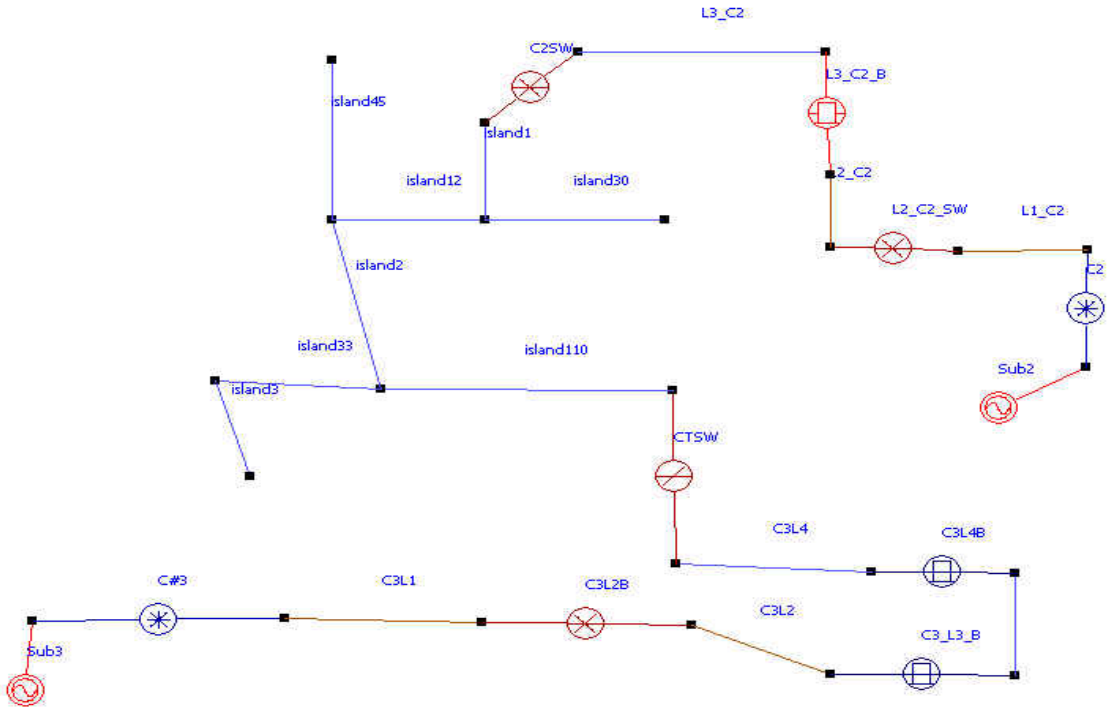

Figure 4.7 Improved System

Both circuits are lightly loaded, so they both have spare capacity. Circuit C3 has the lowest values of line section failure rates (C2 and C3 have annual failure rate of 1.669 and 0.1 respectively). This means that Circuit C3 has a better reliability than Circuit C2. The DAOP analysis result is shown in Figure. 4.7. We can see that both CTSW and C2SW segments shift from C2 to C3. As a result of this, the system reliability is significantly improved as indicated in Table 4.10. For segments CTSW and C2SW, the availability of alternate feeds is the same as in the original system, but in the system with the improved configuration, they have a more reliable feeder path. Thus, these two segments have fewer chances to experience power outages due to the smaller failure of their upstream components.

Table 4.10 Comparison between Original System and Improved System

	Original System	Improved System	Improvement
SAIDI	0.4064	0.2909	28.4%
CAIDI	0.4761	0.4033	15.3%

The DAOP algorithm switches loads from a circuit that has poor failure rates to the circuit that has better reliability, achieving an enhancement in the system reliability. However, system constraints limit the improvement. Referring to the 2-circuit system shown above, if C3 tries to take any more segments beyond CTSW and C2SW, customer level voltage at the end of C3 will drop below 114V, which is the customer voltage limit used for this simulation.

D. Further Comparisons to Minimum Loss Analysis

The next example system has a symmetric topology consisting of two circuits which have the same type of customers and same failure rates, with the number of customers in different segments varying. For this example system, the analysis results from the minimal loss and best reliability are slightly different, as illustrated in figures 4.8 and 4.9. For a system with symmetric topology and similar circuit set up, the tie switch of the two circuits is usually put close to the electrical middle point of the system to minimize the total power loss and optimize the system reliability.

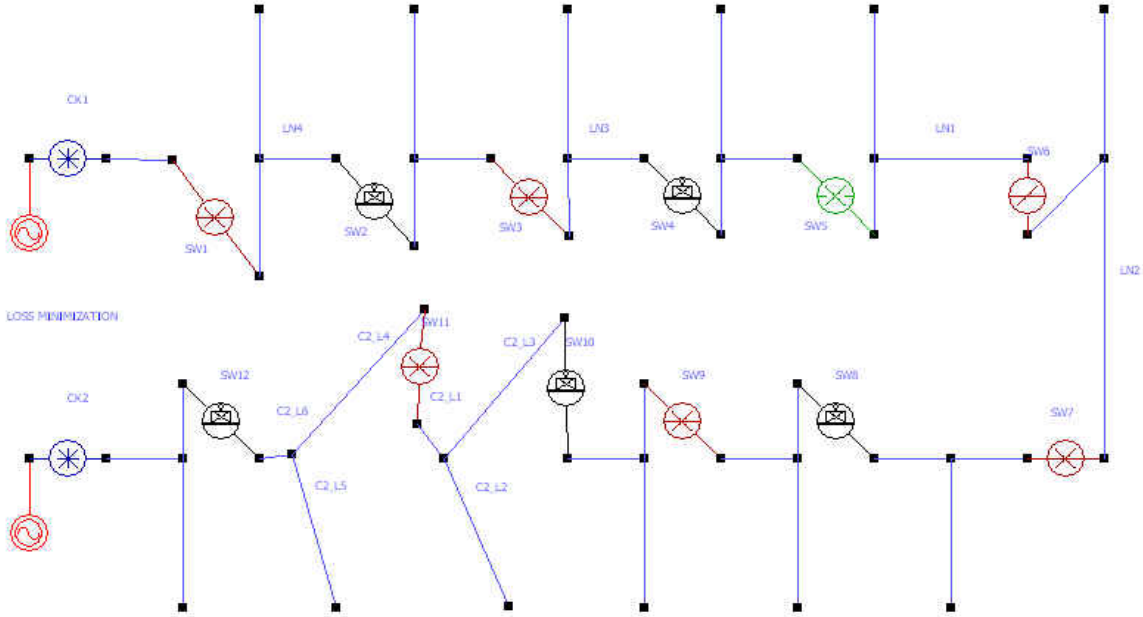

Figure 4.8 Minimum Loss Analysis Result

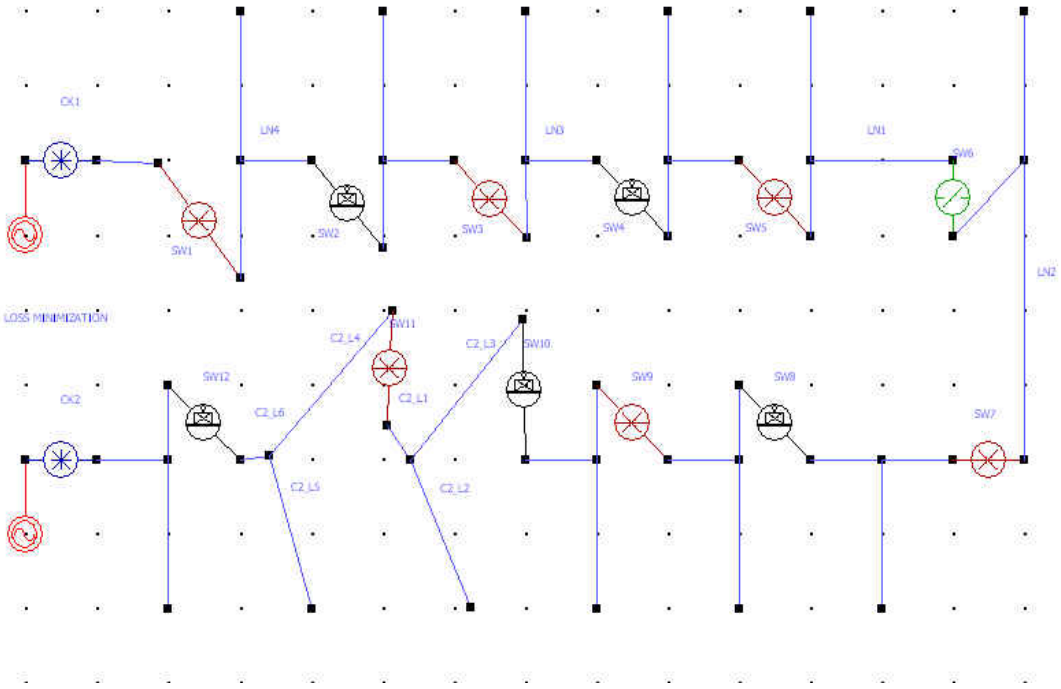

Figure 4.9 Best Reliability Analysis Result

Table 4.11 shows the differences of SAIDI and CAIDI for two switch arrangements for minimal loss and optimal reliability. There are only slight differences between these two arrangements.

Table 4.11 System Reliability Comparison of Switch Arrangements for Minimal Loss and Optimal Reliability

Switch arrangement for Two Criteria	Min Loss	Optimal Reliability	Difference
SAIDI(Hr/Yr)	0.1736	0.1721	0.8%
CAIDI(Hr/Yr)	0.1915	0.1869	2.4%

Figures 4.10 and figure 4.11 show the configuration of a 3-circuit system for minimum loss and best reliability respectively. The minimum loss configuration result is exactly the same as the base case. In the base case, C2 has the best reliability, C1 the worst, and the reliability of C3 is about the middle point of C2 and C1.

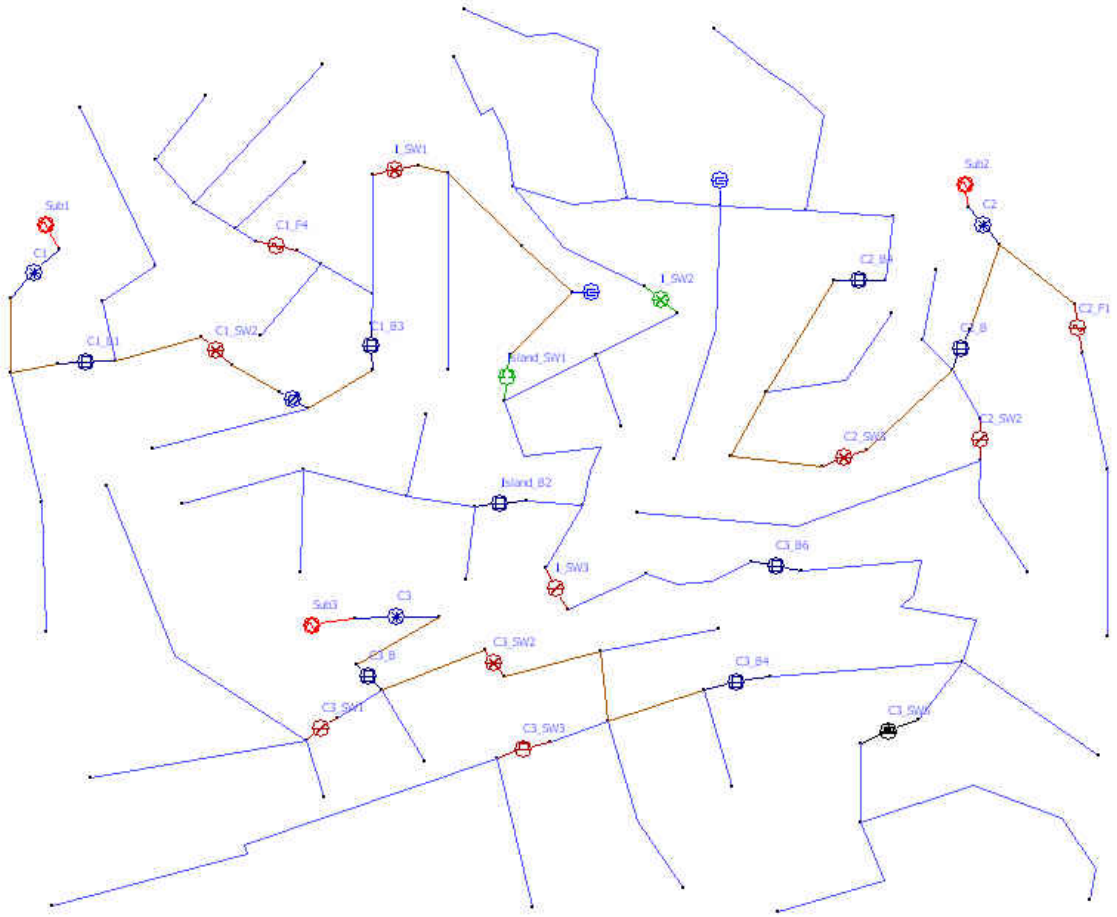

Figure 4.10 Switch arrangement for Minimum Loss

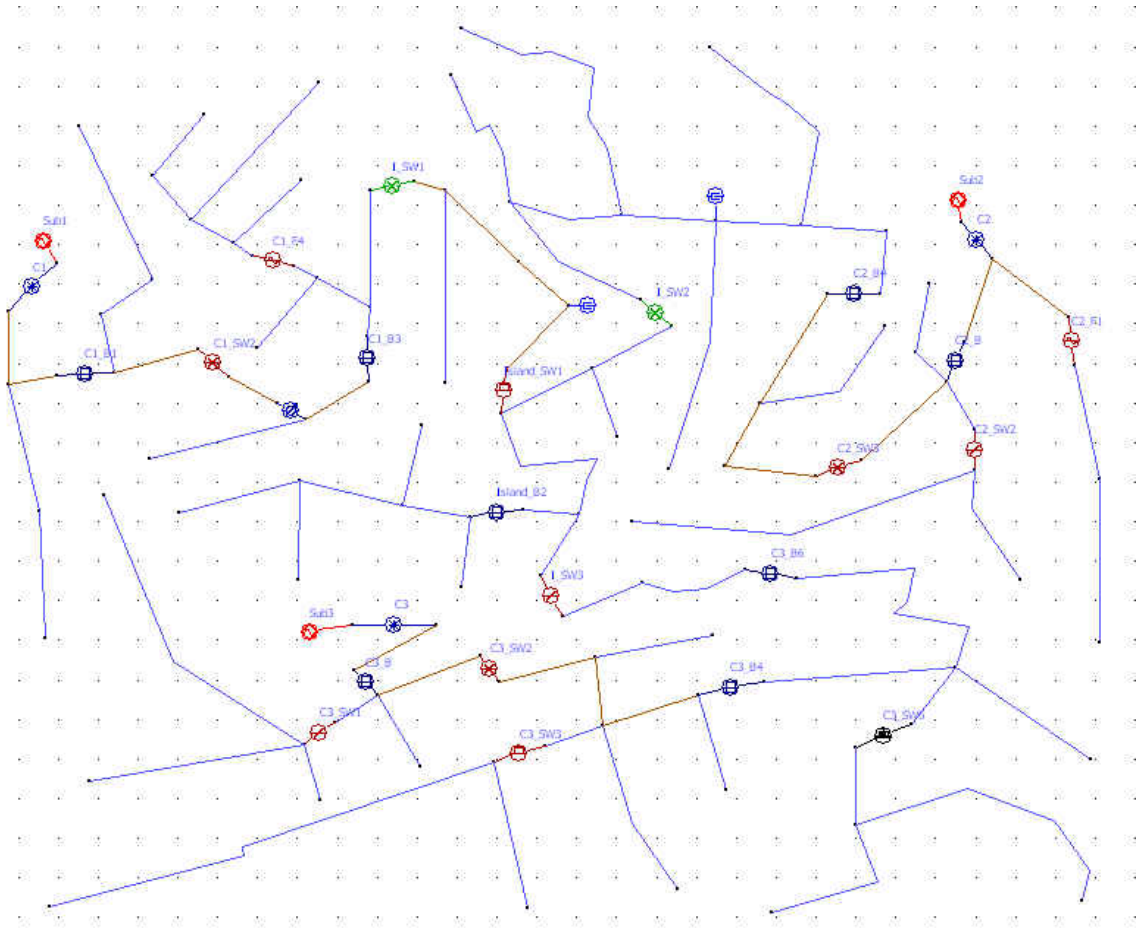

Figure 4.11 Switch Arrangement for Best Reliability

In the minimum loss analysis, the load of segment island_SW1 is attached to C1. On the other hand, the optimal reliability analysis shifts this segment to C3, since C3 has a smaller failure rate than C1. However, shifting the load to C3 increases the total power loss by 8.2% due to the electrical distance from sub3 to the segment island_SW1 being longer than the electrical distance from Sub1 to segment island_SW1. The reliability indices and power loss for the two configurations are listed in Table 4.12.

Table 4.12 System Reliability and Loss Comparison of Switch Arrangements for Minimal Loss and Optimal Reliability

Switch arrangement for Two Criteria	Min Loss	Optimal Reliability	Difference
SAIDI(Hr/Yr)	2.1973	2.0193	8.1%
CAIDI(Hr/Yr)	1.8932	1.7496	7.6%
Loss(KW)	715.31	779.45	8.2%

E. Summary

This work presents a discrete optimization algorithm to optimize system reliability. Load shifting reconfiguration is an effective way to increase distribution system reliability with only the cost of the switching operations. Each DAOP solution presented here was determined with an exhaustive search, and the DAOP algorithm provided the optimum solution on all the systems tested.

Due to the time consuming reliability calculations that are performed for each ending load for each step of the DAOP algorithm, the execution time of the algorithm will grow very large as the system grows large. There are measures that could be investigated which could potentially reduce the solution time. One such measure is placing locks on branches such that they would not be considered during the course of the algorithm.

4.2.3 System Optimization

The work presented in the previous sections of this chapter can be summarized as system optimization. The goal of system optimization is to minimize an objective function without violating constraints. For instance, the objective is to minimize the system reliability index SAIDI without violating current or voltage constraints.

Besides the two measures studied here, applying DGs and reconfiguration, there are several other ways to optimize system reliability, such as feeder path upgrades and adding new tie points. If an alternate path is available to serve power after a fault or equipment failure, and that path is capacity constrained due to small conductor sizes, upgrading the conductor may be a cost-effective way to improve reliability. Increasing the number of tie points enlarges the number of possible alternate feeds. Both of these two methods improve the power exchange capability of the interconnected network.

Another approach to improving system reliability is the addition of sectionalizing devices, both manually operated and automatically operated. Line sectionalizing can be done by placing normally closed sectionalizing devices on a feeder. Adding sectionalizing devices improves reliability by reducing the number of power interruptions caused by down stream faults and also provides more flexibility during post-fault system reconfiguration.

Feeder automation refers to applying supervisory switches such as SCADA-Controlled switches on feeders. These automated switches allow post-fault system reconfiguration to execute faster than with manual switches, so some of the customers in the affected area only experience momentary power outages instead of sustained interruptions.

Objective functions for the different options considered above can be written in terms of maximizing reliability subject to cost constraints. In this way, the effectiveness of each option can be compared. Note that the cost-effectiveness of these approaches may vary widely from region to region.

4.3 From the environmental point of view – storm-dependent failure

Our research focuses on the environmental affects of adverse weather or storms. There are two reasons why we investigate storm data. One is the failure rates and repair times under storm conditions are needed for system reliability evaluations. The second and more important reason is that understanding storm characteristics and their impacts on the reliability of the power system helps the utility improve reliability during storms. This reliability improvement is achieved through improved operations.

Utility companies spend large amounts of money on storm outage restoration. A storm model which can accurately predict time-varying outages for approaching or ongoing storms will help with outage management and reliability improvement. With such a model, both customer down time and outage costs can be reduced.

Single-contingency criterion (N-1 standard) has been used for many years in the power industry. From severe power outages in the past two decades, people comes to realize that the N-1 standard may not be sufficient to preserve a reasonable system reliability level. However, it is also commonly recognized that no utility can financially justify the N-2 or N-3 principle in power system planning. One alternative solution is bringing reliability assessment and management into practice in operations and

maintenance. Storm-dependent failure analysis (to help the operation decision making) is part of this trend.

4.3.1 Introduction

Major impacts of severe weather conditions on electric utility operations are equipment failures and power outages. It is estimated that an average storm costs an average utility about $100k per hour, including materials and labor. For large utilities, storm costs can reach $1000k per hour.

Manpower is a significant part of power restoration cost. A utility usually needs to send out a large number of crews to restore services during a storm. Some of the crews may be borrowed from neighboring companies or are contract crews that are hired during large emergencies. It is a challenging task to manage crews effectively during a major storm. If the number of outages that are going to occur as a function of time can be accurately predicted, then the management of crews and the power restoration can be more effectively planned.

In this work ten years' worth of storm outage data from a utility are investigated. As part of the analysis, storms are classified into six categories. Cumulative outage models for the six storm classifications are developed. For real-time storm tracking, an observer operates on the errors between predicted storm outages and actual storm outages. Simulations demonstrate that outages can be accurately tracked. One-hour and five-hour moving windows are used for predicting outages.

In the data analyzed, more than half of the storm outages during summer are attributed to lightning. Lightning related outages are estimated to cost the nation's utility industry over $100 million annually in materials and labor costs. Accurate forecasts of

outages from storms with intense electrical activity could reduce customer outage time due to better crew management. Here storms with intense lightning activity are analyzed for correlations between lightning density and outages, where the lightning density is calculated inside defined circuit corridors.

4.3.2 Historical Storm Outage Data Analysis

Two sets of historical data were correlated and analyzed: outage data and weather data. The outage data analyzed covers approximately a ten-year period, from July 1995 to September 2004. There are a total of 8367 outage records considered. The weather data comes from three weather stations located in the distribution system. Weather conditions such as wind speed, temperature and other variables are recorded at least every hour at these weather stations.

The analysis uses an hour as the basic unit of time. If there are multiple weather measurements made during an hour at a weather station, the weather data from the multiple records are averaged and the averaged weather variables are used in the analysis. In the outage data, each outage is associated with a substation. Substations are associated with the closest weather station, and thus each outage is associated with a weather station.

A. Storm Classification

Outages that occur in consecutive days are considered caused by the same storm. That is, outages are grouped by storm. Storm types that are considered and the temperature and wind speed ranges that are used to classify the storm are presented in

Table 4.13. Note that the lowest or highest temperature and highest wind speed that occurred during the storm are used to classify the storm.

Table 4.13 Storm type descriptions

Storm Type	Description	Temperature Range (^{o}F)	Wind Speed Range (mph)
H	High temperature	MaxT*>80	WS*<=20
HS	High temperature and Strong wind	MaxT>80	WS>20
L	Low temperature	MinT*<32	WS<=20
LS	Low temperature and Strong wind	MinT<32	WS>20
M	Moderate temperature	MaxT<=80 MinT>=32	WS<=20
MS	Moderate temperature and Strong wind	MaxT<=80 MinT>=32	WS>20
MaxT: maximum temperature; **MinT**: minimum temperature; **WS:** wind speed			

Table 4.13 shows the number of storms of each type found in the outage data set and the number of outages caused by each type of storm. There are only 11 HS storms 18 LS storms in the outage data, but on average, there are 188 outages caused by each HS storm and 190 outages caused by the each LS storm. Note that these are the largest number of outages per storm. This is part of the reason why, as we will see in Figure 4.14 below, the average downtime during HS and LS storms is longer than the other storms. A utility only has certain number of crews, more outages usually means longer downtime.

Table 4.14 Number of outages for each type of storm

Storm Type	Number of Storms	Number of Outages	Average Number of Outages per Storm
H	24	2318	97
HS	11	2072	188
L	12	748	62
LS	18	3419	190
M	22	1030	47

MS	25	3579	143
Total	112	13166	117.6*
*117.6 is the average number of outages per storm across all storm types			

B. Average Hourly Outages and Recoveries

The results thus far of this analysis are presented in the Table 4.15 as six plots. All the plots shown in Table 4.15 are on the same scale, so the quantities of outages and recoveries can be easily compared. Table 4.15 is presented so that a visual comparison among the different storm types can be readily made.

For each storm type, the average number of outages and recovery per hour of storm is calculated. The results are plotted against the elapsed time after storm arrivals. The plots shown in the first column of Table 4.15 show the average number of outages per hour and the plots in the second column show the average number of recoveries per hour. In each plot there are two curves. Each of the curves corresponds to the same temperature range, but different wind speed ranges apply to each of the curves in each plot.

From reviewing the first column of Table 4.15, it may be seen that the maximum of "the number of outages per hour" appears during the first five to ten hours of the storm. It also may be seen that the number of outages dramatically decreases after the first 20 hours (this is true even for storms that last 3-4 days). Also, it should be noted that higher wind speeds result in significant increases in the number outages. From more detailed analysis, the number of hourly outages generally peaks close to when the wind speed is peaking.

It is obvious that the HS storms cause more outages than all other storm types. It seems the system can survive higher wind speeds in the fall and winter, but is more vulnerable to the strong wind storms during summer.

The second column of Table 4.15 shows that the average number of recoveries per hour is fairly even for each type of storm. The recovery curves follow a similar pattern as the outage curves. Usually, the number of recoveries per hour is less than the number of outages per hour during the first ten hours. After the first ten hours, the number of recoveries per hour often starts to exceed the number of outages per hour.

Since all the plots in Table 4.15 are on the same scale, it is easy to observe that the average number of outages caused by storms during moderate weather conditions (M and MS type storms) is less than the average number of outages caused by both high (H and HS) and low temperature storms (L and LS). And generally, the storms with strong winds cause much more damage than the storms in the same temperature range without strong winds.

Table 4.15 Comparative plots of average number of outages and recoveries per hour for different storm types

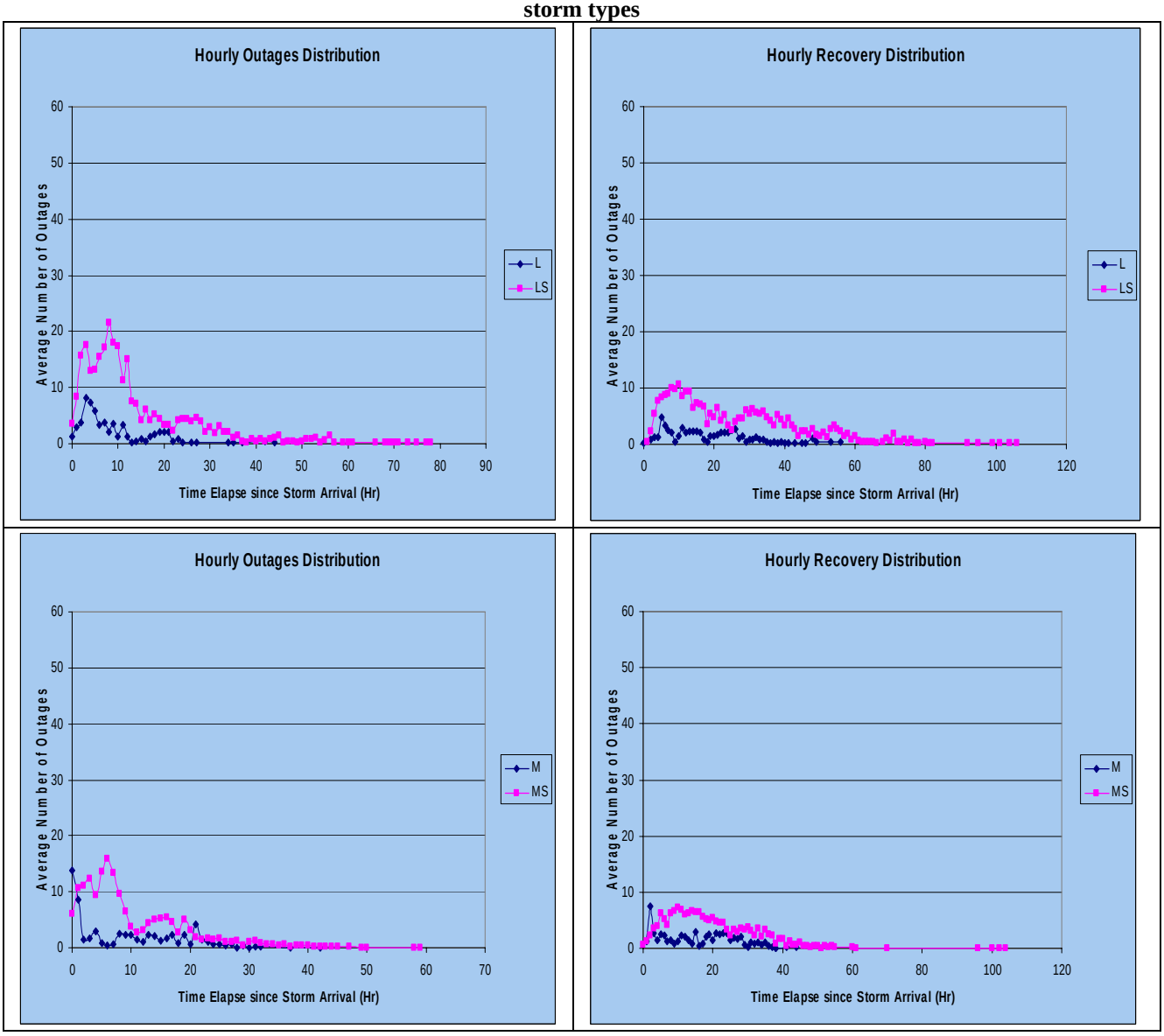

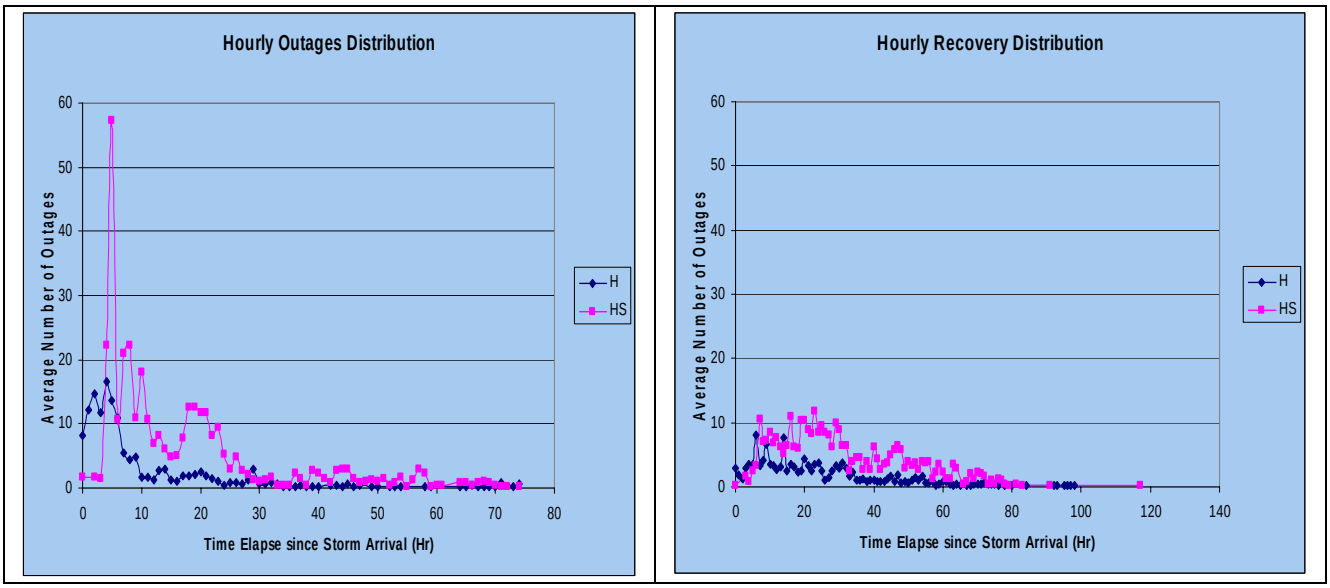

Higher wind speeds result in significant increases in the number of outages. From analyzing storm weather data, the average wind speeds during each hour of a storm may be determined. The results of this analysis are plotted in Figure 4.12, which shows the average hourly wind speeds plotted against the hour of the storm. Comparing the data used to generate Table 4.14 and Figure 2, we found that the average hourly outages generally peak close to when the average wind speed reaches its first peak. This indicates that a general pattern of wind speeds exist in the storms in the recorded area. This also indicates a correlation between wind speed and the number of power outages.

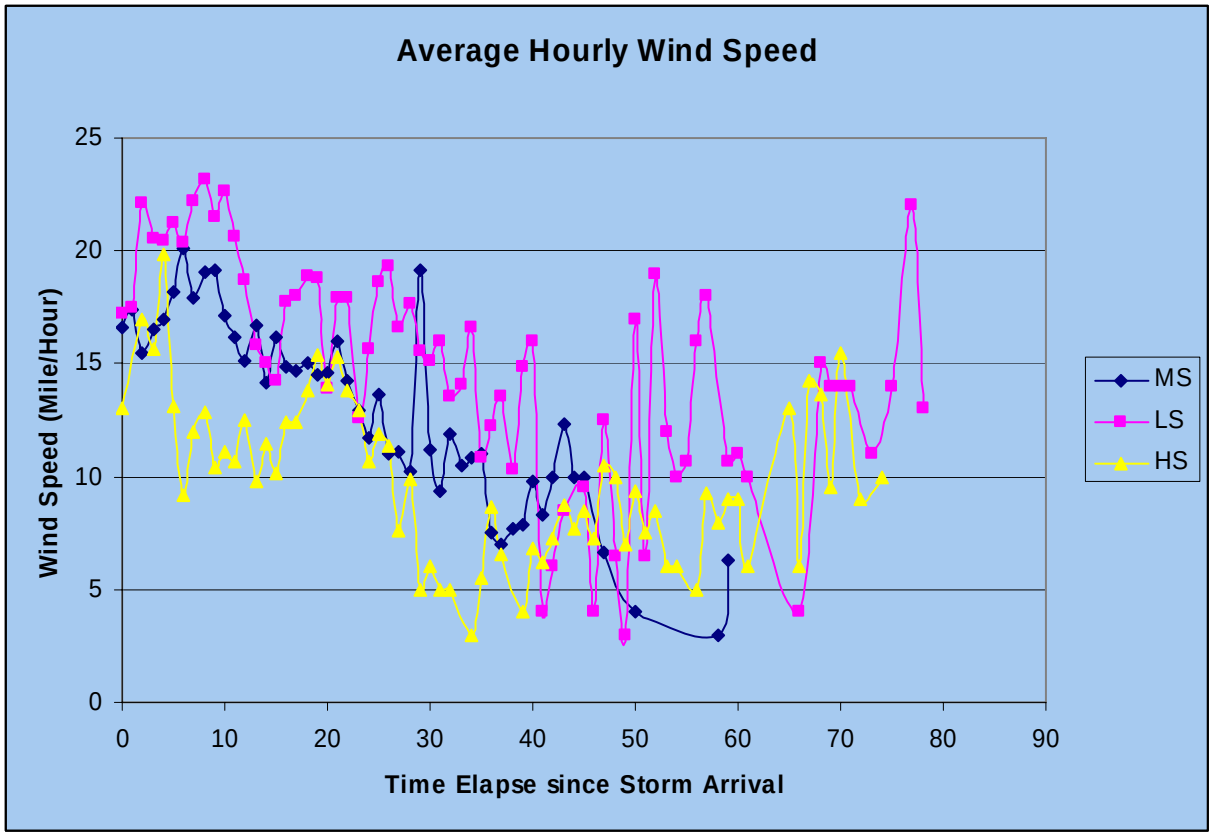

Figure 4.12 Average Hourly Wind Speed for Storms in Three Different Temperature Ranges

C. Downtime and Failure under Storm Condition

Figure 4.13 shows the average downtime for all the storm types. Over all the outage records the Average Downtime is 550 minutes (9.2 hours). The minimum, maximum, and average downtimes are listed in Table 4.16. The largest downtime, 6124 minutes or 4.25 days, occurred during a LS storm.

Figure 4.13 indicates that storms with strong winds generally result in longer downtimes than storms without strong winds. Among them, L and LS have the greatest difference. From Table 4.14 , we see that the number of LS storms is only two times the

number of L storms, but outages caused by LS storms are more than four times the outages caused by L storms. This implies that in low temperature weather, strong winds do more harm to the power system than at other temperature ranges.

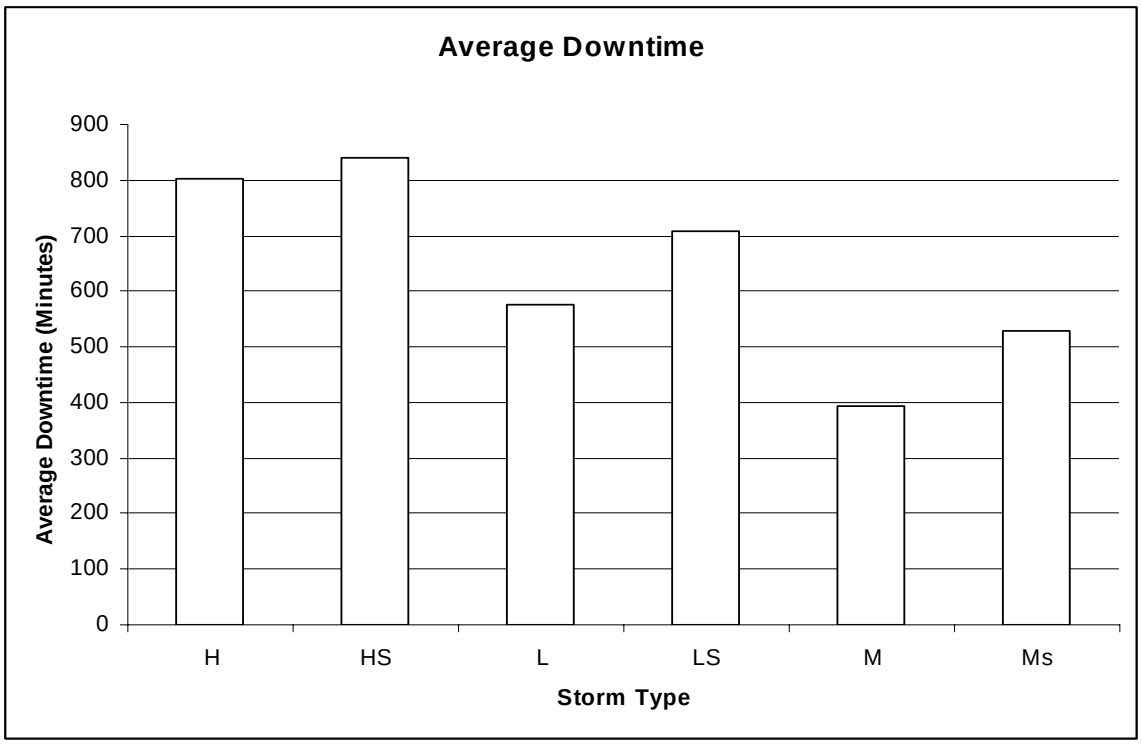

Figure 4.13 Average Downtime per Storm for Storms of Each Type

We notice that HS has the greatest downtime among all the storms. From Table 4.14, HS also has the largest number of outages of the storm types. From this it appears that HS storms result in the most damage to the power system.

The impact of M storms is relatively mild. The number of outages caused by these storms is small and the average downtime of each outage is roughly half the average downtime in HS storms.

Table 4.16 Downtimes for the 1995-2004 Outage Data

Storm Type	Min Downtime (minutes)	Max Downtime (minutes)	Average Downtime (minutes)
H	5	5369	804
HS	3	5860	840
L	8	2651	576
LS	1	6142	707
M	8	3749	393
MS	1	5630	530

For L, LS, M, and MS storm types, the larger the number of outages caused by a storm, the longer downtime customers experience. From this observation, we may imply that as the number of failures increase, it takes crews longer to make each repair. However, the number of outages is not the only factor that affects the down time. If we look at the high temperature storms, the average number of outages caused by an H storm is 145, which is much smaller than the number of outages caused by an HS storm (352). However, the average downtime for an H storm is only a little shorter than the average downtime for an HS storm. The explanation for this may lie in Table 4.17, which lists the number of equipment failures sorted by storm type.

Table 4.17 Number of equipment failures for each storm type

Storm Type	Line Section	Fuse	Switch	Transformer	Regulator
H	826	184	24	184	4
HS	668	29	4	34	0
L	162	2	0	1	0
LS	1186	27	3	61	0
M	318	45	5	56	0
MS	1435	45	7	59	0
Total	4595	332	43	395	4

From the data in Table 4.17, H storms cause the largest number of transformer failures. This may be the reason why the average downtime in an H storm is large, even though there are not a large number of failures.

From Table 4.17, we can see that L storms cause the smallest number of equipment failures. We also notice that in low and moderate temperature weather, strong winds play an important role in line section failures. During LS and MS storms, the line section failures are five to six times as many as the line section failures in L and M storms.

Given the installed number of each type of equipment listed in Table 4.17, the failure rates for each type of equipment as a function of storm type is calculated, as show in Table 4.18. These failure rates may then be used in planning for either the reliability

effect of system design changes or the response needed for a particular approaching storm.

Table 4.18 Component Failure Rate based on Ten-year's Record (1995. 7- 2004. 9)

	Line & Cable			Fuse			Transformer			Switch		
	Tree Contact	Equipment Failure	Lightning	Tree Contact	Equipment Failure	Lightning	Tree Contact	Equipment Failure	Lightning	Tree Contact	Equipment Failure	Lightning
Number of Failure	3145	745	613	33	37	258	61	87	237	11	15	13
Total Number of components	795.30 (miles)			5591			24779			1577		
Annual Failure Rate	0.395	0.094	0.077	0.0015	0.0017	0.0115	0.00025	0.00035	0.00096	0.0007	0.00095	0.000824

D. Curve Fits of Cumulative Outages

Figure 4.14 shows the average cumulative outages per storm as a function of time for high temperature storms. It illustrates on average the total number of outages that the analyzed distribution system experiences by hour of the storm. Note that the cumulative outages change with time in a somewhat smooth fashion. This suggests using cumulative outages for developing analytical storm models. The analytical models may then be used to predict outages that are going to occur due to approaching and/or ongoing storms.

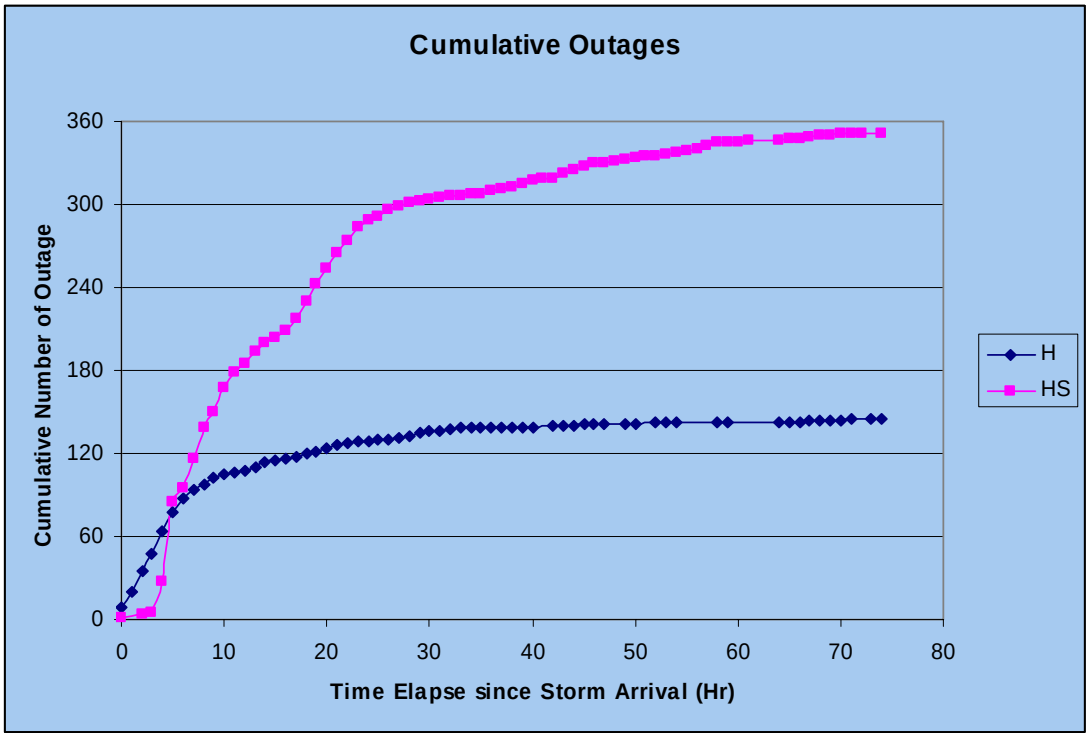

Figure 4.14 Average Cumulative Outages for H and HS Storms

As the end of a storm approaches, the cumulative number of outages gradually flattens out. The cumulative outage curves closely match the characteristics of an exponential distribution. Thus, to model cumulative outages, a least squares approximation is applied to an exponential model as given by:

$$N = A \cdot (1 - \exp(-B \cdot (t - c))) \tag{4.9}$$

where N = number of cumulative outages;

t = number of hours after the first recorded outage; and A, B and C are coefficients that vary with the type of storm.

Figure 4.15 shows the results of the curve fit for H storms. The exponential curve fit model produces results which are in close agreement with the six existing average cumulative storm outage curves with R-squared values [52] in the range of 0.9834 to 0.9957. The R-squared value for the curve shown in Figure 4.15 is 0.9882.

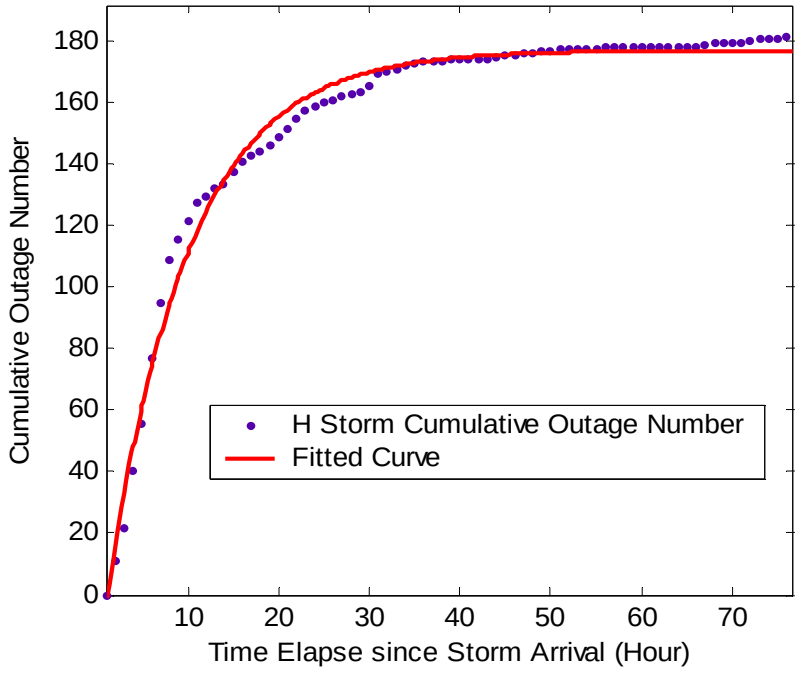

Figure 4.15 Curve Fit for H Storm Cumulative Outages

4.3.3 Storm Outage Forecast

As stated in the previous section, an empirical model is derived from historical data to describe the outage occurrence pattern for each storm type, which can serve as a reference for restoration decision makers before a storm arrives. However, for a specific storm, the real-time outage behavior may differ significantly from the empirical model.

A. Statistical Model with Error Compensation

In order to accurately predict outages for a specific real-time storm, the empirical model (equation 4.9) is combined with error compensation to create an observer, the output of which tracks the actual storm outages. This is illustrated in Figure 4.16, where actual storm outage measurements O_{Ak} are compared with the observer outputs O_{Pk}.

In Figure 4.16, the empirical model takes the actual weather conditions W as an input and creates a prediction of outages $O_{E(k+1)}$. The deviation between the actual outages O_{Ak} and the prediction O_{Pk} serves as input to the feedback stage of the observer. A compensator is used to generate the correction valueΔO_{Ck}, which is used to adjust the prediction $O_{E(k+1)}$.

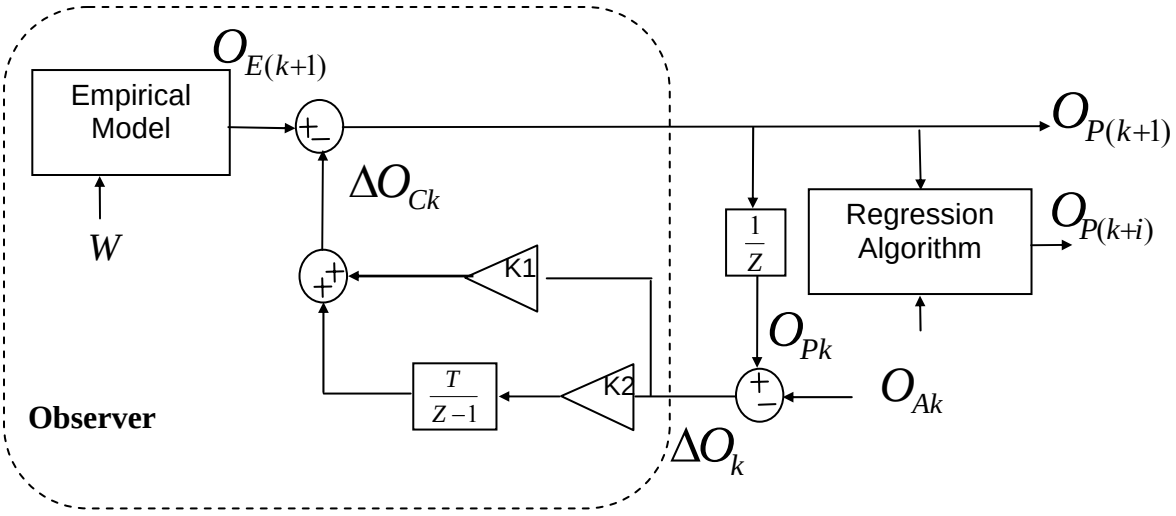

Figure 4.16 Feedforward Prediction Coupled With Feedback Error Correction

W = weather measurements.

$O_{E(k+1)}$= predicted outages at the end of hour (k +1) from empirical model.

O_{Ak} = actual outages measured at end of hour k .

O_{Pk} = predicted outages for hour k at hour (k -1).

$O_{P(k+i)}$ [where i=1, 2, 3, 4, 5] = predicted outages for each of the next five hours at hour k .

$O_k = O_{Pk} - O_{Ak}$.

ΔO_{Ck}= compensator output.

The prediction system provides two forecasts, one hour forecast $O_{P(k+1)}$ and five hour forecast $O_{P(k+i)}$ with i ranged from one to five. The five hour forecast is created by applying a regression algorithm to the one hour forecast and the series of previous actual outages. The regression algorithm attempts to recognize when the steep slope associated with cumulative outage curves is occurring. During this time, different weights are used in the regression to improve the accuracy of the five hour prediction window.

B. Prediction Errors

To evaluate the effectiveness of the forecasting model, simulations based on the 49 actual storms from 1995 to 2004 are used to generate forecast curves and calculate errors.

Figure 4.17and Figure 4.18 illustrate the simulation results for a normal storm, which has an outage pattern close to an exponential distribution, and an abnormal storm, where the outage pattern is different from the modeled exponential distribution. Figure 4.17 illustrates the feed-forward prediction, actual measured storm data, and the one hour forecast. Figure 4.18 illustrates the comparisons for the five hour forecast.

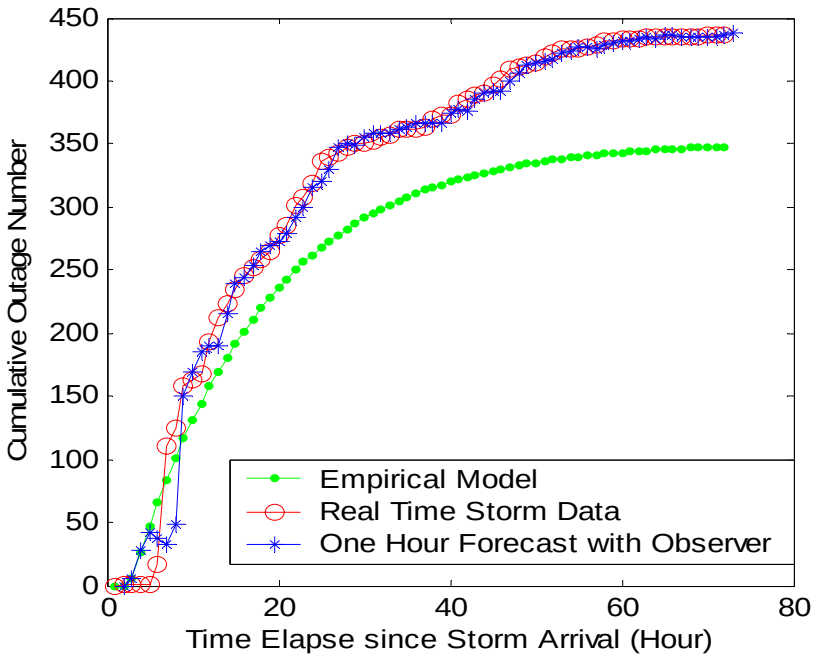

(a) Normal Storm

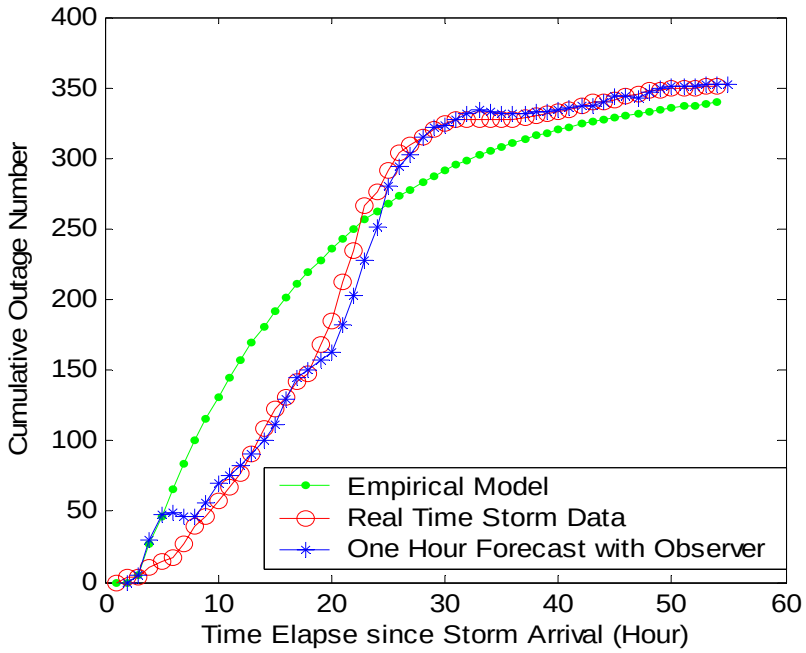

(b) Abnormal Storm

Figure 4.17 One Hour Forecast with Feedback Correction

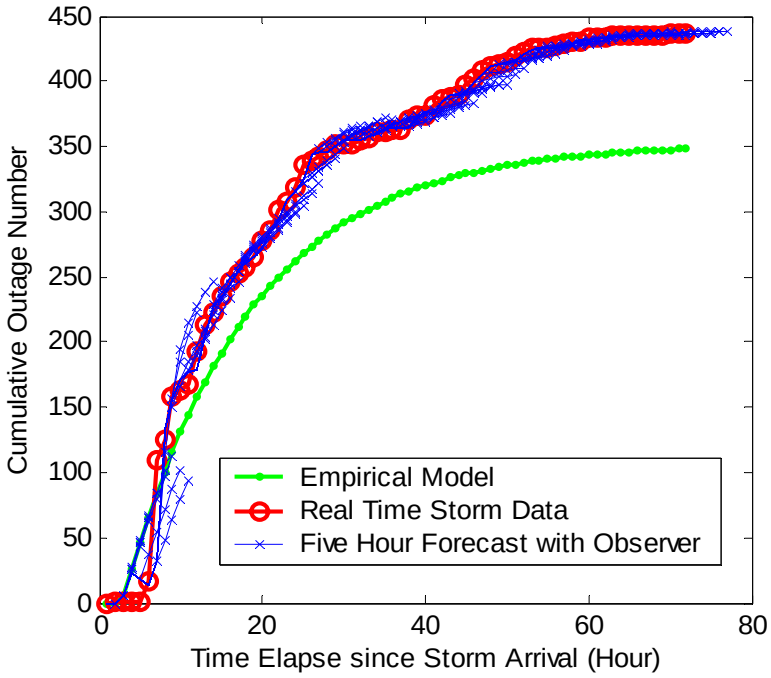

(b) Normal Storm

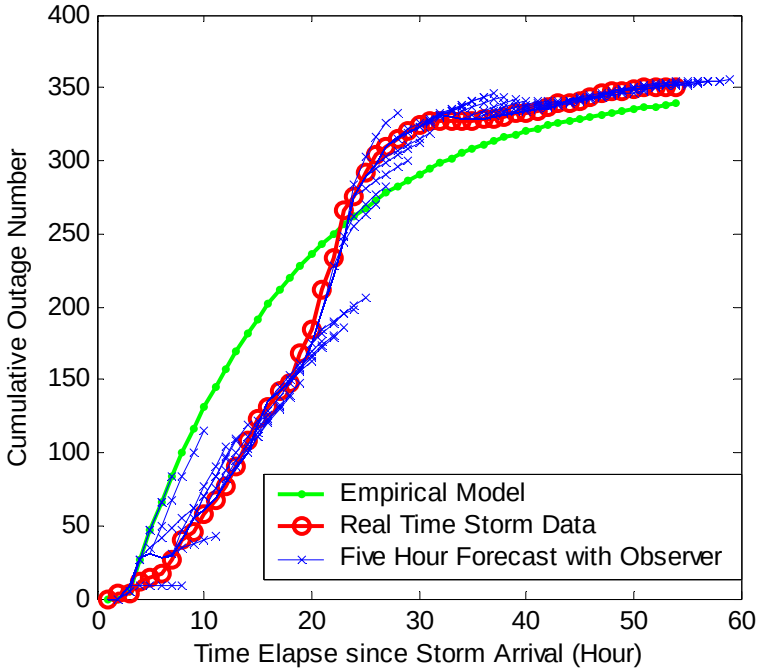

(c) Abnormal Storm

Figure 4.18 Five Hour Forecast with Feedback Correction

The one-hour and five-hour forecasting errors for each storm are calculated using the following equations, respectively.

$$OneHrErr = \frac{1}{N}\sum_{k=1}^{N}\frac{\left|O_{Ak} - O_{Pk}\right|}{O_{Ak}} \cdot 100\,\% \tag{4.10}$$

$$FiveHrErr = \frac{1}{N}\sum_{k=1}^{N}\frac{\left|O_{A(k+5)} - O_{P(k+5)}\right|}{O_{A(k+5)}} \cdot 100\% \tag{4.11}$$

where N = total number of hours for a storm

OneHrErr = one hour forecast error

FiveHrErr = five hour forecast error.

The one-hour and five-hour average forecasting errors for the existing 14 MS storms are 8 % and 16%, respectively. Abnormal storms prediction spikes occur because the abnormal storms do not follow the exponential distribution model.

C. Parameter Sensitivity Study

The forecasting effectiveness relies on error compensation. The performance of the prediction can be considered robust if the predictions are not too sensitive to the values selected for the two parameters, k1 and k2, respectively. A parameter sensitivity study was performed to evaluate the outage prediction variances with changes in the two parameters. For a typical MS storm, Figure 4.19 illustrates that the one hour forecasting errors vary from 4.5% to 6.6% with parameters ranges corresponding to k1 $\in$ [0.7, 1.3]

and k2 ∈ [0.7, 1.6]. The small outage prediction errors indicate that the forecasting system is not too sensitive to the parameter values selected for the compensator.

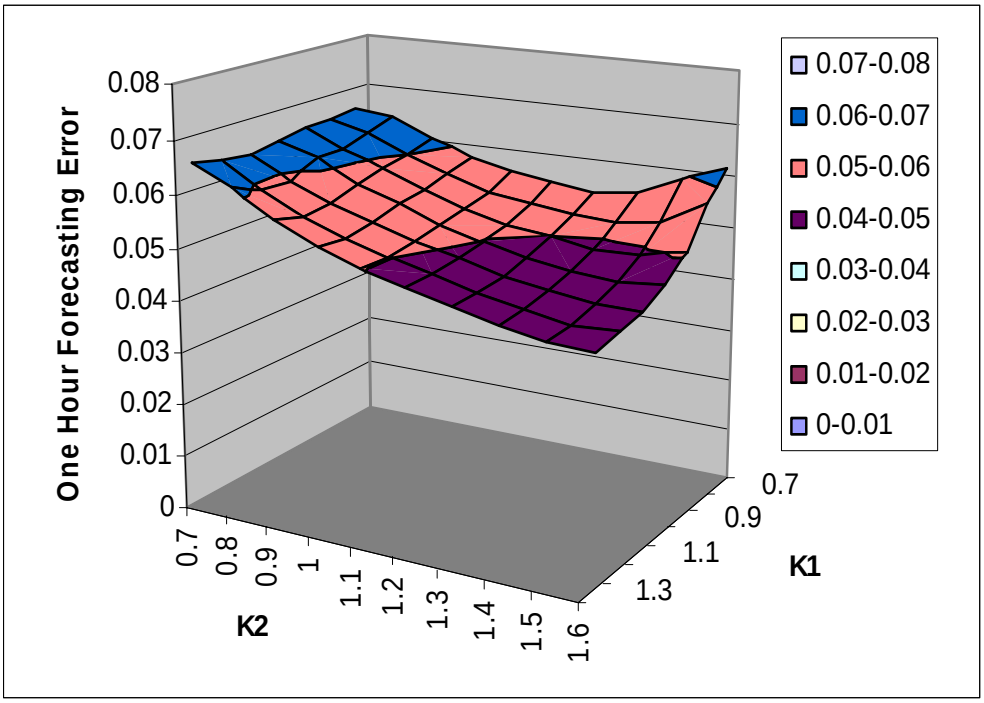

Figure 4.19 Parameter Sensitivity Study

4.3.4 Lightning Outage Analysis

A. Lightning Data

Based on 11 years of lightning data (1994-2004), the average number of flashes in each month of a year are plotted in Figure 4.20, and the average peak current of flashes in each month are shown in Figure 4.21.

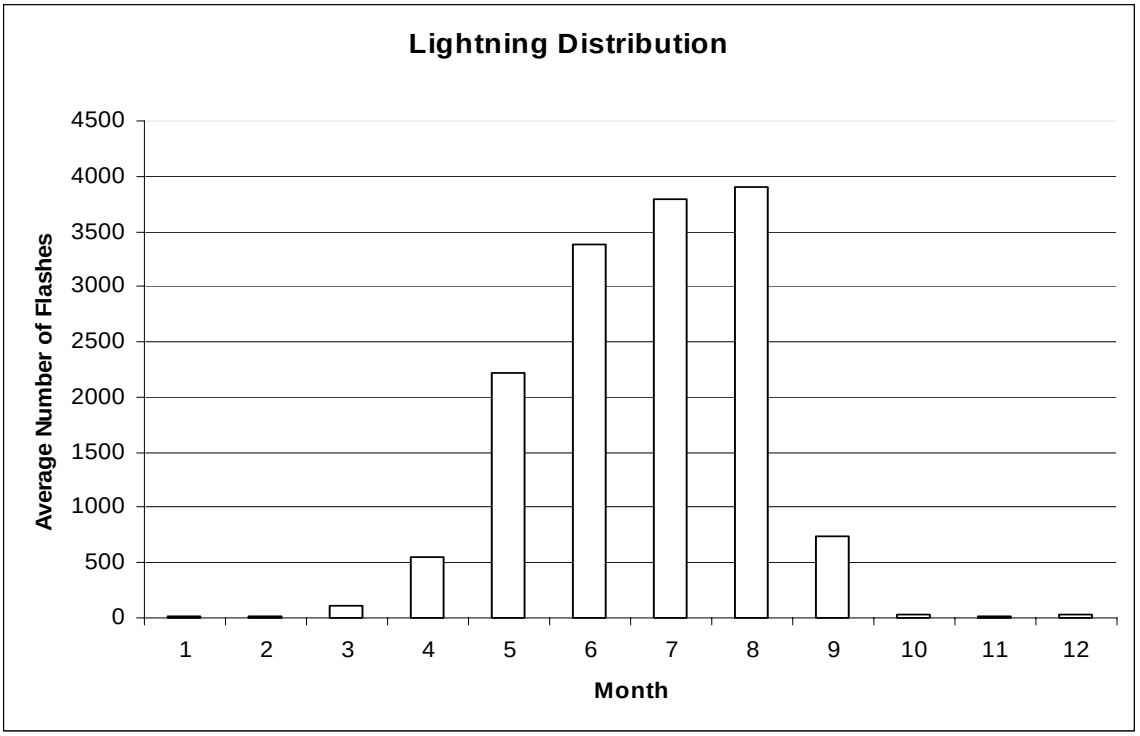

Figure 4.20 Average Number of Flashes in each month

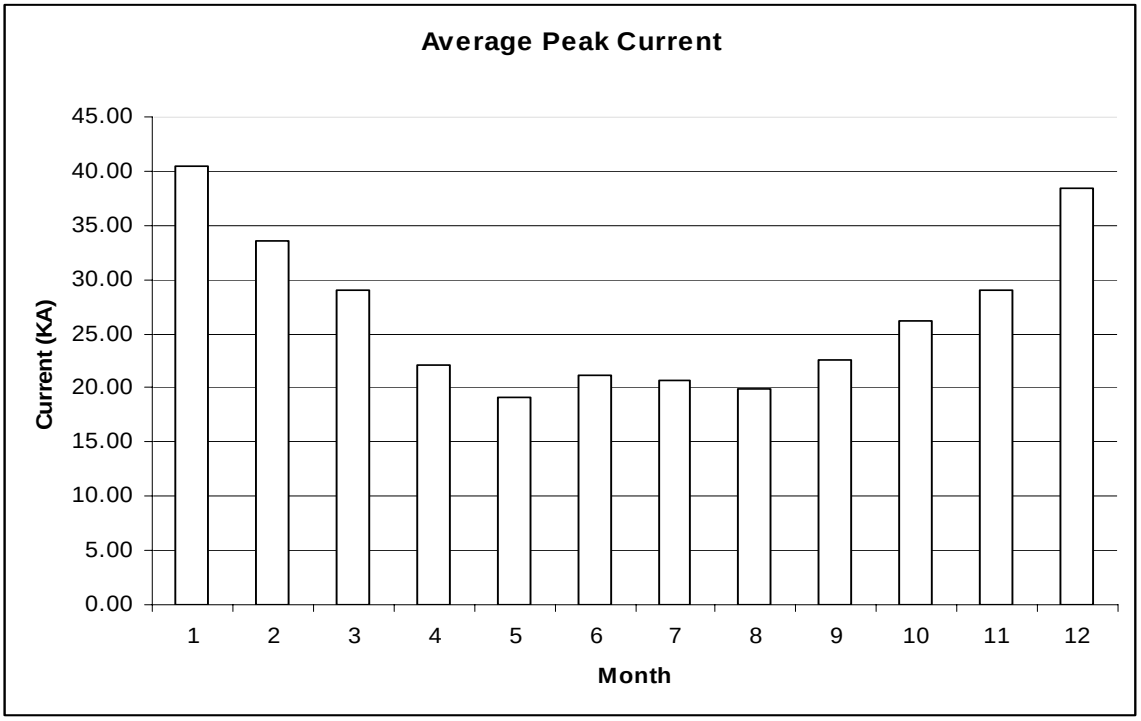

Figure 4.21 Average Peak Current of Flashes in each month

As indicated in Figure 4.21, lightning most frequently occurs in June, July and August. However, the intensity of the lightning shown in Figure 4.21 exhibits a concave curve, which means the flashes in winter have higher peak currents than the flashes that occur in summer.

The numbers that make up figures 4.20 and 4.21 are listed in Table 4.19. Table 4.19 also shows the minimum peak current and maximum peak current in each month.

Table 4.19 Flash Density and Intensity in Each Month

Month	Total Number of Flashes	Average Number of Flashes	Average Peak (KA)	Min Peak (KA)	Max Peak (KA)
1	105	10	40.42	7.80	167.70
2	212	19	33.52	4.20	203.20
3	1170	106	29.08	5.10	275.60
4	6144	559	22.07	4.40	355.80
5	24351	2214	19.17	3.70	380.30
6	37258	3387	21.22	3.80	239.00
7	41662	3787	20.76	3.20	203.40
8	42906	3901	19.87	3.70	201.90
9	8217	747	22.62	3.90	234.30
10	429	39	26.25	5.10	184.20
11	93	8	29.06	4.90	120.10
12	339	31	38.48	6.60	277.40

There are 25 out of the 49 storms from the outage records (1995-2004) that have flashes. The number of flashes in each of these 25 storms and the corresponding storm type are

presented in Table 4.20. Also shown in Table 4.20 are the average current of the flash, the peak current of the flash, and the number of outages in each storm.

Most of the flashes happen in the moderate (M) and high temperature (H) weather. In both cases, lightning may or may not be associated with strong winds. The highest number of lightning flashes in a storm (5110) appears in the moderate temperature weather with no strong winds. There are no outages attributed to flashes during L storms.

The peak currents of flashes in each storm do not show significant variations. If the storms having less than 100 flashes are eliminated, all the average currents will fall into the range of 13-27 kA. On the other hand, the peak flash currents in each storm exhibit larger deviations. The flashes that have a peak current over 100 kA occur in every type of the storm listed in Table 4.20, regardless of the temperature and wind speed. And the highest peak current (234.30 KA) happens in a moderate temperature storm with strong wind.

Table 4.20 Number of flashes in each storm

Storm ID	Number of flashes	Storm Type	Average Current (kA)	Peak Current (kA)	Number of Outages
66	2643	MS	21.41	117.70	28
67	13	MS	32.53	81.40	206
72	1	MS	9.20	9.20	271
73	3	MS	59.90	115.90	130
74	195	MS	22.63	140.30	171
97	1321	MS	21.39	106.60	134
114	58	MS	26.26	234.30	54
85	1790	MS	17.93	98.40	43

92	355	MS	16.29	81.30	104
75	2654	M	18.61	88.50	57
81	135	M	16.71	55.80	87
112	5110	M	17.43	139.10	167
113	648	M	17.71	84.10	8
100	893	M	17.86	72.30	52
82	3046	HS	22.57	134.60	438
84	5027	HS	19.69	109.10	247
93	825	HS	16.91	66.80	369
94	4203	H	20.77	105.40	86
98	1810	H	17.62	105.80	49
99	3994	H	22.55	101.00	142
101	2998	H	21.04	82.40	454
108	2536	H	13.97	119.40	143
102	4477	H	21.06	125.00	347
106	14	LS	33.84	115.70	175
69	1	LS	55.90	55.90	255

The largest number of outages caused by a storm is 438. From the number of outages in each storm, we do not see a clear relationship between the lightning and outages. For example, in HS storms, storm 84 has the highest number of flashes among the three HS storms in the outage records. However, storm 84 has the smallest number of outages among the three HS storms. A similar phenomenon occurs in other storm categories too.

Table 4.21 presents the number of flashes in selected intensity ranges for all storms from 1995 to 2004. From Table 4.21 it may be seen that flashes under 10 kA represent about 10% of the total number of flashes.

Table 4.21 Number of Flashes in Each Intensity Range

Peak Current Range (kA)	Number of Flashes
0-5	399
5-10	14726
10-20	76409
20-30	27677
30-40	10788
40-50	4657
50-100	4234
100-200	362
200-300	16
>300	1
SUM	139269

B. Summer Storm Lightning and Outages

We are interested in predicting outages in H storms that have lightning activity. From the previous section, significant outages occur during high temperature storms that do not have strong winds (H storms) but which do have lightning activity. We will now focus on analyzing four H storms with relatively high lightning activity. Table 4.22 shows the following:

- Number of flashes in each storm
- Average flash current for each storm
- Peak flash current for each storm
- Size of the storm area
- Flash density
- Number of outages caused by the storm

Table 4.22 Storm Information

Storm ID	Number of flashes	Average Current (kA)	Peak Current (kA)	Size of Storm Area(mile^2)	Flash Density (per mile^2)	Number of Outages
94	4203	20.77	105.40	2782.71	1.51	86
99	3994	22.55	101.00	2783.00	1.44	142
102	4477	21.06	125.00	2781.77	1.61	347
101	2998	21.04	82.40	2782.26	1.08	454

All four H storms have similar average flash currents, and the sizes of the storm area are very close. The numbers of flashes in storms with IDs 94, 99, and 102 are close to each other. Storm 101 has around 1000 fewer flashes than the other storms.

The numbers of outages vary significantly among the storms. Also, some storms with fewer flashes have many more outages. Storm 94 has 4203 flashes and 86 power outages where as storm 101 has 2998 flashes and 454 outages. That is, storm 101 has 1205 flashes less but 368 more outages. In percent, storm 101 has 29% fewer flashes but

428% more outages. So a storm with a larger number of flashes does not necessarily result in more outages. A possible relationship between lightning flash density and power outages is investigated in the next two sections.

Table 4.23 shows failures for lines, fuses, cables, transformers, and switches by storm. Under each equipment category, the number of failures due to tree contact, equipment failure, lightning, and/or overloads are enumerated. In Table 4.23, a little over 67.5% of the failures are due to lightning (In the table, we assume tree contact events and lightning and lightning events are statistically independent.)

Table 4.23 Number of Equipment Failures for Different Types of Equipment

Storm ID	Line			Fuse			Cable			Transformer			Switch		
	Tree Contact	Equipment Failure	Lightning	Tree Contact	Over Load	Lightning	Tree Contact	Equipment Failure	Lightning	Tree Contact	Equipment Failure	Lightning	Tree Contact	Equipment Failure	Lightning
94	2	2				26	19		12		2	24			1
99	3		2			37	41	1	19	1	2	26			
102	21		9		1	75	84	2	88	2		51			2
101	4	1	11	2		42	111	4	203	1	1	43	11	6	2
Sum	30	3	22	2	1	180	255	7	322	4	5	144	11	6	5

C. Modeling of Corridors

A circuit corridor represents a symmetrical area around the lines in the circuit model. For instance, a circuit corridor of 200 feet would represent an area that extends 100 feet on either side of every line and cable in the circuit. Flashes for each storm that

occur inside circuit corridors are analyzed. Circuit corridor widths considered are 20, 40, 60, 80, 100, 150, 200, 300, 400, 500, 600, and 800 feet.

For each circuit corridor width and for each storm, the number of flashes with intensity above selected levels of 10, 20, 30, 40, and 50 kA are counted (The lightning activity records in Table 4.21 indicates that flashes under 10 kA represented only about 10% of the total number of flashes from 1995 to 2004. It was decided to focus the analysis on flashes with peak currents over 10kA). That is, for a given circuit corridor width and a given storm, the flashes occurring in the corridor above 10kA are counted. Then, for the same corridor width and storm, the flashes occurring in the corridor above 20kA are counted, and so forth, up to 50 kA. This is repeated for each of the corridor widths and storms selected for study.

The total length of the corridor considered is 831.57 miles. If the half corridor width is 400 feet, the size of the corridor area will be roughly 126 square miles. Based on this corridor area, we compute the flash density within the corridor (flashes under 10 kA are not included). One of the interesting findings from this corridor model is that the lightning density within the circuit corridors is always higher than the density over the entire storm area. This seems to indicate that the lines attract lightning. Note that the areas of the storms analyzed here are much larger that the circuit corridor areas, as shown in Table 4.22. If a circuit corridor of 800 feet is selected, less than 5% of any storm area analyzed overlaps the circuit corridor area.

There are a total of nine H storms. Six H storms have flash records, and four of them have a high density of flashes (High flash density means the number of flashes in a storm is greater than 2990). Figures 4.22-4.25 present analysis results for the four high

flash density H storms referred to as Storm 94, Storm 99, Storm 101, and Storm 102, respectively. Note that in the figure the numbers of flashes are plotted against half the width of the corridor, which may be used as an upper limit on the distance from the flash to the line.

From figures 4.22-4.25 it may be seen that the wider the circuit corridor, the more flashes falling in the range of corridor area. This is to be expected. However, note that as the corridor width is increased above 25 to 75 feet (this increase depends upon the storm), the number of flashes falling within the corridor starts to dramatically increase. Another way to look at this is as follows:

> Over all four figures, the number of flashes falling within the 50-foot (half width is 25 feet) corridor is less than the number of flashes falling between 50 and 100 feet.

For all four storms, when the half corridor width reaches 100 feet, the numbers of flashes inside the corridor is increasing dramatically, especially for flashes above 10 and 20 kA.

From Table 4.21 we may note that over all four storms, 54.8% of the peak current flashes fall between 10 and 20 kA. Flashes with peak currents above 20 kA represent only 34.3%. Also notice that there is a large gap between the number of flashes above 10 kA and the number of flashes above 20 kA for each of the four storms. From figures 4.22-4.25 it is observed that the gaps between the curves become smaller and smaller as the peak currents increase.

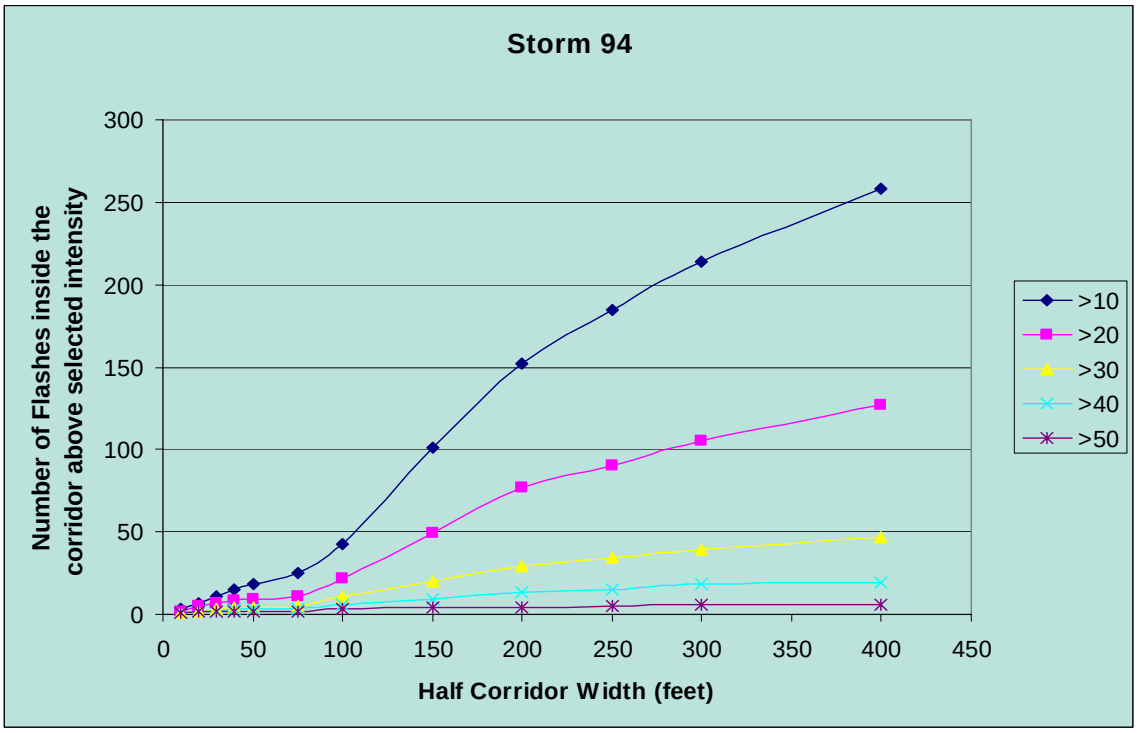

Figure 4.22 Numbers of Flashes above Peak Current Levels in Storm 94 inside Corridors of Different Widths

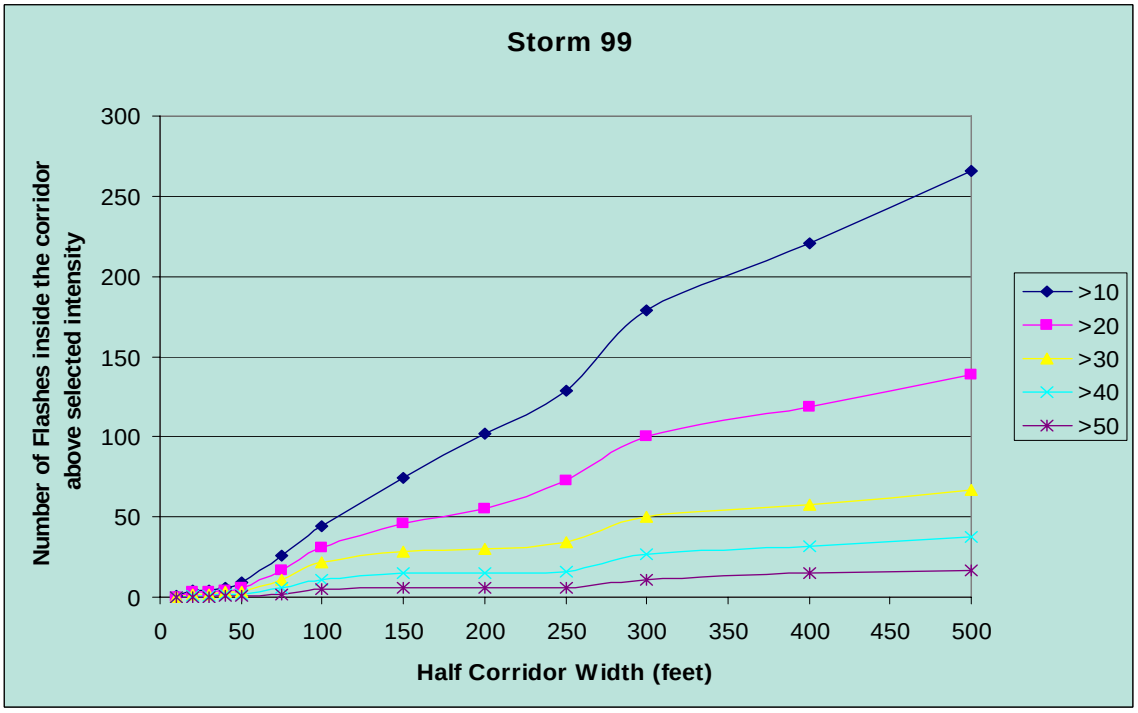

Figure 4.23 Numbers of Flashes above Peak Current Levels in Storm 99 inside Corridors of Different Widths

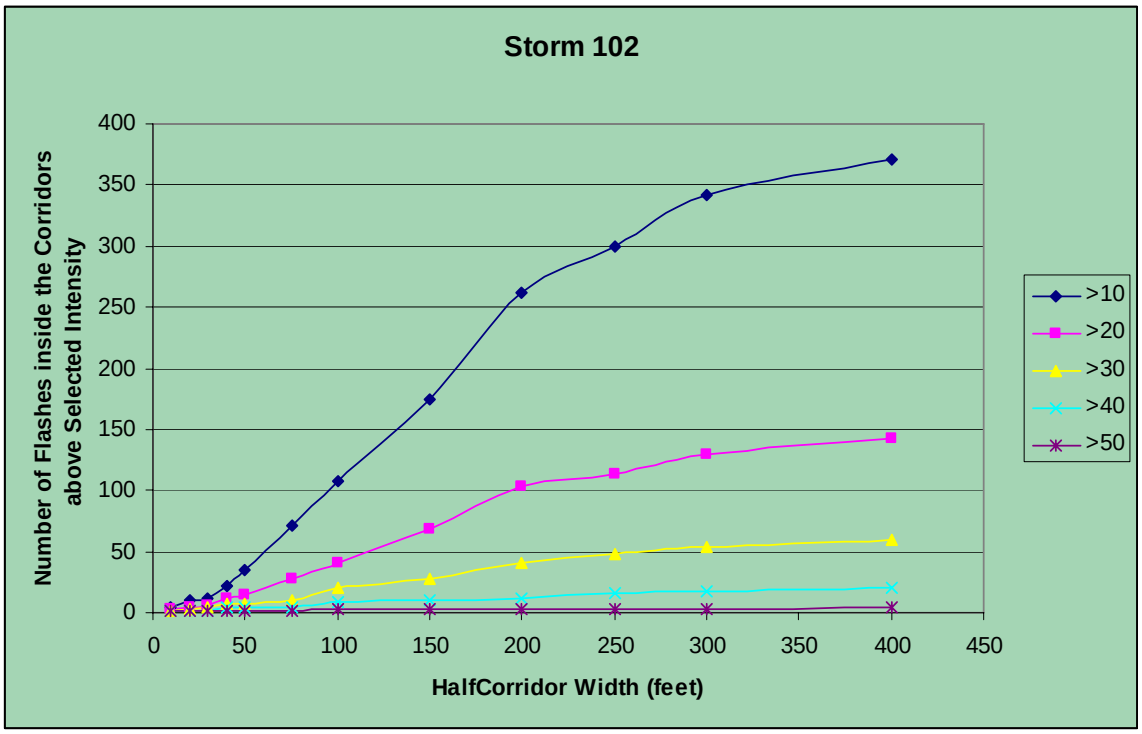

Figure 4.24 Numbers of Flashes above Peak Current Levels in Storm 102 inside Corridors of Different Widths

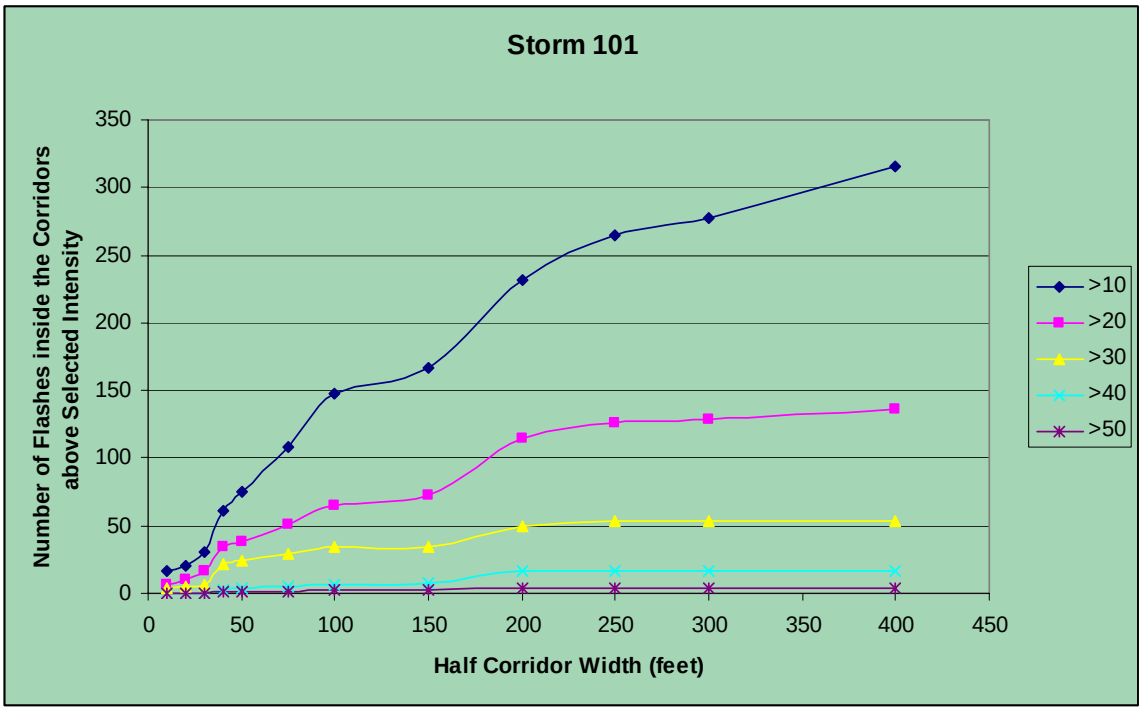

Figure 4.25 Numbers of Flashes above Peak Current Levels in Storm 101 inside Corridors of Different Widths

D. Correlation of Flash Density and Outages

By studying different combinations of lighting intensity ranges and corridor widths, it was discovered that lightning intensities in the range of 10–30 kA within a 400-foot corridor had a high correlation with power outages observed. Fig. 10 shows a plot of 10-30kA flash densities in the 400 foot corridor versus total numbers of outages. The area that was used to compute the flash density is the area of circuits that had one or more flashes during a particular storm.

Figure 4.26 indicates the number of outages due to lightning modeled as a linear function of the lightning density within the 400-foot circuit corridor. The linear curve fit is given by (4) with an R-squared value of 0.9188.

$$N = 58.94D - 27.975 \qquad (4.12)$$

where N = the total number of outages in a storm

D = the 10-30kA flash density within 400-foot circuit corridor.

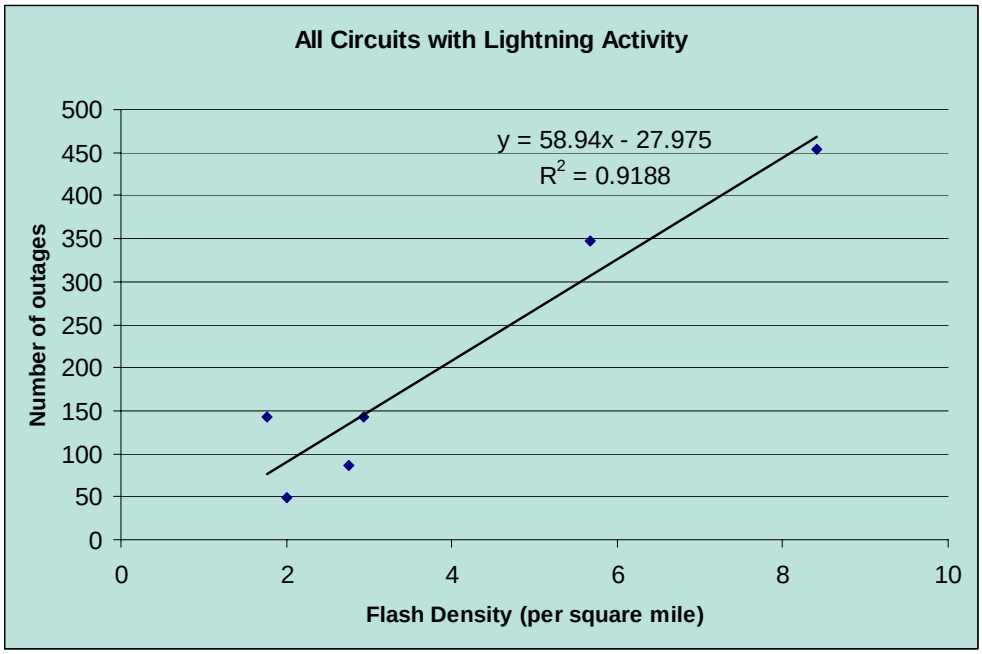

Figure 4.26 Number of Power Outages versus 10-30kA Flash Densities in 400-Foot Corridor over All Circuits with Lightning Activity

It should be noted that there are not many lightning intense storms in the sample, and these particular results are not statistically sustainable. More lightning storm samples are required for a high degree of statistical confidence. However, the analysis here does show promise for being able to estimate the number of outages caused by a storm with lightning activity.

E. Real Time Calculation of Outages

Once there is sufficient lightning storm data to form a statistically sustainable model, the model can be employed in real-time operations for predicting and managing outages. Weather data to implement predictions is available through two different Web enabled interfaces, one for normal weather variables and the other for lightning activity.

The real-time lightning data feed would be used to calculate lightning densities within circuit corridors. The outages can then be predicted in a manner similar to the storm models presented in Section III. The outages can be used to make decisions about the number of crews needed and the distribution of the crews throughout the circuits.

CHAPTER 5 CONCLUSIONS AND FURTHER RESEARCH

5.1 Conclusions

The electric power supply industry, with its humble beginning in the 1880s, has evolved into one of the largest industries in the world. Reliable operation of the electric power system is fundamental to the national economy and the quality of modern society. The complicated power grid is now facing severe challenges to its reliability, which include lack of transmission capability and power infrastructure vulnerability. The recent blackouts, including the one in North America during August 2003, indicated the severity of those challenges. Power outages of the transmission system are more dramatic than distribution system power outages, but many more outages are due to distribution system component failures.

From this study, electrical power distribution reliability can be assessed quantitatively by analytical methods combined with set theory and graph trace analysis. GTA algorithm notation is applied in the solution of reliability assessment. The accuracy of the assessment depends on the accuracy of the component statistical models.

As an effort to enhance the accuracy of reliability assessment, a reconfiguration for restoration algorithm was developed. This algorithm is implemented with Graph Trace Analysis. It takes into account multiple concurrent failures and load priorities. It is shown that reconfiguration for restoration improves system reliability by reducing customer down times following power outages.

Electrical power distribution reliability can be improved from different aspects, from planning to operation to maintenance. This work focuses mainly on a reconfigurable

system design, enhancing system reliability from the configuration point of view. First, it is shown that system reliability can be analyzed as a function of system load. Second, if adding a DG to the system is financially justified, it has been shown that a DG can be placed for either minimum loss or best reliability, and that the optimum placement varies with the criteria selected and the different loadings of the system.

Reconfiguration, resulting in shifting loads around, is a low cost reliability improvement measure if switching operations are permitted. The DAOP algorithm can provide a load distribution plan among multiple adjacent circuits to achieve optimal system reliability.

This work also initiated an investigation on how storms impact the power distribution system and how storm models can help with contingency management and eventually help with reliability improvement. Based on historical storm outage data, a two-stage prediction method is proposed to forecast storm related outages. In the first stage, historical outage and weather data are employed to create empirical models. For different types of storms, the number of outages is modeled as a function of time elapse. In the second stage, observers are employed for tracking and predicting storm outages in real time. The effectiveness of the prediction model is evaluated with simulations using actual storm data. The analysis results presented are system dependent. Different distribution systems may experience different patterns of outages caused by storms. However, the two stage prediction model proposed can be applied to any distribution system.

Lightning is a primary cause of outages during summer storms. Research has been done to seek the relation between summer lightning activities and power outages. The research data indicates that the number of power outages may be modeled as a linear function of lightning density within 400-foot corridors. More statistical data is required to confirm the result.

5.2 Further Research

As mentioned earlier in this dissertation, power system reliability analysis involves technical, economic, and environmental analysis. The content of this study touched parts of these fields. Future work could include the following:

- Continue research on reconfigurable systems with DGs.
- Based on component statistics research, design a data schema to organize and transmit information from system operations to feed reliability analysis.
- Continue research on reconfigurable systems with the goal of achieving reliability levels similar to those attained by adding dedicated redundant components.
- Continue research in storm modeling to improve system reliability, and in particular statistical models involving outages and lightning activity, such as the one proposed here which correlates lightning densities in circuit corridors with outages.

REFERENCE

[1] Roy. Billinton, Ronald N. Allan, *Power-system Reliability in Perspective*, IEE J. Electron. Power, vol.30, pp.231-236, March 1984.

[2] U.S. Department of Energy, Energy Information Administration, *Annual Energy Outlook 2006*, February 2006.

[3] Phili P. Barker, Robert W. De Mello, *Determining the Impact of Distributed Generation on Power System: Part 1- Radial Distribution Systems*, Power Engineering Society Summer Meeting, 2000. IEEE , vol. 3, pp. 1645 – 1656, July 2000.

[4] D. Zhu, R. P. Broadwater, K. Tam, R. Seguin, H. Asgeirsson, *Impact of DG Placement on Reliability and Efficiency with Time-Varying Loads*, IEEE Transactions on Power Systems, Vol. 21, No. 1, Feb 2006.

[5] George Ellis, Observers in Control Systems: A Practical Guide, Academic Press, 2002.

[6] Leite da Silva, A.M.; Cassula, A.M.; Billinton, R.; Manso, L.A.F., *Integrated reliability evaluation of generation, transmission and distribution systems*, IEE Proceedings-Generation, Transmission and Distribution, , Volume 149, Issue 1, Page(s):1 – 6, Jan. 2002

[7] Billinton, R.; Goel, L., *Overall adequacy assessment of an electric power system*, IEE Proceedings-Generation, Transmission and Distribution, Volume 139, Issue 1, Page(s):57 – 63, Jan. 1992

[8] Dixon, G.F.L., Hammersley, H., *Reliability and its cost on distribution systems*. International Conference on Reliability of Power Supply Systems, IEE Conference Publication No. 148, pp. 81-84, London, 1977

[9] Canadian Electrical Association, Equipment Reliability Information Systems, Annual Service Continuity Report on Distribution System Performance in Canadian Electrical Utilities, Final Report, 1990

[10] R. Billinton and R. N. Allan, Reliability Evaluation of Engineering Systems: Concepts and Techniques. 2nd Edn, New York: Plenum, 1992.

[11] Roy Billinton, Kenneth E. Bollinger, *Transmission system Reliability Evaluation Using Markov Processes*, IEEE Trans. Power Apparatus Syst., Vol. PAS-87, no. 2, pp. 538-547, Feb. 1968.

[12] R.N.Allan,R. Billinton, A.M.Breipohl, S.H.Lee, *Bibliography on the application of probability methods in power system reliability evaluation*, IEEE Trans. Power Syst., vol.PAS-103,pp. 275–282, 1984.

[13] R.N.Allan,R. Billinton, A.M.Breipohl, C.H.Grigg, *Bibliography on the application of probability methods in power system reliability evaluation*, IEEE Trans. Power Syst., vol.9, pp.41–49, Feb. 1994.

[14] R.Billinton, R.N.Allan, *Reliability Evaluation of Power Systems*. New York: Plenum, 1984.

[15] R. Billinton, P. Wang, *Network-equivalent approach to distribution system reliability evaluation*, Proc. Inst. Elect. Eng. Gen. Transm. Distrib., vol. 145, no. 2, pp. 149–153,1998.

[16] R.E.BrownandA.P.Hanson, *Impact of two-stage service restoration on distribution reliability*, IEEE Trans. Power Syst., vol. 16, pp.624–629, Nov.2001.

[17] Weixing Li; Peng Wang; Zhimin Li; Yingchun Liu, *Reliability evaluation of complex radial distribution systems considering restoration sequence and network constraints*, Power Delivery, IEEE Transactions Volume 19, Issue 2, April 2004 Page(s):753 – 758

[18] L. Wehenkel. "Automahc learning techniques in power systems." Kluwer Academic, Boston, 1998

[19] P.S. Harish, L.A. Basha, G. Prashant, *Automatic vacuum capacitor switch with modified digital filter design for enhanced speed and power optimization*, Power Systems Conference and Exposition, 2004. IEEE PES, Page(s):568 – 573, vol.1, Oct. 2004.

[20] Appleyard, J.C., Myers, D.A., Niemira, J.K., *Innovations in use of microprocessor relays and controls for improved reliability on the distribution system*, Transmission and Distribution Conference and Exposition, 2001 IEEE/PES Volume 1, 28 Oct.-2 Nov. 2001 Page(s):293 - 298 vol.1

[21] Wolff, Robert F., "Automate Storm Data to Cut Outage Time", Electrical World, PP. 93-94, Nov. 1981.

[22] Brown, R.E, Gupta, S., Christie, R.D., Venkata, S.S., Fletcher, R., "Distribution system reliability assessment: momentary interruptions and storms" Power Delivery, IEEE Transactions, Vol. 12, no. 4, pp.1569 – 1575, Oct. 1997.

[23] Nielsen, T.D., "Improving outage restoration efforts using rule-based prediction and advanced analysis" Power Engineering Society Winter Meeting, 2002. IEEE, Vol. 2, pp. 866 - 869 Jan. 2002.

[24] Takata, H.,Yanase, M., Waki, T., and Hachino, T, "A prediction method of electric power damage by typhoons in Kagoshima via GMDH and NN", Proceedings of the 41st SICE Annual Conference, Vol.4, pp. 2424- 2429 Aug. 2002.

[25] George Ellis, "Observers in Control Systems: A Practical Guide", Academic Press, 2002.

[26] Lubkeman, D., Julian, D.E., "Large scale storm outage management" Power Engineering Society General Meeting, *IEEE*, Vol.1 pp.16 – 22, June 2004.

[27] Wenyuan Li, Risk Assessment of Power Systems models, Methods, and Applications, IEEE Press, Wiley-Interscience, 2005.

[28] http://www.itl.nist.gov/div898/handbook/apr/section1/apr161.htm

[29] Development of Distribution System Reliability and Risk Analysis Models, EPRI Rep. No. EL-2018, Vols.2 and 3, Electric Power Research Inst., Palo Alto, CA Aug. 1981.

[30] Distribution Engineering Workstation Data Schema, Version 1.01, EPRI EL-7249-V5 Project 3079-03 Final Report, Sep. 1995

[31] R.P. Broadwater, J. C. Thompson, T.E. McDermott, *Pointers and linked lists in Electric Power Distribution Circuit Analysis*, Proc. IEEE Power Industry Computer Applications (PICA) Conf. pp. 16-21, MD, 1991.

[32] Jos B. Warmer, Anneke G. Kleppe, *The Object Constraint Language: Precise Modeling With Uml,* Addison-Wesley Professional, 1st edition, Oct. 13, 1998.

[33] http://en.wikipedia.org/wiki/Structured_Query_Language

[34] R. P. Broadwater, J. C. Thompson, S. Rahman, A. Sargent, *An Expert System For Integrated Protection Design With Configurable Distribution Circuits: Part I*, IEEE Transactions on Power Delivery, Vol. 9, No. 2, pp. 1115-1121, Apr. 1994.

[35] Charlie Alan Jones, Operational Extensions to a Power Distribution Design Workstation for Enhanced Emergency Restoration, VA Dec. 1990

[36] R. P. Broadwater, J. C. Thompson, H. Maghdan, and R. E. Lee, *Computer-Aided Protection System Design with Reconfiguration*, IEEE Transactions on Power Delivery, Vol. 6, No. 1, pp. 260-266, January 1991.

[37] Hsu, Y.Y.; Huang, H.M.; Kuo, H.C.; Peng, S.K.; Chang, C.W.; Chang, K.J.; Yu, H.S.; Chow, C.E.; Kuo, R.T.; *Distribution system service restoration using a heuristic search approach,* IEEE Transactions on Power Delivery, Volume 7, Issue 2, Page(s):734 – 740, April 1992.

[38] Dariush Shirmohammadi, *Service Restoration In Distribution Networks Via Network Reconfiguration*, IEEE Transactions on Power Delivery, Vol. 7, No. 2, pp.952-958, Apr. 1992.

[39] C.C Liu, S.J. Lee, S.S. Venkata, *An Expert System Operational Aid for Restoration and Loss Reduction of Distribution Systems*, IEEE Transactions on Power Systems, Vol. 3, No.2, pp. 619-626, May 1988.

[40] Yuan-Yih Hsu; Han-Ching Kuo; *A Heuristic Based Fuzzy Reasoning Approach for Distribution System Service Restoration,* IEEE Transactions on Power Delivery, Volume 9, Issue 2, Page(s):948 – 953, April 1994.

[41] Y. Fukuyama, Hsaio-Dong Chiang, *A Parallel Genetic Algorithm for Service Restoration in Electric Power Distribution Systems*, International Journal of Electrical Power & Energy System, Vol. 18, No.2, PP. 111-119, 1996.

[42] R. Billinton andW. Li, Reliability Assessment of Electric Power Systems Using Monte Carlo Methods. New York: Plenum, 1994.

[43] T. Griffin, K. Tomsovic, D. Secrest, A. Law, Placement of Dispersed Generation Systems for Reduced Losses, Proceedings of the 33rd Annual Hawaii International Conference on Systems Sciences, 2000

[44] K. Nara, Y. Hayashi, K. Ikeda, T. Ashizawa, Application of tabu search to optimal placement of distributed generators, Power Engineering Society Winter Meeting, IEEE, vol.228, pp.918 – 923, Jan.- Feb, 2001.

[45] Kyu-Ho Kim, YuJeong Lee, Sang-bong Rhee, Dispersed Generator Placement using Fuzzy-Ga in Distribution Systems, Power Engineering Society Summer Meeting, 2002 IEEE, Vol. 3, pp. 1148-1153, Chicago, IL, July 2002.

[46] C. Wang, M. H. Nehrir, Analytical Approaches for Optimal Placement of Distributed Generation Sources in Power System, Paper ID: TPWRS-00472_2003, to be published.

[47] Jen-Hao Teng, Tain-Syh Luor, Yi-Hwa Liu, Strategic distributed generator placements for service reliability improvements, Power Engineering Society Summer Meeting, 2002 IEEE, vol.2, pp.719 - 724, July 2002.

[48] R.C. Dugan, T.E. McDermott, G.J. Ball, Planning for distributed generation, Industry Applications Magazine, IEEE, Vol.7, pp. 80-88, Mar/Apr 2001.

[49] Dan Zhu, *Power System Reliability Analysis with Distributed Generators*, Electronic Theses and Dissertations URN-05162003-090532, Dept. of Electrical and Computer Engineering, Virginia Tech, May 2003.

[50] Ann Chambers, Stephanie Hamilton, Barry Schnoor, *Distributed Generation: A Nontechnical Guide*, Oklahoma, PennWell, 2001, pp. 8.

[51] Paul A. Dolloff, Optimization in Electrical Distribution Systems: Discrete Ascent Optimal Programming, PhD Dissertation, Blacksburg, Virginia Tech, February 1996.

[52] Jay Devore, Nicholas Farnum, *Applied statistics for engineers and scientists*, Duxbury Press, 2004.

VITA

Dan Zhu was born in Jiangmen, Guangdong, China 1977. She received her Bachelor of Electrical Engineering degrees from South China Normal University, Guangzhou, China, in June 2000. She worked in the Electric Power Bureau of Jiangmen, China as an assistant engineer after she got her bachelor degree. She came to United States in August 2001, and received her Masters of Science in Electrical Engineering degree from Virginia Tech in 2003. Since then, she has been pursuing her doctoral degree in Virginia Tech. Her research involves algorithms for electric power distribution system reliability assessment. Her research interests are distribution system reliability improvements.